



**A COMPARISON OF MAIN ROTOR SMOOTHING ADJUSTMENTS
USING LINEAR AND NEURAL NETWORK ALGORITHMS**

THESIS

Nathan A. Miller, Captain, USMC

AFIT/GAE/ENY/06-M24

**DEPARTMENT OF THE AIR FORCE
AIR UNIVERSITY**

AIR FORCE INSTITUTE OF TECHNOLOGY

Wright-Patterson Air Force Base, Ohio

APPROVED FOR PUBLIC RELEASE; DISTRIBUTION UNLIMITED

The views expressed in this thesis are those of the author and do not reflect the official policy or position of the United States Air Force, Department of Defense, or the U.S. Government.

AFIT/GAE/ENY/06-M24

**A COMPARISON OF MAIN ROTOR SMOOTHING ADJUSTMENTS
USING LINEAR AND NEURAL NETWORK ALGORITHMS**

THESIS

Presented to the Faculty

Department of Aeronautics and Astronautics

Graduate School of Engineering and Management

Air Force Institute of Technology

Air University

Air Education and Training Command

In Partial Fulfillment of the Requirements for the
Degree of Master of Science in Aeronautical Engineering

Nathan A. Miller, BS

Captain, USMC

March 2006

APPROVED FOR PUBLIC RELEASE; DISTRIBUTION UNLIMITED

**A COMPARISON OF MAIN ROTOR SMOOTHING ADJUSTMENTS
USING LINEAR AND NEURAL NETWORK ALGORITHMS**

Nathan A. Miller, BS
Captain, USMC

Approved:

Donald L. Kunz (Chairman)

Date

Robert A. Canfield (Member)

Date

Paul A. Blue, Maj, USAF (Member)

Date

Abstract

Helicopter main rotor smoothing is a maintenance procedure that is routinely performed to minimize destructive airframe vibrations induced by non-uniform mass and/or aerodynamic distributions in the main rotor system. This important task is both time consuming and expensive, so improvements to the process have been long sought. Traditionally, vibrations have been minimized by calculating adjustments based on an assumed linear relationship between adjustments and vibration response. In recent years, artificial neural networks have been designed to recognize non-linear mappings between adjustments and vibration response. This research was conducted in order observe the mathematical character of the adjustment mapping of the Vibration Management Enhancement Program's PC-Ground Base System (PC-GBS). Flight data from the UH-60, AH-64A, and AH-64D were utilized during the course of this study. What has been determined is that, in a majority of situations, the neural networks of the PC-GBS produce adjustments that can be reproduced by a linear algorithm, thus implying that the character of the mapping is in fact linear.

*This work is dedicated to my wife and best friend for her
support and patience throughout the course of this study.*

Acknowledgments

I would like to express my sincere appreciation to my faculty advisor, Professor Donald Kunz, for sharing his knowledge and providing advice throughout the course of this endeavor. Many days of aimless wandering were avoided by following his excellent directions. I would also like to thank Dr. Jon Keller for providing technical guidance during the course of this research.

Nathan A Miller

Table of Contents

	Page
Abstract	iv
Dedication	v
Acknowledgements	vi
Table of Contents	vii
Nomenclature	x
List of Figures	xi
List of Tables	xii
I. Introduction	1-1
1.1 General	1-1
1.2 Problem Statement	1-3
1.3 Objectives	1-3
1.4 Research Methodology	1-3
1.5 Chapter Summary	1-4
II. Background	2-1
2.1 Introduction	2-1
2.2 General Classification of Vibration	2-1
2.3 Classification of main rotor vibrations	2-2
2.4 Flight Conditions for Vibration Measurement	2-4
2.5 Types of Main Rotor Adjustments	2-4
2.5.1 Adjustments for Mass Imbalance	2-5
2.5.2 Origin of a Mass Imbalance	2-6
2.5.3 Aerodynamic Imbalances	2-7
2.6 Main Rotor Adjustment Fidelity	2-8
2.7 History of Track and Balance	2-9
2.8 Linear Algorithms	2-10
2.8.1 The Aviation Vibration Analyzer	2-10
2.8.2 The Linear Algorithm Defined	2-11
2.8.3 Determining the Linear Sensitivity Coefficient Matrix	2-11
2.9 Application of Adjustment Sets	2-12
2.10 The Linear Assumption Comes into Question	2-14
2.11 The Artificial Neural Network Algorithm	2-15

	Page
2.11.1 The PC-Ground Based System	2-16
2.11.2 PC-GBS Solution Options	2-17
2.11.3 The Neural Networks of PC-GBS	2-17
2.11.4 PC-GBS Performance From and Earlier Study	2-18
2.12 Chapter Summary	2-19
III. Methodology	3-1
3.1 Introduction	3-1
3.2 Origin of Research Data	3-1
3.3 Data Acquisition Techniques	3-3
3.3.1 Removing the Effects of the Solution Optimization Expert	3-3
3.3.2 Removing the Effects of the TON	3-4
3.3.3 Converting Detailed Adjustment Sets into Reduced Adjustment Vectors	3-5
3.4 Overview of Analysis Methods	3-6
3.5 Explanation of Vibration Ranges	3-7
3.6 Calculating the AVA Adjustment Set	3-7
3.7 The Ad Hoc Sensitivity Coefficient Method	3-8
3.7.1 Constructing the Ad-Hoc Sensitivity Coefficient Matrix	3-9
3.8 Database Entries	3-9
3.9 Chapter Summary	3-10
IV. Analysis and Results	4-1
4.1 Introduction	4-1
4.2 Comparison of PC-GBS Adjustments to AVA Adjustments	4-1
4.3 Ad Hoc Coefficient Method	4-5
4.3.1 Small Moves Ad Hoc Coefficient Analysis	4-6
4.3.2 Method of RMS of the Small Moves Ad Hoc Coefficients	4-8
4.3.3 Large Moves Ad Hoc Coefficient Analysis	4-10
4.3.4 Ad Hoc Sensitivity Coefficients as Determined By PC-GBS	4-14
4.5 Chapter Summary	4-16
V. Conclusions and Recommendations	5-1
5.1 Chapter Overview	5-1
5.2 Conclusions of Research	5-1
5.3 Significance of Research	5-2
5.4 Recommendations for Action	5-3
5.5 Summary	5-4

	Page
Appendix A: Aviation Vibration Analyzer Sensitivity Coefficients	A-1
Appendix B: UH-60 Database	B-1
Appendix C: AH-64A Database	C-1
Appendix D: AH-64D Database	D-1
Appendix E: UH-60 Matlab Code	E-1
Appendix F: AH-64A Matlab Code	F-1
Appendix G: AH-64D Matlab Code	G-1
Bibliography	REF-1
Vita	VIT-1

Nomenclature

AVA	Aviation Vibration Analyzer
AEN	Adjustment Evaluation Networks
FPG	Flat Pitch Ground
MRS	Main Rotor Smoothing
PC-GBS	Personal Computer – Ground Based System
RMS	Root Mean Square
RPM	Revolutions Per Minute
SOE	Solution Optimization Expert
TON	Track Optimization Network
UTD	Universal Tracking Device
VMEP	Vibration Management Enhancement Program
VPN	Vibration Prediction Network

List of Figures

	Page
Figure 1. Polar Chart of AH-64D vibrations from PC-GBS	2-3
Figure 2. Universal Static Balance Fixture	2-5
Figure 3. AH-64 Apache with blade weight installed	2-6
Figure 4. A PCR on a UH-60 (left) and a Trim Tab on an OH-58	2-8
Figure 5. Universal Tracking Device mounted on a UH-60	2-14
Figure 6. Schematic of Neural Network Undergoing Training	2-15
Figure 7. Vibration Values Tab of PC-GBS	3-2
Figure 8. Rotor Smoothing Solution Tab of PC-GBS	3-2
Figure 9. UH-60 Blackhawk Blade Map	3-5
Figure 10. UH-60 Bar Chart Comparison of AVA to PC-GBS.....	4-2
Figure 11. Graphical Depiction of Vector Difference	4-3
Figure 12. AH-64A Bar Chart Comparison of AVA to PC-GBS	4-4
Figure 13. AH-64D Bar Chart Comparison of AVA to PC-GBS	4-5
Figure 14. UH-60 Small Moves Ad Hoc Weight Adjustments	4-6
Figure 15. Polar Chart of UH-60 Weight Adjustments	4-10
Figure 16. UH-60 Bar Chart Comparison of RMS of Large Moves to PC-GBS	4-12
Figure 17. AH-64A Bar Chart Comparison of RMS of Small Moves to PC-GBS	4-13
Figure 18. AH-64D Bar Chart Comparison of RMS of Large Moves to PC-GBS	4-13

List of Tables

	Page
Table 1. Vibration Measurement Flight Conditions	2-4
Table 2. Sample Calculation	3-6
Table 3. Vibration Magnitude Ranges by Category	3-7
Table 4. Typical database entry for the UH-60 Blackhawk	3-10
Table 5. Adjustment Move Sizes	3-10
Table 6. UH-60 Small Moves Ad Hoc Comparison	4-7
Table 7. AH-64A Small Moves Ad Hoc Comparison	4-7
Table 8. AH-64D Small Moves Ad Hoc Comparison	4-7
Table 9. UH-60 Comparison for RMS of Small Moves Ad Hoc	4-8
Table 10. AH-64A Comparison for RMS of Small Moves Ad Hoc	4-8
Table 11. AH-64D Comparison for RMS of Small Moves Ad Hoc	4-9
Table 12. Standard Deviations of Differences of RMS of Small Moves Ad Hoc	4-9
Table 13. UH-60 Large Moves Ad Hoc Comparison	4-11
Table 14. AH-64A Large Moves Ad Hoc Comparison	4-11
Table 15. AH-64D Large Moves Ad Hoc Comparison	4-11
Table 16. Standard Deviation Between Ad Hoc RMS and PC-GBS Adjustments.....	4-14
Table 17. UH-60 Ad Hoc Sensitivity Coefficients	4-15
Table 18. AH-64A Ad Hoc Sensitivity Coefficients	4-15
Table 19. AH-64D Ad Hoc Sensitivity Coefficients	4-16

A COMPARISON OF MAIN ROTOR SMOOTHING ADJUSTMENTS USING LINEAR AND NEURAL NETWORK ALGORITHMS

I. Introduction

1.1 General

Since the early days of rotary wing aviation, helicopters have been well known for their unique ability to take off and land vertically as well as for their tendency to vibrate while doing so. Along with providing lift, helicopter main rotors are the source of some of the most destructive vibrations known to the aircraft industry. These one-per-rev vibrations are brought about primarily by non-uniform rotor mass distribution and non-uniform aerodynamic properties among the rotor blades.

In order to alleviate these destructive vibrations, the helicopter main rotor smoothing procedure is periodically performed. Helicopter main rotor smoothing (MRS) is a process in which vibration magnitude and phase are recorded both on the ground and in flight. Then, based on a predetermined relationship between vibrations and corrective adjustments, changes are determined for blade weights, pitch links, and trim tabs. The process usually requires several flights to reduce the vibration to acceptable levels and is therefore time consuming and expensive.

Efforts have long been made to improve the main rotor smoothing process so as to decrease the number of required flights and thus, save time and money. Over the years, data acquisition equipment has become more accurate, dependable, and user friendly. In recent years, a substantial effort has been made to improve the computer software used to convert raw vibration data into corrective main rotor adjustments [1,2,3]. These improvements are centered on the abandonment of the linear assumption relating main rotor adjustments to vibration response.

Due to the complexity of the dynamics involved with a main rotor system, simplifications have to be made about the relationship between vibrations and corrective adjustments. One such simplification is to assume a linear relationship exists between main rotor adjustments and vibration changes. Most MRS algorithms utilize the linear assumption to calculate main rotor adjustments. It is typical that several flights are required in order to smooth vibrations to within acceptable levels. The blame for this poor performance has recently been directed toward the linear assumption.

To this end, a new paradigm has been introduced to the practice of main rotor smoothing. Artificial neural networks have been trained to recognize the relationship between main rotor adjustments and their resulting change in vibrations. This new algorithm makes no assumptions about the mathematical character of the solution space, so it is therefore believed that a higher degree of adjustment accuracy can be realized.

1.2 Problem Statement

Until recently, the mathematical character of the vibration/adjustment solution space had been assumed to be linear; however, this has not been verified by a rigorous study. This thesis shall examine the validity of the linear assumption and shall determine whether higher order algorithms are necessary to accurately calculate main rotor adjustments.

1.3 Objectives

The objective of this research was to characterize the vibration/adjustment solution space as it is understood by a trained neural network, and to search for differences in adjustment solutions produced by a linear algorithm.

1.4 Research Methodology

The objectives of this research were met using two general techniques. The first technique was essentially a detailed comparison of the calculated adjustments from a neural network algorithm to those of a traditional, linear algorithm. If the two algorithms behaved the same, then the conclusion would be that the neural network behaved in a linear fashion. If they produced different results, however, the conclusion would not be as clear cut.

The second technique involved using the neural network to create linear coefficient matrices at multiple locations in the vibration and adjustment spaces. These matrices then became the core of new linear algorithms that were used to calculate adjustments for further comparisons.

1.5 Chapter Summary

Main Rotor Smoothing is an expensive procedure that must be performed periodically on all helicopters. Due to the high cost of fuel, maintenance time, and aircraft unavailability, improvements are sought to reduce the number of flights required to complete a MRS procedure. At the forefront of this effort is the creation of robust algorithms that calculate more accurate adjustment sets than today's linear algorithms. This study will quantify the major differences, if any, between a modern, non-parametric algorithm and traditional, linear algorithms.

II. Background

2.1 Introduction

Vibration is an inherent artifact of all machinery. Typically, in rotating machinery vibrations are often caused by a machine's rotating components having centers of mass that do not lie at the center of rotation. For rotating, aerodynamic components, vibrations can also be caused by non-uniform aerodynamic properties such as blade pitch or camber. In helicopters, vibrations can be quite powerful and lead to shortened component lives as well as crew fatigue. With non-aerodynamic components vibrations can be minimized using precise manufacturing techniques and mass balancing procedures. The rotating, aerodynamic components of the main rotor and tail rotor systems require that specialized vibration reduction procedures be performed. This research is focused on the largest contributor to aircraft vibrations: the main rotor system.

2.2 General Classification of Vibration

Vibrations are usually defined by the oscillatory motion of an object as given by equation (1) [4].

$$x(t) = A \cdot \cos(\omega t - \phi) \quad (1)$$

In this equation, A is the vibration amplitude, or maximum displacement of the object from its mean position, ω is the frequency of the oscillation and ϕ is the phase shift of the steady state response due to damping. In most MRS applications, the vibration displacement x is measured with one or more accelerometers mounted in specific locations on the aircraft.

The frequency of the vibration that MRS is concerned with is the same as that of main rotor system rotation. The phase lag is a product of the structural makeup of the aircraft and is dependent on the location from which vibrations are measured. Therefore, accelerometers must be mounted in the same location each time vibration data is recorded.

2.3 Classification of main rotor vibrations

The main rotor system produces vibrations that are quantified in a number of different ways. Typically, vibration is described as being a vertical vibration or a lateral vibration with respect to the helicopter frame of reference. The amplitude of the vibration is typically measured as velocity, in units of inches-per-second, or IPS. While equation (1) requires amplitude in terms of distance, here we are using amplitude to mean the total distance traveled by the accelerometer in one second. The terms amplitude and magnitude are often used interchangeably when referring to the strength of the vibration. The frequency of the vibration is typically a multiple of the main rotor's period. A 1/rev (pronounced 1-per-rev) vibration produces one vibration cycle for each revolution of the main rotor system. A 1/rev vibration is typically brought about by mass and/or aerodynamic asymmetries in the main rotor system. An n /rev vibration produces n cycles per revolution, where n is the number of blades on the main rotor system. While both types of vibrations are of great importance to helicopter users and designers, only the 1/rev vibrations shall be considered in this study.

In order to further categorize a vibration, a quantity known as phase angle is assigned to the location of peak amplitude. Phase angle is measured from an aircraft specific origin, such as the nose or tail of the aircraft, with increasing phase opposite the direction of main rotor rotation. Test equipment is used to record vertical and lateral vibration amplitude as well as the main rotor angular position. The vibration's peak amplitude is matched with angular position of the main rotor such that a vibration map (see Figure 1) can be plotted with respect to the stationary main rotor. This is particularly useful in determining the corrective action to take in response to vibrations.

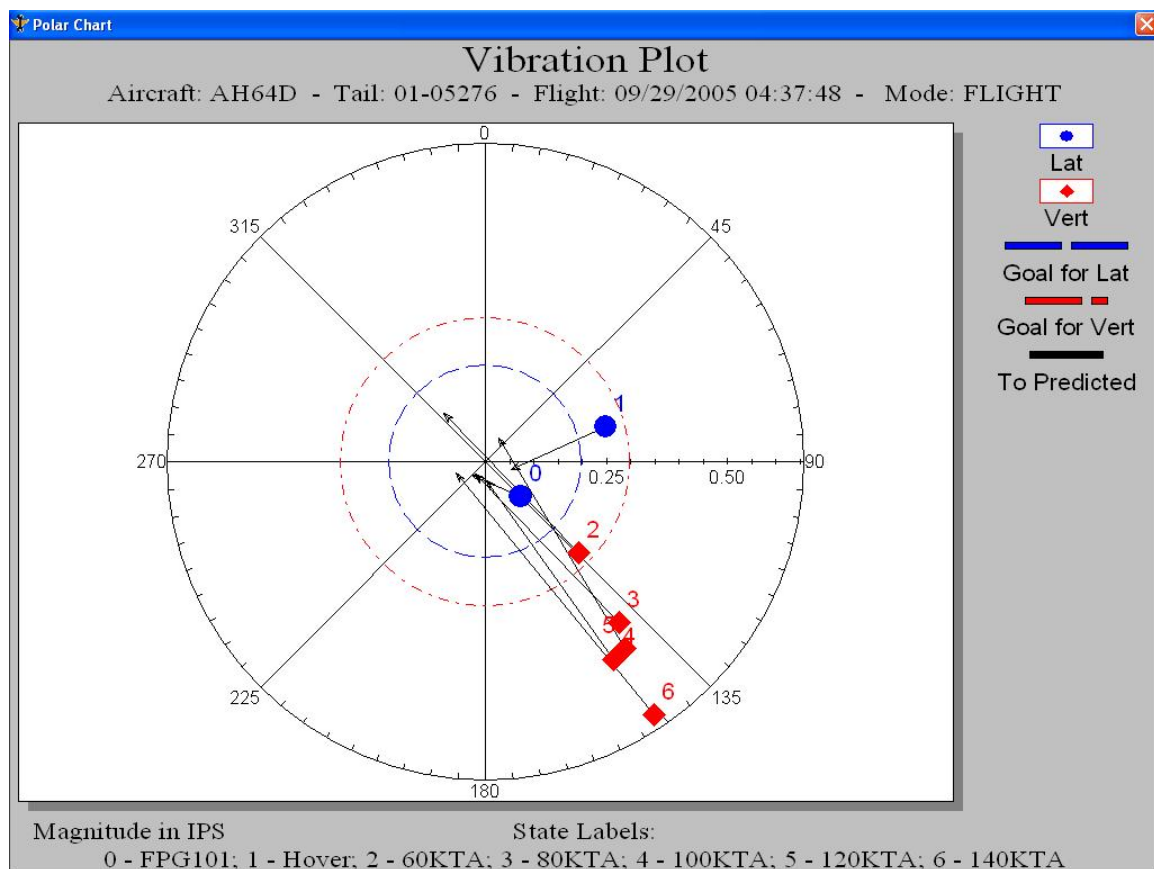


Figure 1. Polar Chart of AH-64D vibrations from PC-GBS. The arrows indicate predicted vibrations following corrective adjustments.

2.4 Flight Conditions for Vibration Measurement

Now that we can quantify a helicopter vibration in terms of direction, magnitude, and phase, we must assign a flight condition at which the vibration should be measured. Typically, a helicopter's vibration characteristics are measured at several specific flight states ranging from on the ground with flat blade pitch at 100% RPM (FPG-100) to maximum level speed (or close to it). Table 1 shows the flight states at which vibration measurements are recorded for two types of helicopter. The quantity of flight states is carefully chosen so as to give a good representation of an aircraft's vibration signature while minimizing the duration of the test flight.

Table 1. Vibration Measurement Flight Conditions

UH-60	AH-64
FPG-100	FPG-100
Hover	Hover
80 Knots	60 Knots
120 Knots	80 Knots
145 Knots	100 Knots
	120 Knots
	140 Knots

2.5 Types of Main Rotor Adjustments

With a clear understanding of what defines a main rotor vibration, it is now important to determine what form the corrective actions should take. In determining this we examine a few of the phenomena that could be responsible for main rotor vibrations. Like any rotating component, the main rotor system could suffer from a mass imbalance. There is also the likelihood that the rotor blades are not aerodynamically identical resulting in non-uniform lift production on the rotor disk.

It is possible that blade stiffness varies from blade to blade allowing some blades to bend and twist more than others at equivalent aerodynamic loads. While this is not a complete list of causes for vibrations, it lends insight into the methods we may employ to help eliminate them. These methods shall include modifying the aerodynamic qualities of the blades as well as modifying their mass.

2.5.1 Adjustments for Mass Imbalance.

To correct for mass imbalances, weights can be added to or subtracted from individual rotor blades. Rotor blades may be balanced prior to installation using devices such as the Universal Static Balance Fixture shown in Figure 2. This piece of equipment allows one to ensure consistency with the spanwise center of mass of each rotor blade prior to installation. This balance technique is an important step in the overall MRS process as it greatly reduces the time spent balancing the mass of the main rotor system after blade installation.



Figure 2. Universal Static Balance Fixture. This piece of equipment is utilized to statically balance the spanwise moment prior to installation [5].

The only weight adjustment method being considered in this study is the addition of blade weights in response to flight test data. Figure 3 shows the rotor hub of an AH-64 Apache with blade weights installed. What follows is a brief explanation of why mass imbalances can occur in a main rotor system.



Figure 3. AH-64 Apache with blade weight installed [5]

2.5.2 Origin of a Mass Imbalance.

Mass imbalances can originate at the manufacturing level, evolve over time, or result from specific events. At the manufacturing level, main rotor system components are fabricated to meet specific engineering tolerances. The size of these tolerances must be small enough to satisfy the demands of the engineer, yet large enough for affordable mass production.

If large enough, which they usually are, these tolerances can lead to mass imbalances in the main rotor system, thus requiring weight adjustments.

Another cause for mass imbalance is that over time, blade erosion occurs due to countless impacts of the rotor blades with sand, dirt, and other debris. Blade erosion causes the rotor system to slowly lose weight. If one of the eroded blades is replaced with a new blade, a mass imbalance is likely to be introduced. Since most helicopter users do not change all of their blades at the same time, mass imbalances are almost sure to be introduced every time a blade is changed.

One final avenue for blade mass imbalance is from a specific event such as a blade repair. A blade repair usually consists of applying a small amount of patching material to the blade to mend a hole or crack. The addition of this material to the rotor blade not only increases the blade mass but also alters its center of moment, thus leading to an increased number of MRS iterations.

2.5.3 Aerodynamic Imbalances.

Aerodynamic imbalances may be created at the same time as mass imbalances. When rotor blades are fabricated, slight imperfections in blade shape cannot be avoided. Even if they were avoided, the overall shape of the blade would be changed by blade erosion during normal flight operations. These aerodynamic imbalances can be dealt with in a number of ways. One way is to change the angle of attack of the blade by adjusting the length of the pitch control rod (PCR). Another is to change the camber of the blade by bending trim tabs located on the blade trailing edge (see Figure 4). While PCR adjustments change the AOA of the entire blade, trim tab adjustments only affects the camber of the blade over the length of the trim tab.

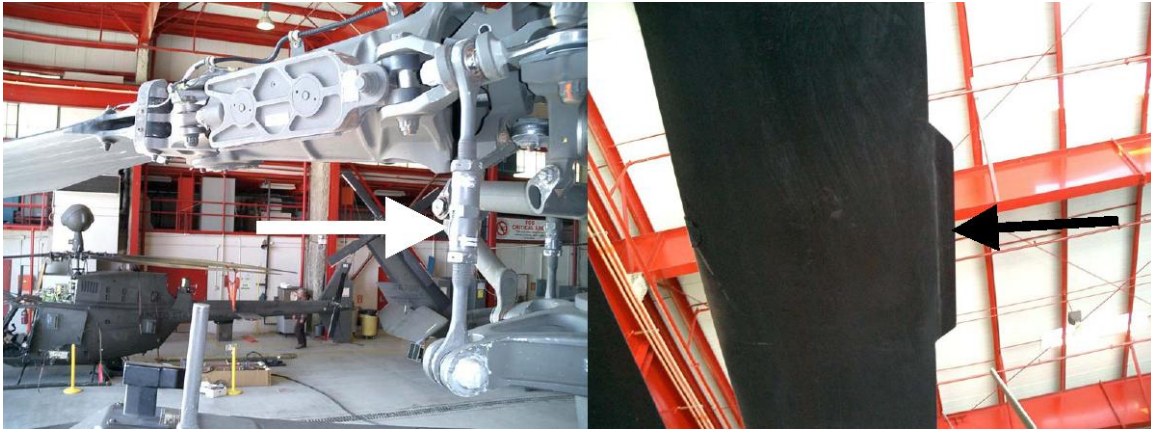


Figure 4. A PCR on a UH-60 (left) and a Trim Tab on an OH-58 [5]

2.6 Main Rotor Adjustment Fidelity

Now that we have discussed adjustment types, it is time to understand the limitations in fidelity of the adjustment sets. Every adjustment type has a minimum allowable magnitude that is set by the manufacturer. For instance, the blade weights may come in one ounce bars or the PCR may have a locking turnbuckle that allows for no less than $\frac{1}{4}$ turn of adjustment. An adjustment set with a higher degree of precision than this basic unit will be rounded off to the nearest basic unit.

There is also the fundamental principle that a calculated adjustment move may have a phase angle anywhere from $0-360^\circ$ but can only be applied on actual blade locations (0° , 90° , 180° , 270° in 4 bladed rotor systems). When an adjustment is calculated at a location between two blades, the adjustment must be divided between the two blades to produce an equivalent result. Most of the time a perfect division of the solution is impossible and more round off error is incurred.

2.7 History of Track and Balance [6,7]

Over the decades since the introduction of the helicopter, vibration reduction procedures have changed greatly. Prior to the incorporation of onboard vibration measuring equipment, rotor tracking was the limit of our capabilities for vibration reduction. Essentially, rotor tracking is an effort to make all rotor blades fly the same path, thus forming a flat rotor disk at 100% RPM. The principle is that the rotor blades are aerodynamically similar if they fly the same path. By incorporating this tracking procedure with a static blade balancing as discussed earlier in section 2.5.1, some vibration reduction is achieved. Unfortunately, early blade tracking techniques could only be accomplished using ground equipment, thus preventing measurements of aerodynamic differences at various flight speeds.

Later, onboard vibration recording equipment was developed and used in conjunction with onboard optical tracking equipment for in flight tracking and balancing of the rotor system. Highly skilled technicians analyzed the magnitude and phase of vibrations as well as track split data in order to determine appropriate adjustment sets for blade pitch, trim tabs, and blade weights. Again, this technique required a great deal of time and skill to accomplish.

Finally, with the advent of high speed digital computers, diagnostic equipment was created that could measure vibrations and blade track as well as calculate adjustment sets. This new equipment not only sped up the rotor smoothing process but also reduced the requisite skill level of the operator. For the past 20 years very little has changed in the overall concept of a main rotor smoothing.

Vibrations and rotor track are still measured in much the same way, albeit more accurately, and adjustments sets still consist of blade weight, pitch link, and trim tab corrections.

2.8 Linear Algorithms

One area that has seen great efforts for improvement in recent years is the computer software used to calculate adjustment sets. There have been efforts to improve this software not only through a more sophisticated user interface, but also through the algorithm that converts raw vibration and track data into useful adjustment sets. Two types of algorithms are being considered in this study. The first type is an algorithm in wide use today that is built on the same linear assumption used since computer automated track and balance began. The second is a state-of-the-art neural network algorithm that is being used by a select few units in the US Army.

2.8.1 The Aviation Vibration Analyzer.

The Aviation Vibration Analyzer (AVA) is a helicopter vibration measurement system that utilizes a linear algorithm in its main rotor smoothing software. That is, we assume that a linear relationship exists between an adjustment and the resulting change in vibration. While this greatly simplifies our calculations, there is the potential that this assumption may not be accurate and could lead to poor adjustment sets in environments where the rotor system behaves in a non-linear fashion.

2.8.2 The Linear Algorithm Defined.

By making the linear assumption, we are able to employ a relatively simple algebraic model to describe the cause and effect of adjustment sets on helicopter vibrations.

$$[C]_{N \times M} \cdot [Adj]_{M \times 1} = [\Delta Vib]_{N \times 1} \quad (2)$$

In Equation (2), $[C]$ is a sensitivity coefficient matrix that is specific to a type, model, and series of helicopter, $[Adj]$ is an adjustment set, and $[\Delta Vib]$ is the change in vibrations brought about by the adjustment set. N stands for the number of specific flight regimes over which data is collected (see Table 1), and M stands for the number of adjustment types (i.e., blade weight, pitch link, and trim tab). The concept of a linear algorithm can be better understood if we first know how the sensitivity coefficient matrix is determined. In doing so, we will look at the case of the UH-60.

2.8.3 Determining the Linear Sensitivity Coefficient Matrix.

A set of sensitivity coefficients for a helicopter is determined through a series of test flights. First, a baseline vibration set is recorded at the N flight conditions before any adjustments have been made. Next, a single adjustment move is applied to the main rotor system (e.g. adding a 5 oz weight to the yellow blade). The helicopter is then flown again at the N flight conditions and a new vibration set is recorded. After landing, the adjustment is removed and a different adjustment type is applied. This process is repeated until vibration responses for all adjustment types have been recorded. When complete, the C matrix is populated in accordance with equation (3).

$$C_{nm} = \frac{Vib_{after\ n} - Vib_{before\ n}}{Adj_m} \quad (3)$$

Typically, several coefficient matrices are combined together in a root-mean-square sense in order to determine a mean coefficient matrix. Due to several factors, such as electronic noise, weather, and differences between like airframes, the average coefficient matrix is only about 20% accurate, and in many cases, worse [3]. For this reason, it is very likely that several test flights will be required to adjust the main rotor system to an acceptable vibration level.

The resulting mean coefficient matrix used in MRS procedures is obtained by rearranging equation 1 and solving for the adjustment set. This is not easily done without the aid of a computer, due to the fact that the linear system typically contains more equations than unknowns. In the case of the AH-64D, there are five unknowns to solve for seven flight regimes. By incorporating a solution algorithm that minimizes the sum of the squares of predicted vibration magnitudes, the best overall adjustment set can be calculated.

2.9 Application of Adjustment Sets

Usually a main rotor smoothing algorithm is written to perform a majority of its calculations in the complex plane. In this fashion, a set of vibrations enters the algorithm and is first converted to a complex number using Equation (4).

$$Vib_{cmplx} = Mag \times [Cos(phase) + i \times Sin(phase)] \quad (4)$$

This complex vibration is then converted into a complex adjustment set as previously described. The complex adjustment set, referred to as a reduced adjustment set, must be implemented as real adjustments on individual blades. This is then called the detailed adjustment set. There is typically more than one detailed adjustment set that corresponds to a single reduced set. For instance, on four-bladed helicopters, a positive adjustment applied to one blade has an equivalent effect on vibration as a negative adjustment applied to the opposite blade (180° phase shift). The difference between applying one versus the other lies in the effect the adjustment has on the track split.

Since a small track split is desired, an additional algorithm is typically incorporated in MRS software to convert reduced adjustments to detailed adjustments while minimizing track split. Such an algorithm would incorporate track data collected with equipment such as the Universal Tracking Device (UDT) shown in Fig. 5. The UTD is an electro-optical device that is usually mounted on the exterior of the aircraft during MRS operations and is able to “see” the flight path of individual blades as they enter its field of view. In recent years it has been shown that track split is not a contributor to main rotor vibrations (post-ground balance) and is optimized mainly for aesthetics.



Figure 5. Universal Tracking Device mounted on a UH-60 [5]

2.10 The Linear Assumption Comes into Question

About a decade ago, Taitel et al[3] questioned the viability of the linear assumption in main rotor smoothing algorithms. It was postulated that the accuracy of the adjustment set might be compromised under certain conditions if higher order main rotor interactions were neglected. This could then result in MRS iterations that require multiple flights. Since multiple flights are typically required to perform a MRS, it was believed that the performance of MRS algorithms could be improved by including the higher order interactions. To this end, neural network architectures were applied to the main rotor smoothing problem. The premise behind this approach was to train neural networks using vibration data from multiple test flights such that the true mathematical relationship between 1/rev vibrations and main rotor adjustments could be learned.

2.11 The Artificial Neural Network Algorithm

In the late 1990's, Wroblewski, et al [2] designed and implemented a neural network based software system for use on the US Army's helicopter fleet. The neural networks were trained with data from approximately thirty test flights per type of helicopter. One of the drawbacks of neural networks is that they are unable to extrapolate the character of the solution space for vibration regimes in which they haven't been trained. Since thirty flights are insufficient to fully train a neural network, modeled data (linear and other) was also incorporated into the training process in order to fill gaps. The intent was that as more flights became available the neural network training could be updated, thus allowing the vibration/adjustment mappings to mature over time.

A neural network is essentially a non-linear algorithm that is able to make predictions based on a history of observations. Figure 6 is a schematic of a neural network undergoing training. What follows is a simplified explanation of how the network is trained to calculate MRS adjustments.

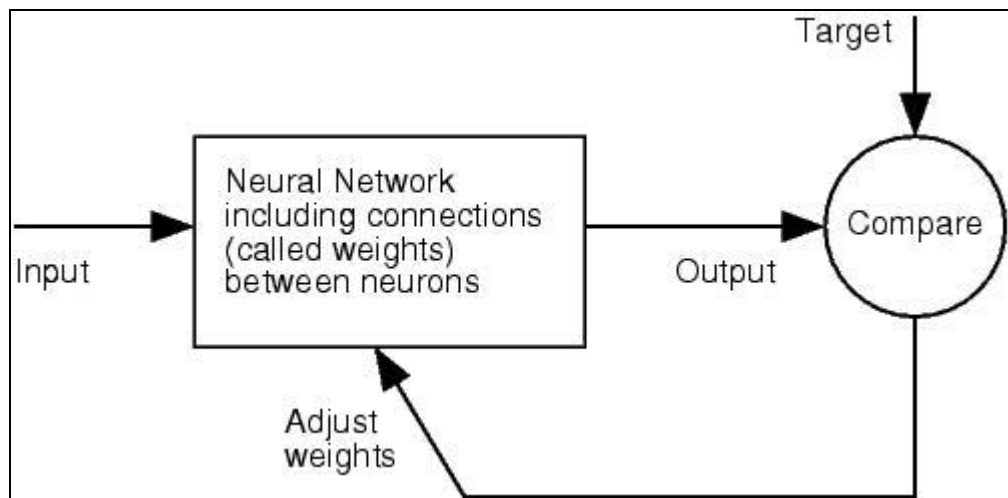


Figure 6. Schematic of Neural Network Undergoing Training [8]

The adjustment portion of the neural network is trained by first recording a baseline vibration set. An adjustment is then applied to the main rotor system and a second vibration set is recorded. The difference vector between the second vibration set and the baseline vibration set is passed through the neural network as the “Input” vibration vector in Fig. 6. A set number of weighted functions operate on the vibration vector to create an adjustment vector, or “Output”. The target value that the output adjustment set is compared to is the negative of the adjustment set that was applied prior to recording the second vibration vector. Based on the comparison, the weights within the neural network are adjusted until the output matches the target. This process is repeated with a variety of adjustment sets until the network is fully trained.

The appealing aspect of using a neural network for MRS procedures is that neural networks can be designed to recognize higher order relationships between adjustments and their vibration response. For this reasons, a properly trained neural network is believed to be capable of describing the relationship between vibrations and adjustments more accurately than a linear algorithm.

2.11.1 The PC-Ground Based System.

The neural network MRS algorithm that was considered in this study was that of the Vibration Management Enhancement Program’s PC-Ground Based System (PC-GBS). This algorithm was designed to work for the same flight regimes as AVA. In fact, vibration data collected with AVA equipment is able to be analyzed by the PC-GBS software. After vibration data has been entered, the default “Best Overall Solution” is calculated to reduce vibration magnitudes to as close to zero as possible in the fewest number of moves.

A secondary consideration for the PC-GBS is to apply the moves such that the main rotor track split is also reduced.

2.11.2 PC-GBS Solution Options.

The user may choose other solution options such as “Resolve to Vibration Limits”, “Limit Solution to x Number of Moves”, or create a “Manual Solution”. If the user chooses the option of “Resolve to Vibration Limits”, an adjustment solution is calculated that will reduce vibration magnitudes to within minimum acceptable limits with the fewest number of moves. If the user chooses “Limit Solution to x Number of Moves”, the number of adjustment moves will not exceed (but can be less than) the x number of moves. Finally, the experienced user may create a solution using a graphical user interface by selecting the “Manual Solution” option. In all cases, PC-GBS predicts the vibration levels and track split following application of the adjustment set.

2.11.3 The Neural Networks of PC-GBS.

The architecture used in the PC-GBS algorithm consists of four neural networks. These are the Adjustment Evaluation Networks (AEN), the Vibration Prediction Network (VPN), the Track Optimization Network (TON), and the Solution Optimization Expert (SOE) [1]. A vibration set passes through these networks, entering as a complex vibration vector and exiting as a set of specific adjustments with a corresponding vibration and track prediction. Each network performs a specific function that shall be described next.

The AEN is a set of networks that provide the mapping of the complex vibration vector to the corresponding complex adjustment space.

Several candidate adjustment sets are calculated and then passed into the VPN where they are mapped back to the vibration space in order to predict a vibration response. Next, the candidate adjustment sets are passed into the TON where they are converted from reduced adjustment sets into detailed adjustments for specific blades. This net incorporates track data from the UTD when converting the complex adjustments into real adjustments. Finally, the SOE reviews the candidate adjustment sets and chooses the best one, based on the predicted vibration levels, the number of actual corrective moves, and the predicted track split. This final selection network is trained through an analysis of real-life examples where the optimal solution was chosen by human experts [1].

2.11.4 PC-GBS Performance From an Earlier Study.

Wroblewski et al [1] discuss the initial results of the PC-GBS algorithm on the AH-64 Apache helicopter. They noted that 2-4 flights were typically required to smooth the rotor. It was not feasible to run parallel flight tests with AVA adjustments, so it was hard to say which algorithm was superior; however, the adjustment solutions were compared between the two algorithms. The neural network consistently offered solutions with fewer numbers of moves and lower predicted vibrations than those of the linear algorithm. This alone represents a noteworthy improvement of the neural network over the linear algorithm.

2.12 Chapter Summary

The problem of main rotor smoothing has long been an expensive challenge in the helicopter industry. Over the years, many improvements have been made to reduce the number of flights required to smooth 1/rev vibrations to within acceptable levels. The most recent improvement, the artificial neural network, has shown potential in reducing the number of iterations (flights) involved in a typical smoothing process. While the core of the software is protected by proprietary rights, its analytical capabilities can be employed to characterize the main rotor solution space as it is known to the trained neural networks.

III. Methodology

3.1 Introduction

The primary goal of this study was to gain insight into a main rotor system's mathematical nature by extracting vibration/adjustment relationships from trained neural networks. By comparing a large population of flight data over a broad spectrum of conditions, characteristics of the main rotor solution space, as learned by the neural network, may be identified.

3.2 Origin of Research Data

Comparisons were made for three different aircraft; the AH-64A Apache, AH-64D Longbow, and UH-60 Blackhawk. Each of these helicopters has a distinct set of trained neural networks contained in the PC-GBS software, as well as its own set of linear sensitivity coefficients. For the purposes of this study, the coefficients from the Aviation Vibration Analyzer system were used (Appendix A). Flight test data from multiple flights of each type of aircraft was compiled in several Microsoft Excel databases (Appendices B, C, D) and was evaluated using Matlab. The flight data utilized in this research was downloaded from an online VMEP database compiled by Intelligent Automation Corporation (IAC) and was evaluated using PC-GBS version 3.0 Build 439 Service Pack 2. For each flight, an Excel database entry was made consisting of vibration vectors (magnitude and phase), predicted vibration vectors, and detailed adjustment values. The data were recorded directly from the Vibration tab (Fig. 7) and the Rotor Smoothing Solution tab (Fig. 8) of the PC-GBS.

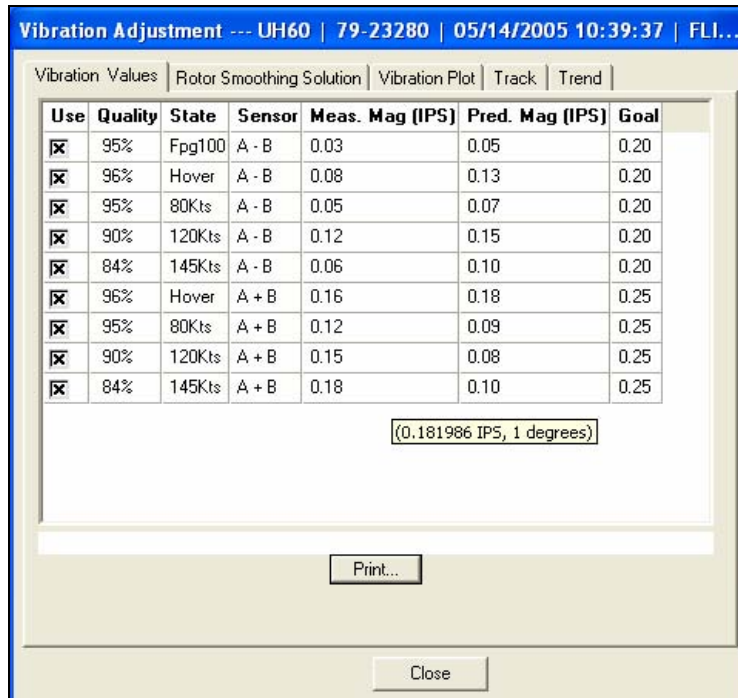


Figure 7. Vibration Values Tab of PC-GBS. Predicted vibration values in this figure correspond to adjustment values of Fig. 8.

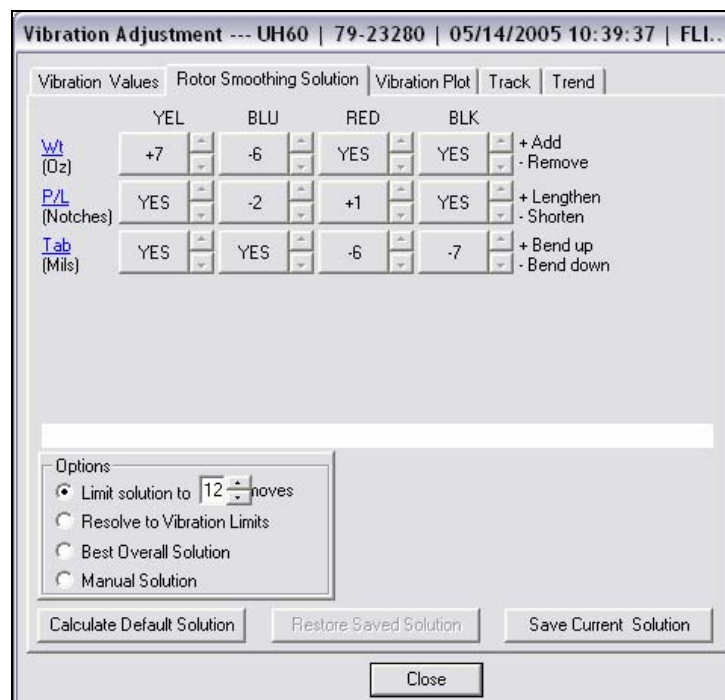


Figure 8. Rotor Smoothing Solution Tab of PC-GBS

3.3 Data Acquisition Techniques

Before proceeding further, it is important to understand the method used to extract data from the PC-GBS. There are four neural networks contained within the PC-GBS. These are the AEN, the VPN, the TON, and the SOE. Of these four networks, only the AEN and the VPN have learned the relationship between main rotor adjustments and vibrations. The effects of the other two networks must therefore be removed from the data in order to obtain a clear picture of the main rotor solution space.

3.3.1 Removing the Effects of the Solution Optimization Expert.

The purpose of the SOE is to choose from an array of possible adjustment sets in accordance with training it received from human experts. The intent of this training was to teach the SOE to offer a solution with the minimum acceptable number of moves. Figures 7 and 8 show the adjustment set and predicted vibration vector when the *maximum* number of moves have been requested. Note that the adjustment set consists of six adjustment moves. Had the “Best Overall Solution” been used, the adjustment set would have been a single move of +1 notch on the yellow pitch link. The selection of this single adjustment move was determined by the SOE. This is obviously a superior adjustment set from the mechanic’s point of view, because it reduces the time to implement adjustments as well as reduces the possibility of making a mistake. The tradeoff for this simpler solution is slightly higher (but still favorable) predicted vibration magnitudes and track split. While the SOE is an incredibly important contributor to the PC-GBS’s performance, for the purposes of this study it only serves to mask our understanding of the AEN.

The SOE was effectively turned off by calculating adjustment sets using the option of *Limit Solution to X Moves* where X was set to the maximum number; as shown in Fig.8. For the AH-64 and UH-60, X was set to 20 and 12 respectively. This number was determined for the UH-60 by multiplying the three adjustment types over the four blades, and for the AH-64 by multiplying the five adjustment types over the four blades. By allowing the maximum number of moves, PC-GBS produces the most highly detailed adjustment set attainable from the AEN. Since maximizing the number of moves is the antithesis of the SOE, it is believed that this procedure effectively disables it.

3.3.2 Removing the Effects of the TON.

Unlike the AEN, the TON is concerned primarily with minimizing the main rotor track split. When a reduced adjustment set is calculated by the AEN, the adjustment magnitudes are all positive numbers with associated phase angles. One could apply this reduced adjustment set to the main rotor system as given, thus resulting in a beneficial change in the main rotor vibration vector. One could just as well apply the negative of the adjustment magnitude at a 180 degree phase shift and achieve the exact same change in the vibration vector. The difference between applying the positive versus the negative adjustment magnitude lies in the effect it has on the main rotor track. One of the purposes of the Track Optimization Network is to determine which adjustment moves to keep as positive magnitudes and which to make negative magnitudes in order to minimize the main rotor track split. The TON makes this determination as it converts a reduced adjustment set to a detailed adjustment set on actual rotor blades.

The method that was used in this study to convert the detailed PC-GBS adjustment sets into reduced adjustment sets automatically converted all magnitudes back to positive values. The next section provides a thorough explanation of this conversion process.

3.3.3 Converting Detailed Adjustment Sets into Reduced Adjustment Vectors.

As discussed earlier, vibration vectors were converted from real vectors to complex vectors in accordance with equation (4), repeated here for convenience.

$$Vib_{cmplx} = Mag \times [Cos(phase) + i \times Sin(phase)] \quad (4)$$

The detailed adjustment sets were converted to complex numbers in much the same way. In the case of the UH-60, equation (5) was used.

$$Adj_{cmplx} = AdjMag \times [Cos(BladePhase - 90) - i \times Sin(BladePhase - 90)] \quad (5)$$

Here, the value for *BladePhase* can only take on values of 0°, 90°, 180°, or 270°, as these are the respective phase angles associated with the black, yellow, blue, and red blades. The value for *AdjMag* is the magnitude of the adjustment move on the blade being considered. Figure 9 shows the top down view of a UH-60 Blackhawk with appropriate phase values assigned to each blade.

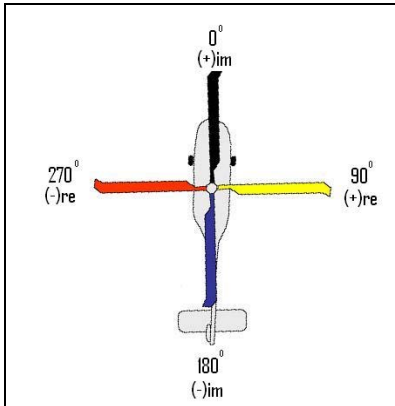


Figure 9. UH-60 Blackhawk Blade Map.

For the UH-60, the Matlab code in Appendix E converts the magnitude of the detailed adjustment on the given blade to a positive or negative, real or imaginary number in accordance with Figure 9 and Equation 5. The complex numbers for each adjustment type (weight, pitch link, trim tab) were then summed, thus producing a single complex number for each adjustment type. This complex adjustment vector was then converted back into real values of magnitude and phase. Table 2 contains sample calculations for two different sets of pitch link adjustments. These two sets of adjustments represent the same reduced adjustment vector, thus emphasizing the fact that the effects of the TON can be removed from the analysis. A similar mapping can be demonstrated for the AH-64A/D adjustments.

Table 2. Sample Calculation. Conversion of UH-60 Pitch Link adjustments into a Reduced Adjustment Vector.

Adjustment Set 1				
Blade Color	Yellow	Blue	Red	Black
Pitch Move	2	1	1	2
Complex Value	2	-i	-1	2i
Complex Vector	1 + i			
Real Vector	Mag: 1.4142		Phase: 45 degrees	
Adjustment Set 2				
Blade Color	Yellow	Blue	Red	Black
Pitch Move	-1	-2	-2	-1
Complex Value	-1	2i	2	-i
Complex Vector	1 + i			
Real Vector	Mag: 1.4142		Phase: 45 degrees	

3.4 Overview of Analysis Methods

With the effects of the TON and SOE effectively removed from the data, the full capabilities of the AEN and VPN could be analyzed. Two methods were used to extract information from the Adjustment Evaluation Networks and the Vibration Prediction Network.

The first method used a graphical and statistical comparison of the reduced adjustment sets of PC-GBS to the reduced adjustment sets of a linear algorithm based on the AVA sensitivity coefficients. The second method also relied heavily on graphical and statistical comparisons; however, the comparisons were made with multiple sets of *ad hoc* linear sensitivity coefficients derived from the PC-GBS. Both methods were applied to databases representative of the full spectrum of vibration regimes.

3.5 Explanation of Vibration Ranges

The comparison of the neural network algorithm and the linear algorithm was carried out for multiple flights in each of the four vibration categories, Good, Above Goal, Caution, and Exceed. A vibration category is assigned to each flight based on the highest vibration magnitude encountered during the flight. Table 3 shows the vibration magnitude ranges associated with each category by type of aircraft. By analyzing the full spectrum of vibration categories, non-linear effects associated with vibration magnitude should be revealed.

Table 3. Vibration Magnitude Ranges by Category

Category	UH-60	AH-64A/D
Good Vert (Lat)	0.0 – 0.25 (0.0 - 0.2)	0.0 – 0.3 (0.0 - 0.2)
Above Vert (Lat)	0.25 – 0.5 (0.2 - 0.5)	0.3 – 0.5 (0.2 - 0.5)
Caution Vert (Lat)	0.5 – 0.8 (0.5 - 0.8)	0.5 – 0.8 (0.5 - 0.8)
Exceed Vert (Lat)	0.8+ (0.8+)	0.8+ (0.8+)

3.6 Calculating the AVA Adjustment Set

The Matlab codes of Appendices E, F, and G were used to calculate reduced AVA adjustments for the UH-60, AH-64A, and AH-64D respectively, using equation (6).

$$[Adj]_{M \times 1} = [C]_{N \times M} \setminus [\Delta Vib]_{N \times 1} \quad (6)$$

In this equation, the adjustment set produces the vibration response, ΔVib , when applied to the main rotor system. Since we wish to zero out our measured vibrations, the ΔVib in equation (6) is set to the negative value of our measured vibration vector.

The C matrix is comprised of the AVA sensitivity coefficients from Appendix A. Since Equation (6) is overdetermined (more equations than unknown), the Matlab Left Divide operation, \backslash , essentially solves Equation (7) where ε is a vector that, when added to ΔVib , satisfies the equality.

$$[Adj]_{M \times 1} = [C]_{N \times M} \backslash ([\Delta Vib]_{N \times 1} + [\varepsilon]_{N \times 1}) \quad (7)$$

The value for ε is calculated such that the sum of the squares of its magnitudes is minimized. This value for ε may be viewed as a predicted vibration vector following application of the Adj vector; however, it corresponds to a reduced adjustment set that has not been distributed to actual rotor blades. Due to round off error associated with mechanical limitations, i.e. weight adjustments in whole ounce increments, the predicted vibration vector will change after a detailed adjustment set has been determined.

3.7 The Ad Hoc Sensitivity Coefficient Method

The second method used in this study offered a good deal more insight into the neural network's mathematical nature than the first method. In the second method, an ad hoc sensitivity coefficient matrix was created for each flight by using the PC-GBS as an adjustment/vibration simulator. This method not only allowed for a straightforward comparison of the ad hoc coefficients to those of AVA, but also to ad hoc coefficients of other flights. In this manner, specific flight regimes could be studied for signs of non-linearity.

3.7.1 Constructing the Ad-Hoc Sensitivity Coefficient Matrix.

The procedures for determining a set of linear sensitivity coefficients were discussed in detail in section 2.8.3. These same procedures were followed in order to determine the ad hoc sensitivity coefficients from PC-GBS. Equation (3), repeated here for convenience, shows the mathematical model used to determining each coefficient.

$$C_{n,m} = \frac{Vib_{after\ n} - Vib_{before\ n}}{Adj_m} \quad (3)$$

To determine the ad hoc coefficients, the PC-GBS was used to predict the vibration vector, $Vib_{after\ n}$, following the application of a single adjustment, Adj_m , to a flight with measured vibration, $Vib_{before\ n}$. This process was repeated for each adjustment type in order to populate the ad hoc sensitivity matrix for each flight.

3.8 Database Entries

Table 4 shows an example of a database entry for a single UH-60 flight. The AVA comparison method uses the measured vibrations, the detailed adjustment set, and their corresponding predicted vibrations. The ad hoc coefficient method uses additional vibration predictions based on application of single adjustment moves to single blades using the Manual Solution option. In the case of Table 4, the smallest allowable adjustment moves were used with PC-GBS to produce the ad hoc predictions.

For each flight, a second database was created using the largest allowable adjustment moves. Table 5 indicates the smallest and largest allowable moves for each aircraft considered in this study. The reasoning behind comparing ad hoc coefficient matrices based on small versus large adjustment moves was to discover non-linearity as a function of adjustment magnitude.

Table 4. Typical database entry for the UH-60 Blackhawk. Magnitude is in IPS. Weight (Wt) is in ounces, Pitch Links (P/L) is in Flats, and Tab is in Mils. Data entered by hand.

Batch 1	Measured Vib		Detailed Adj		Ad Hoc Prediction			Ad Hoc Prediction			Ad Hoc Prediction		
	Before Mag	Before Phase	Pred Mag	Pred Phase	Yellow Wt	After Mag	After Phase	Yellow P/L	After Mag	After Phase	Yellow Tab	After Mag	After Phase
Fpg100 A-B	0.032707	247	0.0197	85	5	0.069268	307	1	0.051184	152	2	0.041347	198
Hover A-B	0.083903	82	0.01359	322		0.065411	85		0.1288	108		0.096912	91
80Kt A-B	0.045817	167	0.047175	220		0.048443	188		0.067723	147		0.051565	155
120Kt A-B	0.121328	70	0.072691	59		0.103722	71		0.149222	85		0.132964	76
145Kt A-B	0.064676	79	0.02042	143		0.047172	84		0.100951	102		0.075388	91
Hover A+B	0.164067	274	0.156546	268		0.164286	274		0.177728	274		0.172191	272
80Kt A+B	0.117083	323	0.074428	285		0.116287	323		0.091119	303		0.100755	307
120Kt A+B	0.149976	349	0.008687	244		0.147891	349		0.080251	342		0.096581	336
145Kt A+B	0.181986	1	0.087178	108		0.179131	1		0.097419	360		0.097789	354
	Yellow			Blue			Red			Black			
	Wt	P/L	Tab	Wt	P/L	Tab	Wt	P/L	Tab	Wt	P/L	Tab	
Detailed	7	0	0	-6	-2	0	0	1	-6	0	0	-7	

Table 5. Adjustment Move Sizes used to determine the ad hoc coefficients.

	UH-60	UH-60	AH-64	AH-64
Weight	5 oz	80 oz	113 grams	1017 grams
Pitch Link	1 Notch	30 Notches	0.5 flats	12 flats
Trim Tab	2 Mils	20 Mils	0.5 degrees	5 degrees

3.9 Chapter Summary

The purpose of this study was to search for non-linear relationships, as learned by a trained neural network, between main rotor adjustments and their resulting change in vibrations. This comparison was made, in part, with the use of a linear algorithm based on the AVA sensitivity coefficients of each aircraft.

Comparisons were made over a broad spectrum of measured vibration amplitudes in an effort to discover whether the shape of the adjustment mapping changes due to the roughness or smoothness of the test flight. The ad hoc coefficient matrices were constructed using both small and large adjustment moves in an effort to discover non-linear effects based on adjustment amplitude. By using these two approaches, the two avenues for non-linear effects have been rigorously explored and any non-linear effects should reveal themselves in the graphical and statistical analysis.

IV. Analysis and Results

4.1 Introduction

The Blackhawk, Apache, and Longbow were studied over a broad spectrum of vibration and adjustment magnitudes. A solid picture has been developed as to how the PC-GBS converts measured vibration vectors into adjustment vectors. Using graphical and statistical analysis, the objectives of this thesis have been met.

4.2 Comparison of PC-GBS Adjustments to AVA Adjustments

A linear algorithm was created for each aircraft based on the sensitivity coefficients of the US Army's Aviation Vibration Analyzer. Figure 10 is a bar chart of the 20 UH-60 flights included in this study. The height of each bar represents the magnitude of the difference between reduced adjustment vectors as determined by the AVA algorithm and the PC-GBS algorithm. Differences that do not exceed the basic adjustment unit are considered to represent identical adjustment calculations.

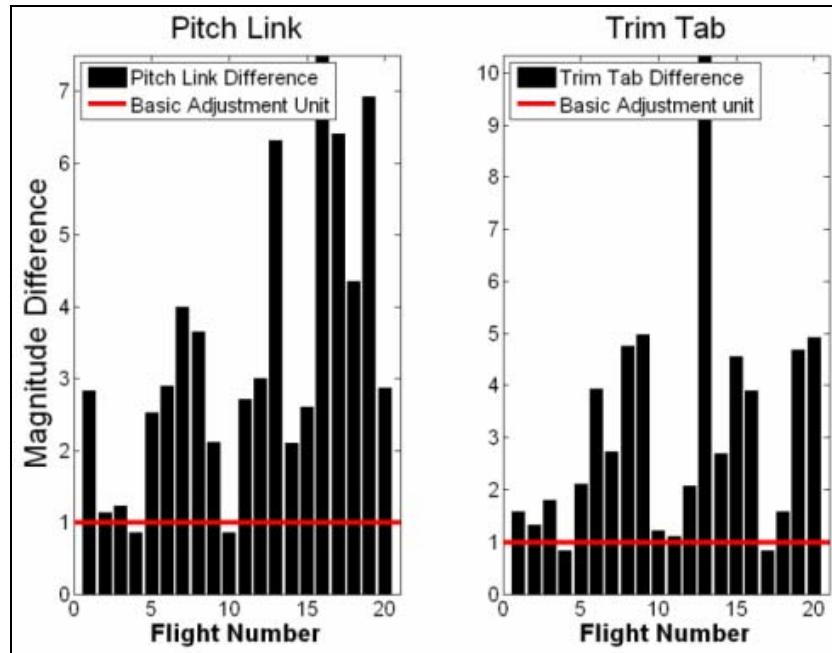


Figure 10. UH-60 Bar Chart Comparison of AVA to PC-GBS. This figure shows the difference between PC-GBS adjustments and AVA adjustments.

Only the Pitch Link and Trim Tab adjustment differences are depicted in Figure 10 as AVA does not produce weight adjustments based on flight data for the UH-60. It is obvious that the amount of difference between the two adjustment sets is significant. These differences were calculated by measuring the length of the vector separating an individual AVA solution from its counterpart PC-GBS solution. These quantities are graphically depicted in Figure 11.

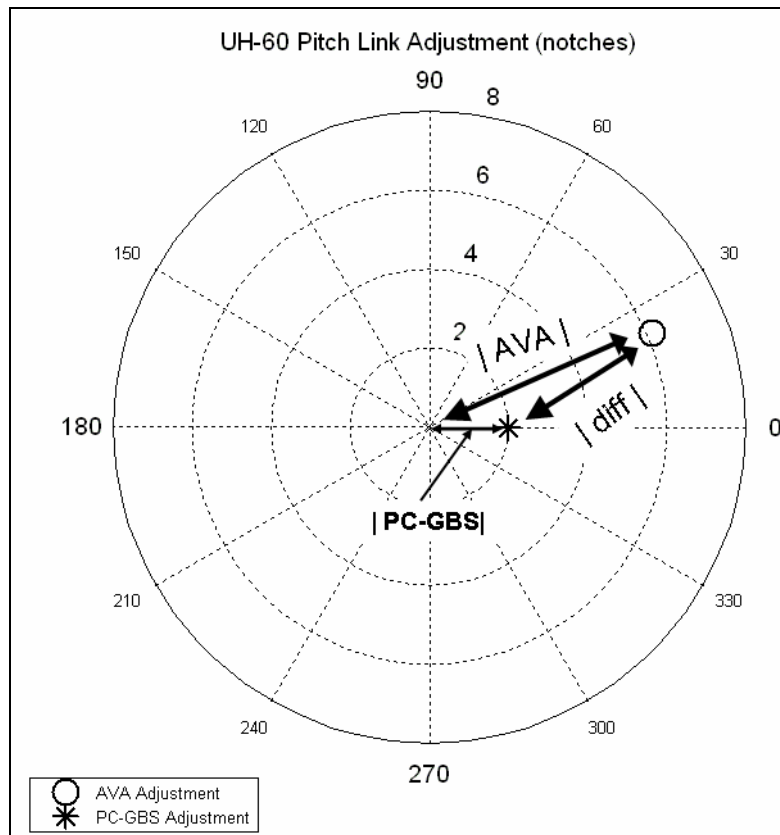


Figure 11. Graphical Depiction of Vector Difference.

Figure 12 shows the magnitude differences between the AH-64A adjustment sets. Again, for the twenty flights considered, the differences between the neural network solution and the AVA solution are often large. This does not imply that a non-linear mapping exists in the PC-GBS. It only means that AVA and PC-GBS produce very different adjustments for the same vibration vector.

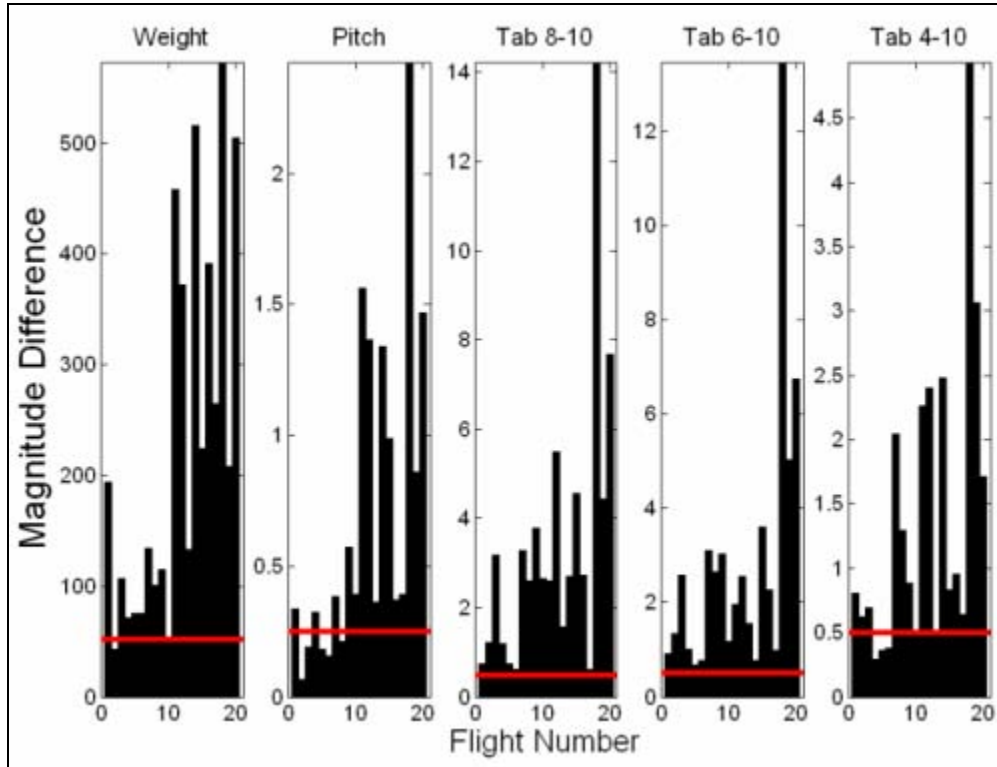


Figure 12. AH-64A Bar Chart Comparison of AVA to PC-GBS. This figure shows the difference between PC-GBS adjustments and AVA adjustments.

Figure 13 shows the magnitude differences between the AH-64D adjustment sets. Unlike the previous comparisons, here the adjustment sets are identical. This indicates that the PC-GBS has learned a linear mapping for the AH-64D that is a near perfect match to the AVA coefficients. This simple analysis has helped to show the similarity of the two algorithms for one aircraft in this study; however, a different method was used to better understand the other two.

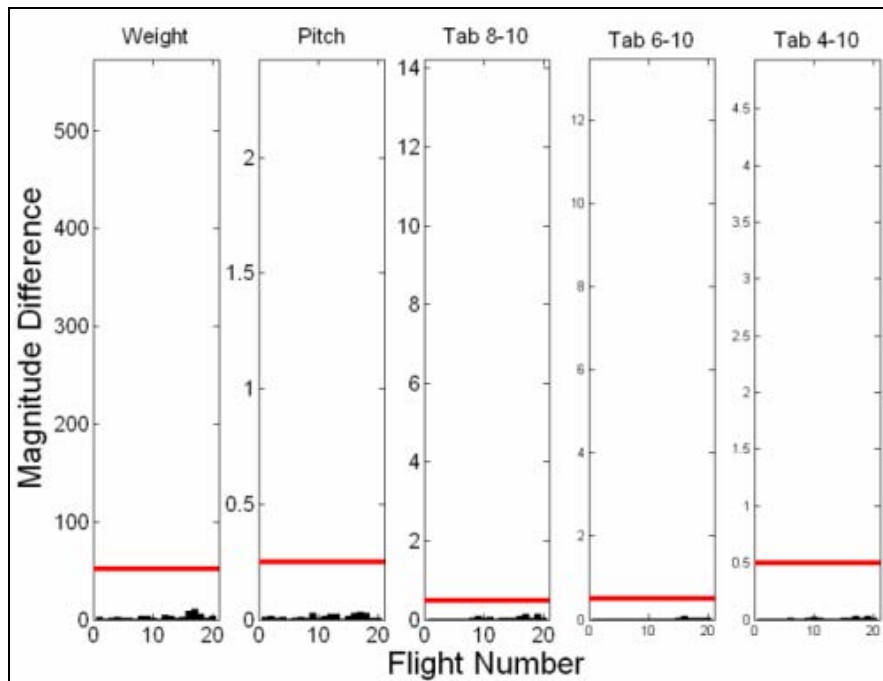


Figure 13. AH-64D Bar Chart Comparison of AVA to PC-GBS. This figure shows the difference between PC-GBS adjustments and AVA adjustments.

4.3 Ad Hoc Coefficient Method

In order to draw conclusions about the characteristics of the adjustment space for the UH-60 and the AH-64A, sets of ad hoc sensitivity coefficients were developed for every flight. These ad hoc coefficients were analogous to the AVA coefficients of Appendix A. These new coefficients were then used to calculate adjustment sets parallel to those of the PC-GBS for the 20 flights analyzed.

4.3.1 Small Moves Ad Hoc Coefficient Analysis.

Figure 14 is the polar plot of the UH-60 weight adjustment sets as determined by the ad hoc coefficients and the PC-GBS for all 20 flights. The ad hoc coefficients used in this set of analyses were developed using the smallest adjustment moves allowable.

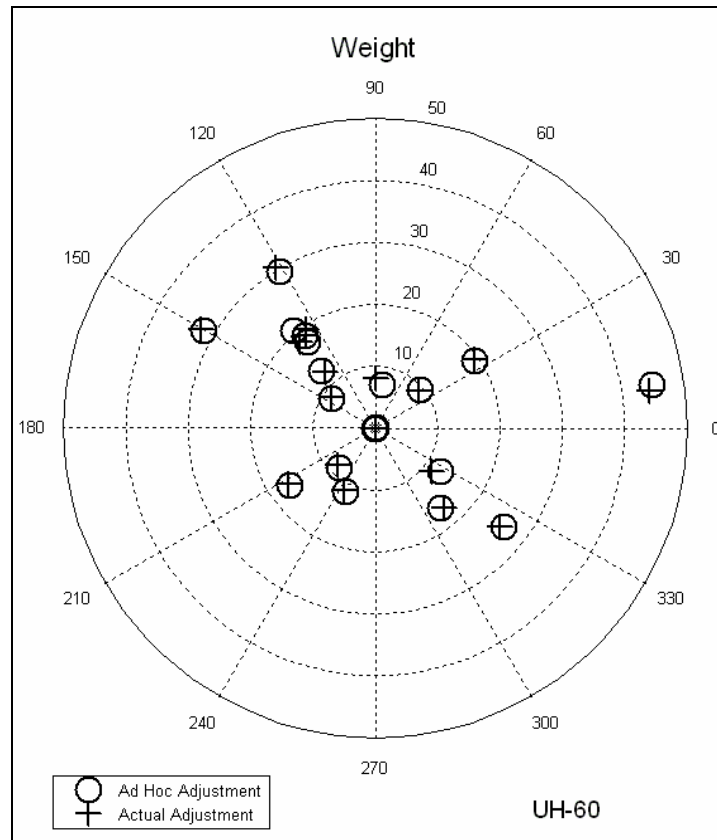


Figure 14. UH-60 Small Moves Ad Hoc Weight Adjustments. This chart represents 20 flights as calculated by the PC-GBS (+) and the small moves ad hoc sensitivity coefficients (O).

For the majority of flights, the + and O markings are on top of one another. This indicates that the adjustment sets as calculated by the ad hoc coefficients and the AEN are nearly identical. The largest magnitude difference between the PC-GBS weight adjustments and those of the ad hoc method is 2.178 oz.

Similar polar plots could be generated for the AH-64A and AH-64D; however, a more concise technique for observing similarities in parallel adjustment sets is to tabulate the largest magnitude of dissimilarity for each adjustment type (weight, pitch link, tab).

For every flight, a difference vector separating parallel adjustments was determined, as was shown in Fig 11. Table 6 contains the magnitude of the largest difference vector per adjustment type. As a reference, the table also contains the minimum adjustment unit that is mechanically allowable on the UH-60. Tables 7 and 8 contain similar information for the AH-64A and AH-64D.

Table 6. UH-60 Small Moves Ad Hoc Comparison. This table shows the largest difference between small moves ad hoc adjustment sets and PC-GBS adjustment sets.

UH-60	Weight	Pitch Link	Tab
Largest Adjustment Difference	2.178	1.253	4.699
Basic Adjustment Unit	1 oz	1 Notch	1 Mil

Table 7. AH-64A Small Moves Ad Hoc Comparison. This table shows the largest difference between small moves ad hoc adjustment sets and PC-GBS adjustment sets.

AH-64A	Weight	Pitch Link	Tab 8-10	Tab 6-10	Tab 4-10
Largest Adj Difference	43.78	0.417	0.960	0.838	0.471
Basic Adjustment Unit	52 grams	0.25 Flats	0.5 deg	0.5 deg	0.5 deg

Table 8. AH-64D Small Moves Ad Hoc Comparison. This table shows the largest difference between small moves ad hoc adjustment sets and PC-GBS adjustment sets.

AH-64D	Weight	Pitch Link	Tab 8-10	Tab 6-10	Tab 4-10
Largest Adj Difference	96.37	0.492	2.063	1.248	0.437
Basic Adjustment Unit	52 grams	0.25 Flats	0.5 deg	0.5 deg	0.5 deg

For all three aircraft, it is seen that the largest adjustment difference is usually greater than the basic adjustment unit. This indicates that the PC-GBS may, under certain circumstances, produce slightly different adjustment sets than the ad hoc linear coefficient algorithm.

Since the AH-64D has already been shown to behave like AVA, yet still has magnitude differences exceeding the minimum adjustment unit, the values noted in these tables should not be interpreted as proof of non-linearity in the AEN or VPN of PC-GBS.

4.3.2 Method of Root Mean Squares of the Small Moves Ad Hoc Coefficients.

During the course of this analysis, it was observed that the ad hoc coefficient matrices were virtually identical from flight to flight. For each type aircraft, the ad hoc coefficient matrices were summed into a single root-mean-square (RMS) coefficient matrix. All flights for each aircraft were then re-evaluated using the respective single RMS matrix. Tables 9, 10, and 11 are analogous to Tables 6-8 in that they show the maximum difference encountered between the PC-GBS solution and the ad hoc RMS solution. Also contained in these tables are the largest differences between individual ad hoc coefficient adjustments and PC-GBS adjustments from tables 6-8.

Table 9. UH-60 Comparison for RMS of Small Moves Ad Hoc. This Table shows the largest difference between RMS of small moves ad hoc and PC-GBS adjustment sets.

UH-60 Small Moves	Weight	Pitch Link	Tab
Largest Individual Difference	2.178	1.253	4.699
Largest RMS Difference	1.402	0.475	1.166
Basic Adjustment Unit	1 oz	1 Notch	1 Mil

Table 10. AH-64A Comparison for RMS of Small Moves Ad Hoc. This Table shows the largest difference between RMS of small moves ad hoc and PC-GBS adjustment sets.

AH-64A Small Moves	Weight	Pitch Link	Tab 8-10	Tab 6-10	Tab 4-10
Largest Individual Difference	43.78	0.417	0.960	0.838	0.471
Largest RMS Difference	33.901	0.410	0.426	0.363	0.337
Basic Adjustment Unit	52 grams	0.25 Flats	0.5 deg	0.5 deg	0.5 deg

Table 11. AH-64D Comparison for RMS of Small Moves Ad Hoc. This Table shows the largest difference between RMS of small moves ad hoc and PC-GBS adjustment sets.

AH-64D Small Moves	Weight	Pitch Link	Tab 8-10	Tab 6-10	Tab 4-10
Largest Individual Difference	96.37	0.492	2.063	1.248	0.437
Largest RMS Difference	14.698	0.066	0.219	0.125	0.043
Basic Adjustment Unit	52 grams	0.25 Flats	0.5 deg	0.5 deg	0.5 deg

The most important thing to learn from studying these tables is that, for each type of helicopter, a single set of linear sensitivity coefficients is able to produce reduced adjustment sets that are virtually identical to those of the AEN of PC-GBS. This is proof that the AEN calculates reduced adjustment sets using a linear mapping. Table 12 offers the standard deviation of the difference between PC-GBS adjustments and those produced with the RMS of the large-move ad hoc method. The values in this table are less than the basic adjustment unit, thus proving that a majority of ad hoc adjustments are identical to those of the PC-GBS. Figure 15 is a similar polar plot to figure 14 except that the single RMS matrix of the small moves ad hoc coefficients was used to calculate parallel adjustments to those of PC-GBS.

Table 12. Standard Deviation of Differences of RMS of Small Moves Ad Hoc. This table shows standard deviation of the difference in adjustments as determined by the PC-GBS and the RMS of the small move ad hoc coefficients.

	Weight	Pitch Link	Trim Tab		
UH-60	0.342 oz	0.1 Notch	0.36 Mil		
	Weight	Pitch Link	Tab 8-10	Tab 6-10	Tab 4-10
AH-64A	7.86 g	0.10 Flats	0.12 deg	0.10 deg	0.08 deg
AH-64D	3.43 g	0.01 Flats	0.04 deg	0.03 deg	0.01 deg

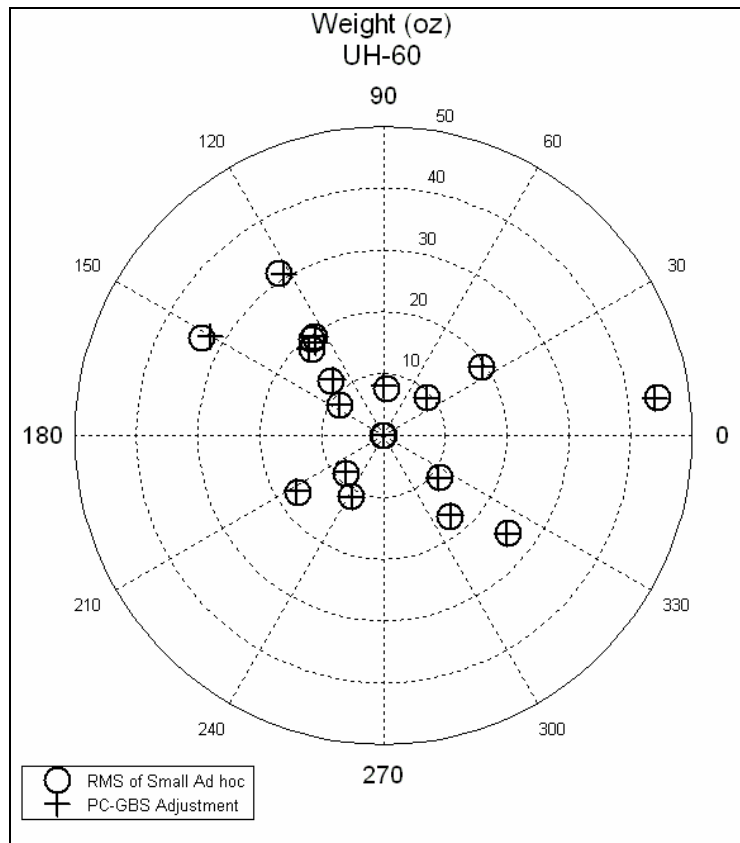


Figure 15. Polar Chart of UH-60 Weight Adjustments. This chart represents 20 flights as calculated by the PC-GBS (+) and the single RMS of the small moves ad hoc sensitivity coefficients (O).

The preceding analysis included an equal distribution of flights from each of the four vibration categories. The results of that analysis showed a high degree of linearity exists in the AEN and VPN networks regardless of measured vibration magnitude. The next section will address the effects of high magnitude adjustments on the VPN.

4.3.3 Large Moves Ad Hoc Coefficient Analysis.

In order to determine whether large adjustment magnitudes produce non-linear predictions from the VPN, a second set of ad hoc coefficients was created for each flight using the maximum allowable adjustment magnitude of Table 5.

It was believed that these new coefficients would produce different adjustment sets than the previous small move coefficients if any non-linear mappings had been learned by the VPN. As tables 13-15 show, this is not the case. Here are tabulated the largest magnitude of the difference vector between adjustments as determined by PC-GBS and the large-move-ad-hoc-coefficients. Also contained in these tables are the largest differences between individual ad hoc coefficient adjustments and PC-GBS adjustments.

Table 13. UH-60 Large Moves Ad Hoc Comparison. This Table shows the largest difference between large moves ad hoc and PC-GBS adjustment sets.

UH-60 Large Moves Ad Hoc	Weight	Pitch Link	Tab
Largest Individual Difference	1.069	0.392	0.394
Largest RMS Difference	0.779	0.393	0.523
Basic Adjustment Unit	1 oz	1 Notch	1 Mil

Table 14. AH-64A Large Moves Ad Hoc Comparison. This Table shows the largest difference between large moves ad hoc and PC-GBS adjustment sets.

AH-64A	Weight	Pitch Link	Tab 8-10	Tab 6-10	Tab 4-10
Largest Individual Difference	37.938	0.672	0.596	0.333	0.366
Largest RMS Difference	39.219	0.647	0.486	0.360	0.318
Basic Adjustment Unit	52 grams	0.25 Flats	0.5 deg	0.5 deg	0.5 deg

Table 15. AH-64D Large Moves Ad Hoc Comparison. This Table shows the largest difference between large moves ad hoc and PC-GBS adjustment sets.

AH-64D	Weight	Pitch Link	Tab 8-10	Tab 6-10	Tab 4-10
Largest Individual Difference	16.369	0.076	0.259	0.106	0.063
Largest RMS Difference	9.786	0.041	0.151	0.055	0.026
Basic Adjustment Unit	52 grams	0.25 Flats	0.5 deg	0.5 deg	0.5 deg

These tables show that for the UH-60 and the AH-64D, the respective RMS values of the large moves coefficients produced adjustment sets that were virtually identical to those of the PC-GBS. For the AH-64A, a comparison of Tables 14 and 7 reveal that the RMS of the small moves ad hoc coefficients actually provides a better match to adjustments of the PC-GBS.

Figures 16, 17, and 18 illustrate the magnitude difference between adjustments as calculated by the PC-GBS and the single RMS matrix of the appropriate ad hoc coefficients for the three helicopters.

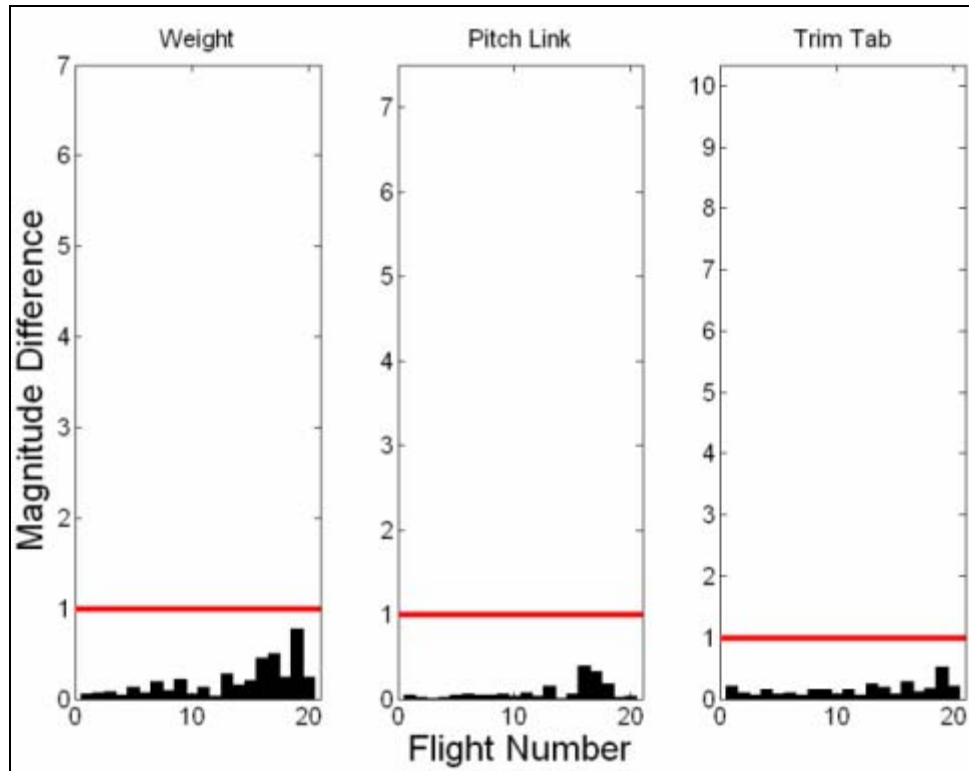


Figure 16. UH-60 Bar Chart Comparison of RMS of Large Moves to PC-GBS. This chart shows the magnitude difference between the PC-GBS adjustments and those based on the RMS of large move ad hoc coefficients. The red bar indicates the basic adjustment unit magnitude.

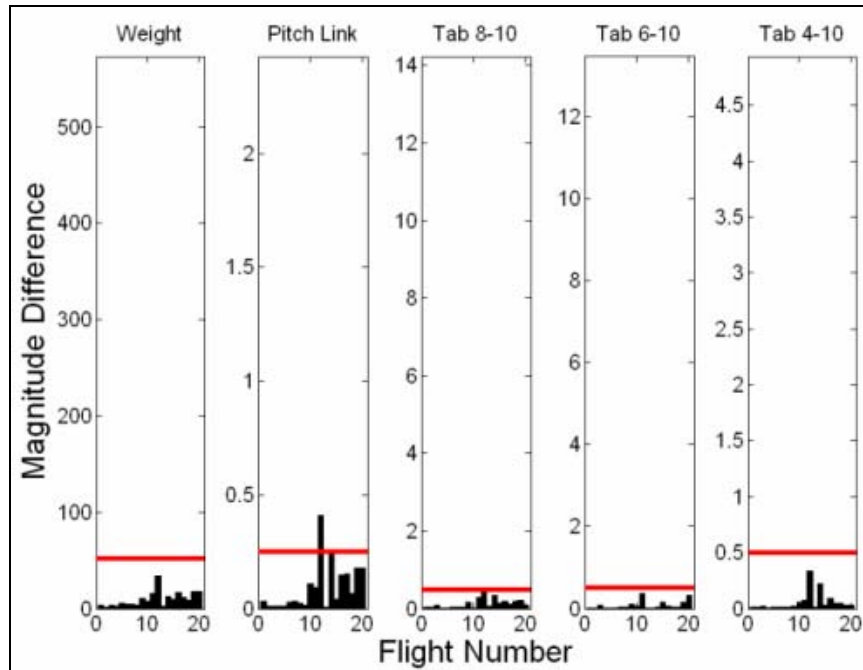


Figure 17. AH-64A Bar Chart Comparison of RMS of Small Moves to PC-GBS. This chart shows the magnitude difference between the PC-GBS adjustments and those based on the RMS of small move ad hoc coefficients. The red bar indicates the basic adjustment unit magnitude.

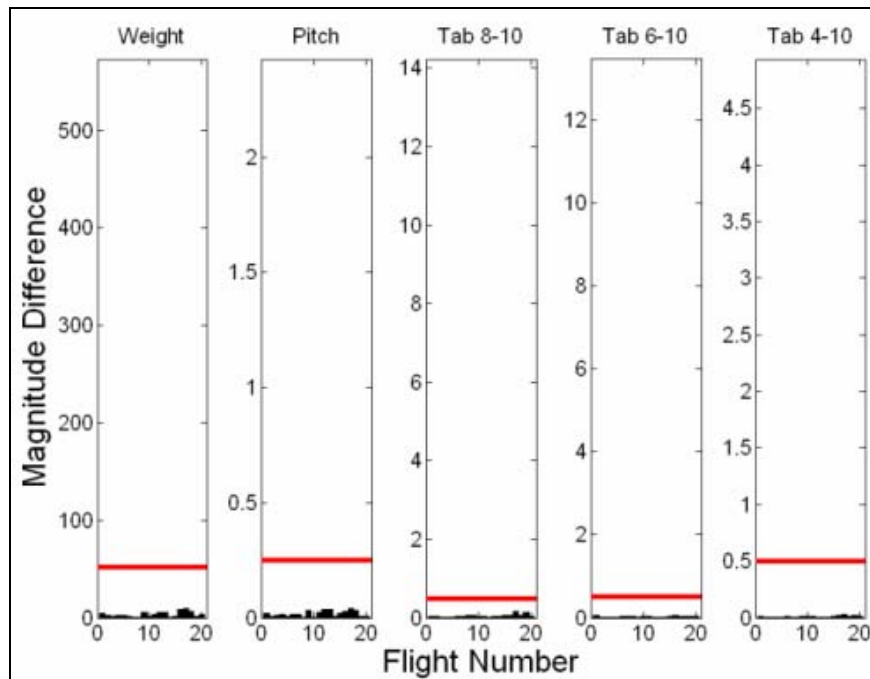


Figure 18. AH-64D Bar Chart Comparison of RMS of Large Moves to PC-GBS. This chart shows the magnitude difference between the PC-GBS adjustments and those based on the RMS of large move ad hoc coefficients. The red bar indicates the basic adjustment unit magnitude.

Figures 16-18 show that a single set of linear coefficients will almost always provide reduced adjustment sets that are identical to those calculated by the AEN. Table 16 contains the standard deviation of the difference between PC-GBS adjustments and those produced by the RMS of the appropriate ad hoc coefficients.

Table 16. Standard Deviation Between Ad Hoc RMS and PC-GBS Adjustments. This table shows standard deviation of the difference in adjustments as determined by the PC-GBS and the RMS of the indicated ad hoc coefficients.

	Weight	Pitch Link	Trim Tab		
UH-60 Large Moves RMS	0.187 oz	0.1 Notch	0.11 Mil		
	Weight	Pitch Link	Tab 8-10	Tab 6-10	Tab 4-10
AH-64A Small Moves RMS	7.86 g	0.10 Flats	0.12 deg	0.10 deg	0.08 deg
AH-64D Large Moves RMS	2.63 g	0.01 Flats	0.04 deg	0.02 deg	0.01 deg

These standard deviation values are all less than the size of the basic adjustment unit.

This means that a vast majority of the reduced adjustments, as calculated by this RMS method, will produce identical detailed adjustments to those of the PC-GBS.

4.3.4 Ad Hoc Sensitivity Coefficients as Determined By PC-GBS.

Tables 17, 18, and 19 contain the RMS values of the ad hoc sensitivity coefficients for the UH-60, AH-64A, and AH-64D as determined in this study. The coefficients for the UH-60 and the AH-64D were determined by taking the RMS of the large move ad hoc sensitivity coefficients. The coefficients for the AH-64A were determined by taking the RMS of the small moves ad hoc sensitivity coefficients. These coefficients may be encoded into a linear algorithm such as AVA in order to produce reduced adjustment sets that are virtually identical to those determined by the PC-GBS. Of course some form of post processing will be required in order to convert the reduced adjustment sets to detailed adjustment sets with the same performance capabilities as those of the PC-GBS.

Table 17. UH-60 Ad Hoc Sensitivity Coefficients. These coefficients were determined by taking the RMS of the large moves ad hoc coefficients.

	Weight		Pitch Link		Tab	
UH-60	Mag	Phase	Mag	Phase	Mag	Phase
FPG100(A-B)	0.012437	335.1	0.061253	119.9	0.014479	146.7
Hover(A-B)	0.003777	258.1	0.062257	140.9	0.008360	128.8
80Kts(A-B)	0.003672	261.0	0.027984	114.8	0.005148	99.7
80Kts(A+B)	0.000018	309.2	0.043495	187.9	0.016227	197.2
120Kts(A-B)	0.003595	250.2	0.042692	127.8	0.007671	116.6
120Kts(A+B)	0.000057	273.8	0.068672	176.9	0.028640	191.4
145Kts(A-B)	0.003700	249.2	0.046724	132.0	0.008472	139.5
145Kts(A+B)	0.000041	311.3	0.081355	182.9	0.040795	190.3
Hover(A+B)	0.000006	15.9	0.013415	278.9	0.004451	243.3

Table 18. AH-64A Ad Hoc Sensitivity Coefficients. These coefficients were determined by taking the RMS of the small moves ad hoc coefficients.

AH-64A	Weight	Pitch Link	Tab 8-10	Tab 6-10	Tab 4-10
Magnitude	ips/gram	ips/flat	ips/deg	ips/deg	ips/deg
FPG100(Lat)	0.000593	0.041779	0.000165	0.000139	0.000135
Hover(Lat)	0.000515	0.185371	0.028842	0.064399	0.104124
60Kt(Vert)	0.000358	0.030565	0.148199	0.250506	0.295098
80Kt(Vert)	0.000012	0.079075	0.334511	0.501796	0.751610
100Kt(Vert)	0.000009	0.129714	0.357461	0.546680	0.797509
120Kt(Vert)	0.000011	0.159954	0.440764	0.660609	0.969146
140Kt(Vert)	0.000018	0.235513	0.562146	0.824348	1.323498
Phase	deg	deg	deg	deg	deg
FPG100(Lat)	169.0	20.7	338.3	344.3	0.8
Hover(Lat)	166.4	54.7	71.1	61.6	51.3
60Kt(Vert)	224.9	220.0	247.9	246.0	259.4
80Kt(Vert)	44.0	268.5	251.5	264.2	262.3
100Kt(Vert)	101.2	267.4	261.6	256.1	260.3
120Kt(Vert)	42.5	248.6	252.5	256.0	260.2
140Kt(Vert)	22.9	246.1	243.6	249.8	238.2

Table 19. AH-64D Ad Hoc Sensitivity Coefficients. These coefficients were determined by taking the RMS of the large moves ad hoc coefficients.

AH-64D	Weight	Pitch Link	Tab 8-10	Tab 6-10	Tab 4-10
Magnitude	ips/gram	ips/flat	ips/deg	ips/deg	ips/deg
FPG101(Lat)	0.000491	0.044240	0.000000	0.000000	0.000000
Hover(Lat)	0.000456	0.155225	0.000000	0.000000	0.000000
60Kt(Vert)	0.000468	0.038996	0.159772	0.336765	0.647302
80Kt(Vert)	0.000452	0.063262	0.170617	0.287236	0.735197
100Kt(Vert)	0.000480	0.113166	0.187719	0.314955	0.655976
120Kt(Vert)	0.000451	0.180973	0.214903	0.372574	0.695178
140Kt(Vert)	0.000449	0.242108	0.305237	0.444347	0.903616
Phase	deg	deg	deg	deg	deg
FPG101(Lat)	163.0	15.5	165.9	165.9	165.9
Hover(Lat)	171.1	57.6	238.3	238.9	238.9
60Kt(Vert)	212.0	286.3	263.6	270.5	256.0
80Kt(Vert)	204.7	273.2	261.6	261.3	259.2
100Kt(Vert)	216.0	262.1	258.7	268.3	256.7
120Kt(Vert)	219.7	256.1	255.8	258.7	255.0
140Kt(Vert)	235.7	247.3	250.3	260.4	250.6

4.5 Chapter Summary

The Adjustment Evaluation Networks and the Vibration Prediction Network of the PC-GBS have been isolated and studied in detail. Graphical and statistical analyses have shown that in all vibration categories, the AEN calculates adjustment sets using a linear mapping. The prediction capabilities of the VPN have also been shown to behave in a purely linear fashion with respect to adjustment magnitude. This overall lack of non-linear behavior indicates that the neural networks of the PC-GBS have learned that a linear relationship exists between adjustments and vibration response, thus validating the linear assumption.

V. Conclusions and Recommendations

5.1 Chapter Overview

Due to the difficulty in making MRS adjustments on many helicopters, it was strongly believed that the linear assumption was flawed. For this reason, neural networks were used to determine a non-linear mapping of the solution space of main rotor vibrations in order to produce more accurate adjustments. This study has shown that the mapping of these networks is essentially linear. Therefore, the performance gains of the PC-GBS are not due to unique, non-linear mappings, but rather to accurate linear mappings and improved post-processing of the reduced adjustment sets.

5.2 Conclusions of Research

The goal of this study was to characterize the vibration/adjustment mapping as it is known to a trained neural network. This goal was achieved through analysis of the AEN and VPN in the PC-GBS. By studying multiple flights over a broad range of vibration and adjustment magnitudes, it was determined that the PC-GBS mappings can almost always be described accurately with linear sensitivity coefficients.

In a study conducted by Wroblewski et al [1], the PC-GBS algorithm outperformed the AVA algorithm by consistently producing adjustment sets for the AH-64 with fewer moves and lower predicted vibrations. It is now apparent that the success that the PC-GBS has enjoyed is not due to the inclusion of higher-order interactions in the vibration response, but rather to improved accuracy in a traditional linear mapping, the effects of the SOE, and other improvements.

The SOE has made large improvements in decreasing the chances of human error in main rotor smoothing iterations by selecting adjustment sets with minimal numbers of moves. While there is a slight tradeoff in predicted vibration levels, this is more than justified when these few adjustment moves are applied correctly the first time. Future rotor smoothing algorithms must also account for the human element in order to surpass the performance of the PC-GBS. Until the day that adjustment mechanisms are engineered to be error proof, mistakes will continue to reduce main rotor smoothing performance.

5.3 Significance of Research

Helicopter main rotor smoothing is an extremely expensive and time consuming task that must be periodically performed on all helicopters. Small improvements to the process have the potential to save millions of dollars annually. In recent years, efforts have been made to design non-linear algorithms for the task of main rotor smoothing. This research has shown that a set of non-linear neural networks have essentially learned that the vibration response is linear. Assuming that the neural networks in the PC-GBS are fully trained, the significance of this research is that the linear assumption is completely adequate for calculating adjustments. Software designers can safely continue to use the linear assumption and seek improvements to MRS performance elsewhere.

This research has also shown that a fair amount of disparity exists between the adjustments offered by the AVA algorithm and those of the PC-GBS, which is now known to be linear. Due to the improved performance that has been noted by Wroblewski et al, it is believed that the linear mapping of the PC-GBS is superior to that of AVA for the AH-64A and the UH-60. The mapping for the AH-64D is, of course, identical.

The US Army currently performs MRS procedures on these three aircraft with the Aviation Vibration Analyzer and, to a lesser extent, the PC-GBS. Until such time as the PC-GBS is used on all Army helicopters, the sensitivity coefficients that have been determined in this research are offered as a free upgrade to the AVA systems. An improvement in performance should be expected from incorporating these updated coefficients.

5.4 Recommendations for Action

One other area where the PC-GBS has shown great potential in improving MRS performance is the incorporation of the Solution Optimization Expert. The SOE improves the MRS process by selecting adjustment sets with minimal numbers of moves. This not only shortens maintenance time, but also minimizes the chances for error.

It is well known that human error is a common occurrence during adjustment application. For this reason, new adjustment mechanisms must be devised that reduce or eliminate the chances for mistakes. Something as simple as an engraved numbering scheme on the pitch links, much like on a micrometer, could virtually eliminate the chances of applying pitch adjustments in the wrong direction or on the wrong blade.

This research has shown that the linear assumption is still valid; however, linear algorithms must still be replaced. By their very nature, linear algorithms require that specific flight profiles be flown while vibration and track data are recorded. Pilot error can lead to poor data acquisition and therefore, poor adjustment sets. A rotor smoothing process that utilizes continuous vibration measurements could potentially alleviate the requirement of strict adherence to flight regimes. This type of system has been examined by Branhof et al [9] and has been determined to provide adjustments that improve vibration levels. Further efforts should be made to develop algorithms that do not require that specific flight profiles be flown while recording vibration data.

5.5 Summary

There are many improvements that still need to be made to the main rotor smoothing process. The ultimate goal is to one day have a system that can produce adjustment sets from a single set of flight data that will reduce any vibrations to within acceptable levels. This thesis has reported on one of the latest efforts in MRS algorithm modernization. While the use of neural networks in MRS applications has proven to be beneficial, the underlying method that the PC-GBS neural networks uses for mapping the solution space is not unique.

Appendix A: AVA Sensitivity Coefficients

UH60 Coefficients

adjustment = Hub Weight, Pitch Link, Trim Tabs
unit = Oz, Notches, Mils

Hover A - B

Coeff = {0.0 IPS/oz, 0 deg}, {0.046 IPS/notch, 147.3 deg}, {0.0162 IPS/mil, 146.7 deg}

80Kts A + B

Coeff = {0.0 IPS/oz, 0 deg}, {0.0410 IPS/notch, 196.2 deg}, {0.0296 IPS/mil, 196.2 deg}

80Kts A - B

Coeff = {0.0 IPS/oz, 0 deg}, {0.0289 IPS/notch, 126.7 deg}, {0.0105 IPS/mil, 122.4 deg}

120Kts A + B

Coeff = {0.0 IPS/oz, 0 deg}, {0.0516 IPS/notch, 189.6 deg}, {0.0413 IPS/mil, 191.7 deg}

120Kts A - B

Coeff = {0.0 IPS/oz, 0 deg}, {0.0369 IPS/notch, 138.0 deg}, {0.0113 IPS/mil, 136.7 deg}

145Kts A + B

Coeff = {0.0 IPS/oz, 0 deg}, {0.066 IPS/notch, 192.7 deg}, {0.053 IPS/mil, 192.0 deg}

145Kts A - B

Coeff = {0.0 IPS/oz, 0 deg}, {0.046 IPS/notch, 147.0 deg}, {0.018 IPS/mil, 139.0 deg}

AH64A Coefficients

adjustment = Hub Weight, Pitch Link, Tab 8-10, Tab 6-10, Tab 4-10
units = Grams, Flats, Degrees, Degrees, Degrees

FPG100 LAT

Coeff = {0.00033 IPS/gram, 165°}, {0.044 IPS/flat, 21°}, {0 IPS/°, 0°}, {0,0}, {0,0}

Hover LAT

Coeff = {0.00037 IPS/gram, 169°}, {0.143 IPS/flat, 51°}, {0 IPS/°, 0°}, {0,0}, {0,0}

60K VERT

Coeff = {0.000331 IPS/gram, 231°}, {0.054 IPS/flat, 274°}, {0.141 IPS/°, 255°}, {0.255 IPS/°, 246°}, {0.286 IPS/°, 273°}

80K VERT

Coeff = {0.000269 IPS/gram, 234°}, {0.062 IPS/flat, 283°}, {0.227 IPS/°, 267°}, {0.329 IPS/°, 260°}, {0.363 IPS/°, 270°}

100K VERT

Coeff = {0.000390 IPS/gram, 232°}, {0.106 IPS/flat, 265°}, {0.264 IPS/°, 269°}, {0.434 IPS/°, 260°}, {0.485 IPS/°, 273°}

120K VERT

Coeff = {0.000369 IPS/gram, 242°}, {0.156 IPS/flat, 240°}, {0.405 IPS/°, 262°}, {0.613 IPS/°, 253°}, {0.630 IPS/°, 266°}

140K VERT

Coeff = {0.000287 IPS/gram, 250°}, {0.224 IPS/flat, 239°}, {0.436 IPS/°, 249°}, {0.664 IPS/°, 245°}, {0.689 IPS/°, 267°}

AH64D Coefficients

adjustment = Hub Weight, Pitch Link, Tab 8-10, Tab 6-10, Tab 4-10

units = Grams, Flats, Degrees, Degrees, Degrees

FPG100 LAT

Coeff = {.0004936 IPS/gram, 163.0°}, {.04448 flat/°, 15.5°}, {0 IPS/°, 0°}, {0, 0°}, {0, 0°}

Hover LAT

Coeff = {.0004580 IPS/gram, 171.2°}, {.1560 flat/°, 57.5°}, {0 IPS/°, 0°}, {0, 0°}, {0, 0°}

60KTA VERT

Coeff = {.0004696 IPS/gram, 211.9 °}, {.03924 flat/°, 286.6°}, {.1605 IPS/°, 263.5°}, {.3385 IPS/°, 270.6°}, {.6507 IPS/°, 256.1°}

80KTA VERT

Coeff = {.0004546 IPS/gram, 204.7°}, {.06359 flat/°, 273.2°}, {.1714 IPS/°, 261.6°}, {.2886 IPS/°, 261.3°}, {.7391 IPS/°, 259.2°}

100KTA VERT

Coeff = {.0004825 IPS/gram, 215.9°}, {.1137 flat/°, 262.0°}, {.1888 IPS/°, 258.8°}, {.3168 IPS/°, 268.4°}, {.6596 IPS/°, 256.7°}

120KTA VERT

Coeff = {.0004547 IPS/gram, 219.6°}, {.1819 flat/°, 256.1°}, {.2161 IPS/°, 255.8°}, {.3747 IPS/°, 258.6°}, {.6992 IPS/°, 255.0°}

140KTA VERT

Coeff = {.0004519 IPS/gram, 235.6°}, {.2434 flat/°, 247.2°}, {.3071 IPS/°, 250.3°}, {.4467 IPS/°, 260.5°}, {.9085 IPS/°, 250.5°}

Appendix B: UH-60 Database

Note: All data in this appendix was manually typed into Microsoft Excel spreadsheets. The data was originally presented with a graphic user interface in the PC-GBS program.

UH-60 Flight Log					
Flight #	Type	BUNO	Date	Time	Vib Category
1	UH-60	79-23280	5/14/2005	103937	good
2	UH-60	81-23550	11/27/2003	104807	good
3	UH-60	80-23470	2/15/2005	161139	good
4	UH-60	84-23981	8/20/2004	115128	good
5	UH-60	95-26658	2/28/2004	100113	good
6	UH-60	80-23470	10/26/2003	112939	above
7	UH-60	80-23470	2/13/2005	130352	above
8	UH-60	79-23280	4/2/2003	181046	above
9	UH-60	79-23280	8/22/2003	102945	above
10	UH-60	79-23280	10/9/2003	100510	above
11	UH-60	79-23280	10/21/2003	103923	above
12	UH-60	84-23981	2/28/2003	181616	above
13	UH-60	84-23981	1/5/2004	44045	above
14	UH-60	83-23921	12/2/2005	162722	caution
15	UH-60	80-23470	2/13/2005	145852	caution
16	UH-60	80-23470	2/13/2005	121244	caution
17	UH-60	95-26659	3/17/2004	102442	caution
18	UH-60	81-23550	8/4/2003	114453	caution
19	UH-60	84-23981	11/23/2003	81228	exceed
20	UH-60	91-26330	9/16/2003	132022	exceed

VMEP Solution												
Flight #	Yellow			Blue			Red			Black		
	Wt	P/L	Tab	Wt	P/L	Tab	Wt	P/L	Tab	Wt	P/L	Tab
1	7	0	0	-6	-2	0	0	1	-6	0	0	-7
2	0	0	2	0	0	-7	0	1	0	0	-2	0
3	-7	-1	0	-5	0	0	0	0	0	0	0	0
4	0	-1	3	0	0	4	0	0	0	0	1	0
5	0	0	0	10	0	0	5	-2	0	0	0	5
6	16	0	0	-11	-3	0	0	0	0	0	0	0
7	-11	0	0	-16	0	-4	0	-2	0	0	-3	0
8	20	0	6	16	0	3	0	-2	0	0	0	0
9	11	0	-2	0	2	0	0	-1	0	-13	0	10
10	0	0	0	0	0	-3	0	-2	2	0	-3	0
11	0	0	0	0	0	-4	6	-2	9	-6	-3	0
12	-14	0	-8	9	2	3	0	-1	0	0	0	0
13	0	4	0	-6	0	0	-44	0	6	0	0	0
14	9	0	0	7	0	0	0	0	-16	0	0	-2
15	-12	0	0	-14	0	0	0	1	0	0	-2	-11
16	-16	0	0	-26	0	0	0	-4	9	0	-5	20
17	-11	-2	7	-15	0	0	0	0	0	0	-4	20
18	-8	0	0	-9	0	0	0	0	10	0	-4	19
19	-28	0	0	-16	0	-16	0	0	20	0	0	0
20	0	0	0	-8	0	15	0	0	20	0	0	0

Full Soln

Flight #	Before Mag	Before Phase	Pred Mag	Pred Phase	Yellow Wt	After Mag	After Phase	Yellow P/L	After Mag	After Phase	Yellow Tab	After Mag	After Phase
1													
Fpg100 A-B	0.032707	247	0.0197	85	5	0.069268	307	1	0.051184	152	2	0.041347	198
Hover A-B	0.083903	82	0.01359	322		0.065411	85		0.1288	108		0.096912	91
80Kt A-B	0.045817	167	0.047175	220		0.048443	188		0.067723	147		0.051565	155
120Kt A-B	0.121328	70	0.072691	59		0.103722	71		0.149222	85		0.132964	76
145Kt A-B	0.064676	79	0.02042	143		0.047172	84		0.100951	102		0.075388	91
Hover A+B	0.164067	274	0.156546	268		0.164286	274		0.177728	274		0.172191	272
80Kt A+B	0.117083	323	0.074428	285		0.116287	323		0.091119	303		0.100755	307
120Kt A+B	0.149976	349	0.008687	244		0.147891	349		0.080251	342		0.096581	336
145Kt A+B	0.181986	1	0.087178	108		0.179131	1		0.097419	360		0.097789	354

Flight #	Vib Mag	Vib Phase	Pred Mag	Pred Phase	Yellow Wt	After Mag	After Phase	Yellow P/L	After Mag	After Phase	Yellow Tab	After Mag	After Phase
2													
Fpg100 A-B	0.123726	121	0.047083	100	5	0.081083	97	1	0.18681	121	2	0.152567	126
Hover A-B	0.027149	201	0.052165	29		0.041329	222		0.081229	158		0.037668	174
80Kt A-B	0.004418	64	0.02832	15		0.013692	264		0.031764	109		0.014868	91
120Kt A-B	0.029976	147	0.02966	62		0.032046	180		0.073063	136		0.045286	137
145Kt A-B	0.04869	261	0.067846	308		0.066435	257		0.042052	197		0.042265	239
Hover A+B	0.163819	16	0.155879	11		0.163762	16		0.162791	11		0.157802	13
80Kt A+B	0.125195	50	0.132697	32		0.124163	51		0.09655	69		0.09819	61
120Kt A+B	0.183337	88	0.125869	60		0.183109	89		0.197626	109		0.179883	107
145Kt A+B	0.176624	137	0.089133	186		0.178737	138		0.243284	152		0.238748	154

Flight #	Vib Mag	Vib Phase	Pred Mag	Pred Phase	Yellow Wt	After Mag	After Phase	Yellow P/L	After Mag	After Phase	Yellow Tab	After Mag	After Phase
3													
Fpg100 A-B	0.03638	331	0.023388	70	5	0.096599	333	1	0.036389	92	2	0.005196	351
Hover A-B	0.084397	59	0.127113	26		0.066325	55		0.112495	94		0.091682	70
80Kt A-B	0.141022	224	0.121409	236		0.156057	228		0.134744	212		0.135442	220
120Kt A-B	0.188868	226	0.171848	242		0.205598	228		0.188196	213		0.184501	221
145Kt A-B	0.104637	101	0.093494	67		0.090338	108		0.147993	111		0.119648	106
Hover A+B	0.081093	167	0.087003	159		0.08104	167		0.076929	176		0.083628	173
80Kt A+B	0.078236	214	0.044569	240		0.079445	214		0.120591	205		0.111787	209
120Kt A+B	0.067702	247	0.078086	301		0.068724	246		0.114155	211		0.113317	221
145Kt A+B	0.139082	125	0.117409	91		0.140772	126		0.198099	147		0.192785	149

Flight #	Vib Mag	Vib Phase	Pred Mag	Pred Phase	Yellow Wt	After Mag	After Phase	Yellow P/L	After Mag	After Phase	Yellow Tab	After Mag	After Phase
4													
Fpg100 A-B	0.065383	16	0.035052	12	5	0.117679	356	1	0.078001	67	2	0.050358	44
Hover A-B	0.030869	289	0.081646	291		0.047527	276		0.041575	165		0.015436	263
80Kt A-B	0.042057	84	0.025012	71		0.024201	88		0.068372	97		0.052784	88
120Kt A-B	0.088015	150	0.069855	165		0.087869	162		0.129982	143		0.102513	146
145Kt A-B	0.024951	13	0.028618	322		0.020008	326		0.04203	102		0.020133	60
Hover A+B	0.098902	58	0.103693	66		0.098717	58		0.088973	52		0.089629	57
80Kt A+B	0.046546	308	0.027918	291		0.046047	306		0.046151	249		0.047083	265
120Kt A+B	0.152539	332	0.101525	332		0.15071	331		0.093166	313		0.112091	312
145Kt A+B	0.087242	309	0.014692	197		0.085445	308		0.078107	247		0.087801	250

Flight #	Vib Mag	Vib Phase	Pred Mag	Pred Phase	Yellow Wt	After Mag	After Phase	Yellow P/L	After Mag	After Phase	Yellow Tab	After Mag	After Phase
5													
Fpg100 A-B	0.164886	8	0.052168	197	5	0.217559	359	1	0.151814	31	2	0.142606	16
Hover A-B	0.110756	317	0.0843	177		0.120421	309		0.047315	311		0.09254	318
80Kt A-B	0.138877	332	0.040756	11		0.145008	326		0.117165	341		0.132097	336
120Kt A-B	0.165934	305	0.057836	250		0.175768	300		0.122132	304		0.149506	306
145Kt A-B	0.15523	329	0.016932	324		0.158113	323		0.110025	337		0.136924	331
Hover A+B	0.048921	168	0.035917	229		0.048873	168		0.045825	184		0.051937	178
80Kt A+B	0.195477	92	0.126838	125		0.195211	92		0.195851	105		0.189549	102
120Kt A+B	0.073415	41	0.104117	236		0.071677	42		0.053381	107		0.036529	96
145Kt A+B	0.249527	44	0.062149	321		0.247478	44		0.193362	60		0.1844	59

Flight #	Vib Mag	Vib Phase	Pred Mag	Pred Phase	Yellow Wt	After Mag	After Phase	Yellow P/L	After Mag	After Phase	Yellow Tab	After Mag	After Phase
6													
Fpg100 A-B	0.071631	169	0.039252	276	5	0.020056	217	1	0.123017	147	2	0.101456	162
Hover A-B	0.235183	49	0.073489	329		0.218362	46		0.240397	64		0.238165	53
80Kt A-B	0.121482	52	0.027723	352		0.105876	48		0.136762	63		0.128917	56
120Kt A-B	0.163799	55	0.013991	300		0.146516	54		0.181446	69		0.171929	60
145Kt A-B	0.283022	45	0.116078	18		0.266013	43		0.288889	54		0.28187	49
Hover A+B	0.125287	168	0.088157	159		0.12524	168		0.121108	174		0.127871	172
80Kt A+B	0.40637	116	0.284325	125		0.406641	117		0.422615	122		0.413406	121
120Kt A+B	0.27158	89	0.062613	97		0.271377	89		0.282599	103		0.265621	102
145Kt A+B	0.085521	77	0.167117	280		0.084935	79		0.102317	130		0.09478	134

Flight #	Vib Mag	Vib Phase	Pred Mag	Pred Phase	Yellow Wt	After Mag	After Phase	Yellow P/L	After Mag	After Phase	Yellow Tab	After Mag	After Phase
7													
Fpg100 A-B	0.343202	265	0.046506	95	5	0.367909	273	-1	0.394559	270	2	0.32991	260
Hover A-B	0.091605	278	0.161325	62		0.108966	274		0.143072	295		0.076931	271
80Kt A-B	0.224173	222	0.078613	207		0.238623	224		0.233878	228		0.218869	219
120Kt A-B	0.39421	236	0.219135	232		0.411574	236		0.409215	241		0.38694	233
145Kt A-B	0.110259	205	0.110074	95		0.124712	210		0.106653	229		0.119414	197
Hover A+B	0.091364	141	0.092323	169		0.091223	141		0.101648	136		0.089653	146
80Kt A+B	0.080271	273	0.084629	196		0.080538	272		0.08742	302		0.094859	252
120Kt A+B	0.265887	288	0.15114	261		0.265406	287		0.296279	300		0.265814	274
145Kt A+B	0.139524	4	0.088816	94		0.136674	4		0.218119	4		0.05463	355

Flight #	Vib Mag	Vib Phase	Pred Mag	Pred Phase	Yellow Wt	After Mag	After Phase	Yellow P/L	After Mag	After Phase	Yellow Tab	After Mag	After Phase
8													
Fpg100 A-B	0.090777	122	0.023738	216	5	0.05125	84	1	0.153956	122	-2	0.06588	113
Hover A-B	0.110572	17	0.134221	127		0.101542	8		0.090868	52		0.116635	9
80Kt A-B	0.212216	328	0.13177	318		0.219209	324		0.188618	333		0.21861	326
120Kt A-B	0.32375	321	0.176085	313		0.328891	318		0.280973	323		0.336991	320
145Kt A-B	0.018327	342	0.16691	155		0.024277	294		0.0336	117		0.033726	331
Hover A+B	0.111057	312	0.138663	293		0.111222	312		0.122806	309		0.108312	317
80Kt A+B	0.361304	337	0.189272	316		0.360281	337		0.323352	333		0.386371	340
120Kt A+B	0.461297	334	0.166561	300		0.45943	334		0.396855	330		0.507014	338
145Kt A+B	0.333519	9	0.161466	131		0.330687	9		0.249109	11		0.413915	9

Flight #	Vib Mag	Vib Phase	Pred Mag	Pred Phase	Yellow Wt	After Mag	After Phase	Yellow P/L	After Mag	After Phase	Yellow Tab	After Mag	After Phase
9													
Fpg100 A-B	0.247293	120	0.053574	191	-5	0.301827	127	1	0.310507	120	2	0.275717	123
Hover A-B	0.029988	97	0.114688	140		0.048492	91		0.087807	128		0.046248	110
80Kt A-B	0.154695	333	0.10163	316		0.149204	339		0.1328	340		0.147883	336
120Kt A-B	0.075135	320	0.035242	232		0.06992	334		0.033244	336		0.06002	326
145Kt A-B	0.073574	343	0.017912	286		0.075849	357		0.040392	21		0.056884	351
Hover A+B	0.172685	306	0.209098	305		0.172932	306		0.185022	304		0.177226	303
80Kt A+B	0.118899	324	0.180323	310		0.118026	323		0.092378	303		0.102162	308
120Kt A+B	0.078203	131	0.072629	265		0.079619	133		0.137788	153		0.120858	157
145Kt A+B	0.311925	113	0.084439	140		0.31296	113		0.349783	126		0.34161	127

Flight #	Vib Mag	Vib Phase	Pred Mag	Pred Phase	Yellow Wt	After Mag	After Phase	Yellow P/L	After Mag	After Phase	Yellow Tab	After Mag	After Phase
10													
Fpg100 A-B	0.141422	268	0.092054	4	5	0.174379	287	1	0.094671	247	2	0.128042	256
Hover A-B	0.20833	211	0.191414	152		0.222382	214		0.238706	196		0.212487	206
80Kt A-B	0.17198	257	0.092927	270		0.189913	257		0.150418	250		0.161925	256
120Kt A-B	0.284234	280	0.17768	299		0.299123	279		0.246274	276		0.268491	279
145Kt A-B	0.119453	230	0.058056	133		0.137225	232		0.122686	207		0.120867	221
Hover A+B	0.155949	299	0.176863	288		0.156142	299		0.168902	297		0.161464	296
80Kt A+B	0.372482	302	0.272648	300		0.3721	302		0.356858	295		0.365229	297
120Kt A+B	0.167834	291	0.01736	281		0.16723	290		0.153804	266		0.168196	270
145Kt A+B	0.070084	228	0.146776	148		0.072039	226		0.143597	203		0.14812	207

Flight #	Vib Mag	Vib Phase	Pred Mag	Pred Phase	Yellow Wt	After Mag	After Phase	Yellow P/L	After Mag	After Phase	Yellow Tab	After Mag	After Phase
11													
Fpg100 A-B	0.094397	194	0.028446	131	5	0.061013	233	1	0.128226	166	2	0.118311	183
Hover A-B	0.096156	220	0.124352	115		0.112297	225		0.126183	190		0.098419	209
80Kt A-B	0.189777	287	0.139536	303		0.205902	284		0.161227	285		0.178636	287
120Kt A-B	0.15312	287	0.093446	331		0.167124	283		0.11329	278		0.13684	285
145Kt A-B	0.144485	204	0.091786	138		0.158739	208		0.166455	188		0.153684	198
Hover A+B	0.223468	301	0.228018	299		0.223659	301		0.236355	299		0.228745	299
80Kt A+B	0.276624	296	0.230493	319		0.276358	296		0.266003	287		0.273132	289
120Kt A+B	0.199556	236	0.035045	334		0.200924	235		0.244749	221		0.246428	226
145Kt A+B	0.30721	183	0.156248	129		0.310082	183		0.39244	183		0.393314	184

Flight #	Vib Mag	Vib Phase	Pred Mag	Pred Phase	Yellow Wt	After Mag	After Phase	Yellow P/L	After Mag	After Phase	Yellow Tab	After Mag	After Phase
12													
Fpg100 A-B	0.088372	303	0.040087	340	5	0.142768	316	1	0.025421	306	2	0.061214	290
Hover A-B	0.138989	236	0.044676	103		0.156993	238		0.148198	211		0.135446	229
80Kt A-B	0.074038	212	0.03868	133		0.087231	221		0.076244	190		0.070957	204
120Kt A-B	0.104176	265	0.065874	358		0.121074	262		0.078311	242		0.09079	259
145Kt A-B	0.189213	257	0.070583	314		0.207116	256		0.166941	243		0.181655	252
Hover A+B	0.023186	98	0.048864	119		0.022969	99		0.009461	98		0.016388	117
80Kt A+B	0.246438	239	0.087278	213		0.247341	239		0.27691	232		0.272864	235
120Kt A+B	0.278277	254	0.064167	2		0.279056	253		0.303205	240		0.310735	244
145Kt A+B	0.322668	237	0.07209	66		0.324228	236		0.378857	226		0.386504	227

Flight #	Vib Mag	Vib Phase	Pred Mag	Pred Phase	Yellow Wt	After Mag	After Phase	Yellow P/L	After Mag	After Phase	Yellow Tab	After Mag	After Phase
13													
Fpg100 A-B	0.457242	183	0.028405	324	5	0.405699	187	1	0.489631	177	2	0.482902	181
Hover A-B	0.147058	1	0.053746	232		0.142737	353		0.105347	23		0.135795	7
80Kt A-B	0.171925	60	0.071035	57		0.155019	58		0.189928	68		0.18043	63
120Kt A-B	0.214342	48	0.103124	77		0.197622	46		0.225867	59		0.220478	52
145Kt A-B	0.13403	329	0.118282	265		0.137117	322		0.08882	338		0.115646	331
Hover A+B	0.160661	92	0.131253	83		0.160441	92		0.147	91		0.152469	93
80Kt A+B	0.176284	9	0.097421	21		0.175006	9		0.131059	9		0.142106	7
120Kt A+B	0.20973	10	0.131168	43		0.207565	10		0.14083	16		0.149039	9
145Kt A+B	0.10178	292	0.079618	231		0.100729	290		0.109462	245		0.118944	247

Flight #	Vib Mag	Vib Phase	Pred Mag	Pred Phase	Yellow Wt	After Mag	After Phase	Yellow P/L	After Mag	After Phase	Yellow Tab	After Mag	After Phase
14													
Fpg100 A-B	0.043871	326	0.077443	179	5	0.103587	331	1	0.029493	83	2	0.012464	322
Hover A-B	0.250402	299	0.131275	278		0.263887	297		0.192677	292		0.232501	299
80Kt A-B	0.076905	324	0.02997	20		0.085938	314		0.053517	339		0.069111	331
120Kt A-B	0.164148	237	0.171274	194		0.181595	238		0.156085	221		0.156969	231
145Kt A-B	0.334668	321	0.185128	315		0.339695	318		0.287052	322		0.316082	321
Hover A+B	0.228697	89	0.172602	102		0.228478	89		0.215184	88		0.220307	90
80Kt A+B	0.444824	35	0.233458	63		0.443627	35		0.405011	38		0.412136	36
120Kt A+B	0.401959	15	0.102478	137		0.399825	15		0.33457	18		0.341561	15
145Kt A+B	0.644317	356	0.075764	255		0.641461	356		0.560175	355		0.560864	354

Flight #	Vib Mag	Vib Phase	Pred Mag	Pred Phase	Yellow Wt	After Mag	After Phase	Yellow P/L	After Mag	After Phase	Yellow Tab	After Mag	After Phase
15													
Fpg100 A-B	0.363445	249	0.044457	32	5	0.372994	259	1	0.328144	241	2	0.358174	244
Hover A-B	0.177773	202	0.128494	41		0.189922	206		0.216621	187		0.184672	197
80Kt A-B	0.256493	215	0.109086	253		0.26965	218		0.253309	209		0.252327	213
120Kt A-B	0.409914	219	0.195748	244		0.42562	220		0.412123	213		0.40729	216
145Kt A-B	0.214618	163	0.18547	83		0.217979	168		0.25717	158		0.231814	162
Hover A+B	0.074173	173	0.152435	165		0.074143	173		0.071581	183		0.077653	179
80Kt A+B	0.304634	276	0.037687	283		0.304827	276		0.309864	267		0.313194	270
120Kt A+B	0.579386	275	0.144156	297		0.579373	275		0.574319	268		0.58879	269
145Kt A+B	0.479439	271	0.137422	89		0.47938	271		0.489705	261		0.499899	261

Flight #	Vib Mag	Vib Phase	Pred Mag	Pred Phase	Yellow Wt	After Mag	After Phase	Yellow P/L	After Mag	After Phase	Yellow Tab	After Mag	After Phase
16													
Fpg100 A-B	0.374782	269	0.090561	58	5	0.403091	277	1	0.3231	263	2	0.359229	265
Hover A-B	0.161809	285	0.158173	63		0.178094	282		0.116625	266		0.145586	282
80Kt A-B	0.222461	240	0.045509	248		0.239399	241		0.207602	233		0.214348	238
120Kt A-B	0.418754	261	0.24027	271		0.435896	260		0.390419	256		0.40572	260
145Kt A-B	0.04873	345	0.212789	42		0.048966	324		0.027232	58		0.03286	359
Hover A+B	0.163275	130	0.086611	142		0.163106	130		0.151703	133		0.159739	133
80Kt A+B	0.155919	152	0.113375	176		0.156862	152		0.19397	160		0.181803	160
120Kt A+B	0.416578	109	0.260885	98		0.417116	109		0.44748	117		0.428989	117
145Kt A+B	0.624346	102	0.279851	86		0.624957	102		0.642935	109		0.633334	110

Flight #	Vib Mag	Vib Phase	Pred Mag	Pred Phase	Yellow Wt	After Mag	After Phase	Yellow P/L	After Mag	After Phase	Yellow Tab	After Mag	After Phase
17													
Fpg100 A-B	0.031618	317	0.050796	59	5	0.090624	329	1	0.033769	106	2	0.005643	234
Hover A-B	0.117707	204	0.079119	36		0.13068	211		0.157628	183		0.124324	196
80Kt A-B	0.073185	186	0.041995	66		0.080352	199		0.08699	168		0.075076	178
120Kt A-B	0.076669	171	0.059912	59		0.082855	183		0.112975	156		0.087716	163
145Kt A-B	0.224682	199	0.117649	225		0.2376	202		0.2482	188		0.234957	195
Hover A+B	0.033688	339	0.069537	300		0.033768	339		0.042207	323		0.034119	324
80Kt A+B	0.232903	94	0.096333	66		0.23267	94		0.233676	105		0.227422	102
120Kt A+B	0.399486	99	0.084833	82		0.399681	100		0.420277	109		0.402528	108
145Kt A+B	0.574942	96	0.089234	116		0.575259	96		0.585438	104		0.575537	105

Flight #	Vib Mag	Vib Phase	Pred Mag	Pred Phase	Yellow Wt	After Mag	After Phase	Yellow P/L	After Mag	After Phase	Yellow Tab	After Mag	After Phase
18													
Fpg100 A-B	0.10891	151	0.050044	16	5	0.049047	147	1	0.166536	140	2	0.140336	150
Hover A-B	0.097986	189	0.056474	54		0.107456	199		0.148636	171		0.108782	181
80Kt A-B	0.058938	188	0.003668	189		0.066904	203		0.072991	166		0.060728	177
120Kt A-B	0.065231	187	0.023473	325		0.075608	198		0.096004	164		0.073046	174
145Kt A-B	0.119797	145	0.060929	39		0.117981	154		0.167161	142		0.138326	144
Hover A+B	0.115527	42	0.144143	29		0.115383	42		0.108682	36		0.106987	40
80Kt A+B	0.144347	147	0.099493	6		0.145216	147		0.180683	156		0.168551	156
120Kt A+B	0.450975	142	0.091338	63		0.452588	143		0.511043	147		0.493166	148
145Kt A+B	0.709512	146	0.080946	148		0.711889	146		0.778737	150		0.773768	150

Flight #	Vib Mag	Vib Phase	Pred Mag	Pred Phase	Yellow Wt	After Mag	After Phase	Yellow P/L	After Mag	After Phase	Yellow Tab	After Mag	After Phase
19													
Fpg100 A-B	0.065843	279	0.148752	218	5	0.111037	305	1	0.025188	206	2	0.050843	251
Hover A-B	0.198795	64	0.175332	18		0.180366	62		0.220988	80		0.206389	68
80Kt A-B	0.095744	76	0.077975	67		0.07789	76		0.119454	85		0.105878	79
120Kt A-B	0.226021	87	0.123039	62		0.209508	89		0.260607	93		0.240341	89
145Kt A-B	0.321385	81	0.255459	44		0.303864	82		0.353312	87		0.331272	84
Hover A+B	0.164591	216	0.056255	240		0.164717	216		0.171195	220		0.172808	217
80Kt A+B	0.588989	171	0.199789	198		0.590158	171		0.632033	172		0.619995	172
120Kt A+B	0.947801	168	0.314875	210		0.949888	169		1.01837	169		1.004095	170
145Kt A+B	1.537488	163	0.547287	187		1.540229	163		1.617413	164		1.614839	164

Flight #	Vib Mag	Vib Phase	Pred Mag	Pred Phase	Yellow Wt	After Mag	After Phase	Yellow P/L	After Mag	After Phase	Yellow Tab	After Mag	After Phase
20													
Fpg100 A-B	0.442209	204	0.064965	271	5	0.405373	210	1	0.454472	196	2	0.460267	201
Hover A-B	0.174997	177	0.077556	318		0.18026	183		0.230026	168		0.188225	173
80Kt A-B	0.138393	102	0.10312	24		0.122097	105		0.166499	104		0.149506	102
120Kt A-B	0.135376	119	0.133645	9		0.125465	126		0.178895	122		0.151953	119
145Kt A-B	0.341969	151	0.154564	112		0.34101	154		0.388051	148		0.36026	150
Hover A+B	0.049651	199	0.115483	126		0.04972	199		0.053708	213		0.056565	205
80Kt A+B	0.459304	223	0.103606	169		0.46043	222		0.49719	220		0.490632	221
120Kt A+B	0.678619	229	0.036912	41		0.680173	229		0.725206	224		0.727371	226
145Kt A+B	1.151947	229	0.134108	242		1.15381	229		1.212255	226		1.219836	227

Flight #	Before Mag	Before Phase	Pred Mag	Pred Phase	Yellow Wt	After Mag	After Phase	Yellow P/L	After Mag	After Phase	Yellow Tab	After Mag	After Phase
1													
Fpg100 A-B	0.032707	247	0.0197	85	80	0.993553	333	30	1.813004	121	20	0.285169	153
Hover A-B	0.083903	82	0.01359	322		0.217932	256		1.909229	139		0.232944	114
80Kt A-B	0.045817	167	0.047175	220		0.293496	252		0.867441	117		0.127949	119
120Kt A-B	0.121328	70	0.072691	59		0.165645	250		1.345842	124		0.252069	96
145Kt A-B	0.064676	79	0.02042	143		0.231657	246		1.437952	130		0.208562	124
Hover A+B	0.164067	274	0.156546	268		0.164172	274		0.565151	277		0.244803	263
80Kt A+B	0.117083	323	0.074428	285		0.118343	323		1.222679	192		0.272916	218
120Kt A+B	0.149976	349	0.008687	244		0.151708	348		1.904632	178		0.434758	199
145Kt A+B	0.181986	1	0.087178	108		0.183913	0		2.252873	183		0.634939	193

Flight #	Vib Mag	Vib Phase	Pred Mag	Pred Phase	Yellow Wt	After Mag	After Phase	Yellow P/L	After Mag	After Phase	Yellow Tab	After Mag	After Phase
2													
Fpg100 A-B	0.123726	121	0.047083	100	80	0.894825	339	30	1.960873	120	20	0.405038	139
Hover A-B	0.027149	201	0.052165	29		0.317759	254		1.881627	142		0.17746	137
80Kt A-B	0.004418	64	0.02832	15		0.289636	261		0.842267	115		0.106583	98
120Kt A-B	0.029976	147	0.02966	62		0.282459	244		1.309011	128		0.179457	121
145Kt A-B	0.04869	261	0.067846	308		0.343268	251		1.369656	133		0.149647	156
Hover A+B	0.163819	16	0.155879	11		0.164222	16		0.416319	302		0.123108	343
80Kt A+B	0.125195	50	0.132697	32		0.124965	50		1.215092	184		0.230021	180
120Kt A+B	0.183337	88	0.125869	60		0.181511	88		2.071132	172		0.558862	173
145Kt A+B	0.176624	137	0.089133	186		0.173296	137		2.564042	180		0.931555	182

Flight #	Vib Mag	Vib Phase	Pred Mag	Pred Phase	Yellow Wt	After Mag	After Phase	Yellow P/L	After Mag	After Phase	Yellow Tab	After Mag	After Phase
3													
Fpg100 A-B	0.03638	331	0.023388	70	80	1.03471	335	30	1.813185	119	20	0.254791	146
Hover A-B	0.084397	59	0.127113	26		0.225102	265		1.888799	138		0.212508	107
80Kt A-B	0.141022	224	0.121409	236		0.416202	249		0.807597	124		0.119095	178
120Kt A-B	0.188868	226	0.171848	242		0.467965	241		1.272416	136		0.199781	180
145Kt A-B	0.104637	101	0.093494	67		0.215097	234		1.497649	130		0.260065	125
Hover A+B	0.081093	167	0.087003	159		0.080646	167		0.380723	268		0.133662	207
80Kt A+B	0.078236	214	0.044569	240		0.07812	215		1.380062	189		0.4014	201
120Kt A+B	0.067702	247	0.078086	301		0.068932	249		2.091228	179		0.614206	197
145Kt A+B	0.139082	125	0.117409	91		0.135666	125		2.527629	180		0.886971	182

Flight #	Vib Mag	Vib Phase	Pred Mag	Pred Phase	Yellow Wt	After Mag	After Phase	Yellow P/L	After Mag	After Phase	Yellow Tab	After Mag	After Phase
4													
Fpg100 A-B	0.065383	16	0.035052	12	80	1.047449	337	30	1.826668	118	20	0.252719	135
Hover A-B	0.030869	289	0.081646	291		0.330151	261		1.849551	141		0.139282	133
80Kt A-B	0.042057	84	0.025012	71		0.252749	261		0.878326	113		0.144195	95
120Kt A-B	0.088015	150	0.069855	165		0.287559	232		1.366173	129		0.231705	129
145Kt A-B	0.024951	13	0.028618	322		0.283846	253		1.394808	131		0.156444	132
Hover A+B	0.098902	58	0.103693	66		0.099073	58		0.335922	290		0.013274	17
80Kt A+B	0.046546	308	0.027918	291		0.047845	308		1.285933	190		0.312348	205
120Kt A+B	0.152539	332	0.101525	332		0.154667	331		1.928613	179		0.46573	203
145Kt A+B	0.087242	309	0.014692	197		0.09065	309		2.399551	185		0.780793	196

Flight #	Vib Mag	Vib Phase	Pred Mag	Pred Phase	Yellow Wt	After Mag	After Phase	Yellow P/L	After Mag	After Phase	Yellow Tab	After Mag	After Phase
5													
Fpg100 A-B	0.164886	8	0.052168	197	80	1.135672	340	30	1.781108	115	20	0.198906	113
Hover A-B	0.110756	317	0.0843	177		0.371266	273		1.755722	141		0.059665	113
80Kt A-B	0.138877	332	0.040756	11		0.362199	282		0.732769	108		0.112171	19
120Kt A-B	0.165934	305	0.057836	250		0.405185	270		1.112223	128		0.02774	2
145Kt A-B	0.15523	329	0.016932	324		0.356016	275		1.25242	130		0.031173	81
Hover A+B	0.048921	168	0.035917	229		0.048475	168		0.38724	272		0.11165	218
80Kt A+B	0.195477	92	0.126838	125		0.194455	92		1.296957	179		0.331686	163
120Kt A+B	0.073415	41	0.104117	236		0.07329	39		2.002688	176		0.507608	187
145Kt A+B	0.249527	44	0.062149	321		0.249061	43		2.254299	179		0.621972	178

Flight #	Vib Mag	Vib Phase	Pred Mag	Pred Phase	Yellow Wt	After Mag	After Phase	Yellow P/L	After Mag	After Phase	Yellow Tab	After Mag	After Phase
6													
Fpg100 A-B	0.071631	169	0.039252	276	80	0.923969	334	30	1.882477	122	20	0.356794	151
Hover A-B	0.235183	49	0.073489	329		0.150736	308		1.869642	134		0.310739	81
80Kt A-B	0.121482	52	0.027723	352		0.195814	278		0.899455	108		0.205243	74
120Kt A-B	0.163799	55	0.013991	300		0.13535	268		1.336653	121		0.272268	85
145Kt A-B	0.283022	45	0.116078	18		0.122263	321		1.440219	121		0.317302	77
Hover A+B	0.125287	168	0.088157	159		0.124841	168		0.376096	261		0.171045	198
80Kt A+B	0.40637	116	0.284325	125		0.405112	116		1.481608	173		0.558549	151
120Kt A+B	0.27158	89	0.062613	97		0.269737	89		2.08241	169		0.5765	164
145Kt A+B	0.085521	77	0.167117	280		0.083311	75		2.412573	181		0.784034	185

Flight #	Vib Mag	Vib Phase	Pred Mag	Pred Phase	Yellow Wt	After Mag	After Phase	Yellow P/L	After Mag	After Phase	Yellow Tab	After Mag	After Phase
7													
Fpg100 A-B	0.343202	265	0.046506	95	80	1.154576	319	-30	2.129105	294	20	0.32885	214
Hover A-B	0.091605	278	0.161325	62		0.388697	263		1.934472	319		0.099537	157
80Kt A-B	0.224173	222	0.078613	207		0.487856	244		0.928616	282		0.190742	195
120Kt A-B	0.39421	236	0.219135	232		0.676483	242		1.449609	293		0.347157	213
145Kt A-B	0.110259	205	0.110074	95		0.382061	237		1.372509	308		0.237481	164
Hover A+B	0.091364	141	0.092323	169		0.090976	140		0.473521	106		0.11232	191
80Kt A+B	0.080271	273	0.084629	196		0.081306	273		1.298521	4		0.352912	210
120Kt A+B	0.265887	288	0.15114	261		0.268098	288		2.168018	350		0.603242	217
145Kt A+B	0.139524	4	0.088816	94		0.141326	3		2.577311	3		0.67606	192

Flight #	Vib Mag	Vib Phase	Pred Mag	Pred Phase	Yellow Wt	After Mag	After Phase	Yellow P/L	After Mag	After Phase	Yellow Tab	After Mag	After Phase
8													
Fpg100 A-B	0.090777	122	0.023738	216	80	0.92103	338	30	1.930995	120	20	0.375149	141
Hover A-B	0.110572	17	0.134221	127		0.26753	279		1.812448	138		0.162829	90
80Kt A-B	0.212216	328	0.13177	318		0.423857	289		0.67382	105		0.163615	357
120Kt A-B	0.32375	321	0.176085	313		0.497562	288		0.970806	123		0.195454	341
145Kt A-B	0.018327	342	0.16691	155		0.295825	253		1.387674	132		0.152936	137
Hover A+B	0.111057	312	0.138663	293		0.111411	312		0.499837	286		0.165589	282
80Kt A+B	0.361304	337	0.189272	316		0.362454	337		1.011703	198		0.236642	276
120Kt A+B	0.461297	334	0.166561	300		0.463386	334		1.649025	183		0.349527	245
145Kt A+B	0.333519	9	0.161466	131		0.335067	8		2.112659	182		0.483904	191

Flight #	Vib Mag	Vib Phase	Pred Mag	Pred Phase	Yellow Wt	After Mag	After Phase	Yellow P/L	After Mag	After Phase	Yellow Tab	After Mag	After Phase
9													
Fpg100 A-B	0.247293	120	0.053574	191	80	0.806763	345	30	2.088473	120	20	0.523627	134
Hover A-B	0.029988	97	0.114688	140		0.274036	256		1.890617	140		0.193434	124
80Kt A-B	0.154695	333	0.10163	316		0.37334	284		0.725277	107		0.123841	14
120Kt A-B	0.075135	320	0.035242	232		0.321469	263		1.208787	127		0.089399	97
145Kt A-B	0.073574	343	0.017912	286		0.300273	263		1.342468	130		0.106645	123
Hover A+B	0.172685	306	0.209098	305		0.173007	306		0.561767	287		0.227578	286
80Kt A+B	0.118899	324	0.180323	310		0.120161	323		1.22529	192		0.272465	218
120Kt A+B	0.078203	131	0.072629	265		0.075867	132		2.117212	175		0.615087	185
145Kt A+B	0.311925	113	0.084439	140		0.3086	112		2.568264	176		0.935508	171

Flight #	Vib Mag	Vib Phase	Pred Mag	Pred Phase	Yellow Wt	After Mag	After Phase	Yellow P/L	After Mag	After Phase	Yellow Tab	After Mag	After Phase
10													
Fpg100 A-B	0.141422	268	0.092054	4	80	1.060332	328	30	1.722304	122	20	0.247485	176
Hover A-B	0.20833	211	0.191414	152		0.468413	239		1.94552	147		0.284686	175
80Kt A-B	0.17198	257	0.092927	270		0.466076	260		0.712456	123		0.086278	230
120Kt A-B	0.284234	280	0.17768	299		0.552079	265		1.037024	135		0.143805	263
145Kt A-B	0.119453	230	0.058056	133		0.411222	244		1.391404	137		0.206292	175
Hover A+B	0.155949	299	0.176863	288		0.156229	299		0.550626	284		0.218743	279
80Kt A+B	0.372482	302	0.272648	300		0.373768	302		1.20532	204		0.428946	255
120Kt A+B	0.167834	291	0.01736	281		0.170091	291		1.997786	181		0.568251	208
145Kt A+B	0.070084	228	0.146776	148		0.070879	230		2.495251	184		0.8742	193

Flight #	Vib Mag	Vib Phase	Pred Mag	Pred Phase	Yellow Wt	After Mag	After Phase	Yellow P/L	After Mag	After Phase	Yellow Tab	After Mag	After Phase
11													
Fpg100 A-B	0.094397	194	0.028446	131	80	0.928254	331	30	1.874974	123	20	0.36207	158
Hover A-B	0.096156	220	0.124352	115		0.383688	249		1.897601	144		0.192219	159
80Kt A-B	0.189777	287	0.139536	303		0.473525	271		0.656232	117		0.087989	295
120Kt A-B	0.15312	287	0.093446	331		0.42181	263		1.144496	131		0.026426	201
145Kt A-B	0.144485	204	0.091786	138		0.411954	235		1.458929	137		0.266749	169
Hover A+B	0.223468	301	0.228018	299		0.223759	301		0.617465	287		0.282001	285
80Kt A+B	0.276624	296	0.230493	319		0.277892	296		1.251084	200		0.392955	241
120Kt A+B	0.199556	236	0.035045	334		0.200341	236		2.178004	181		0.729814	202
145Kt A+B	0.30721	183	0.156248	129		0.305386	183		2.758963	183		1.125045	188

Flight #	Vib Mag	Vib Phase	Pred Mag	Pred Phase	Yellow Wt	After Mag	After Phase	Yellow P/L	After Mag	After Phase	Yellow Tab	After Mag	After Phase
12													
Fpg100 A-B	0.088372	303	0.040087	340	80	1.069339	333	30	1.747431	120	20	0.212009	156
Hover A-B	0.138989	236	0.044676	103		0.43392	251		1.857802	145		0.182418	175
80Kt A-B	0.074038	212	0.03868	133		0.346404	252		0.831048	120		0.101003	142
120Kt A-B	0.104176	265	0.065874	358		0.388874	254		1.203984	131		0.08389	157
145Kt A-B	0.189213	257	0.070583	314		0.483466	252		1.299999	139		0.187353	203
Hover A+B	0.023186	98	0.048864	119		0.02305	97		0.378737	279		0.071079	233
80Kt A+B	0.246438	239	0.087278	213		0.246874	240		1.467644	195		0.53305	215
120Kt A+B	0.278277	254	0.064167	2		0.279688	254		2.137508	184		0.742155	211
145Kt A+B	0.322668	237	0.07209	66		0.323924	237		2.639592	189		1.062665	203

Flight #	Vib Mag	Vib Phase	Pred Mag	Pred Phase	Yellow Wt	After Mag	After Phase	Yellow P/L	After Mag	After Phase	Yellow Tab	After Mag	After Phase
13													
Fpg100 A-B	0.457242	183	0.028405	324	80	0.626516	315	30	2.075305	131	19	0.69725	170
Hover A-B	0.147058	1	0.053746	232		0.306239	286		1.762414	138		0.135084	70
80Kt A-B	0.171925	60	0.071035	57		0.14673	285		0.952014	106		0.255815	74
120Kt A-B	0.214342	48	0.103124	77		0.120104	292		1.33749	119		0.300237	75
145Kt A-B	0.13403	329	0.118282	265		0.345596	272		1.278389	130		0.037634	102
Hover A+B	0.160661	92	0.131253	83		0.160571	92		0.244898	284		0.094956	117
80Kt A+B	0.176284	9	0.097421	21		0.17695	9		1.131844	188		0.137755	208
120Kt A+B	0.20973	10	0.131168	43		0.210795	9		1.859153	176		0.335527	192
145Kt A+B	0.10178	292	0.079618	231		0.105101	292		2.416867	185		0.765277	198

Flight #	Vib Mag	Vib Phase	Pred Mag	Pred Phase	Yellow Wt	After Mag	After Phase	Yellow P/L	After Mag	After Phase	Yellow Tab	After Mag	After Phase
14													
Fpg100 A-B	0.043871	326	0.077443	179	80	1.03779	335	30	1.797667	119	20	0.246057	147
Hover A-B	0.250402	299	0.131275	278		0.516871	277		1.636209	144		0.089559	282
80Kt A-B	0.076905	324	0.02997	20		0.335205	273		0.772848	112		0.072465	51
120Kt A-B	0.164148	237	0.171274	194		0.448978	245		1.236283	135		0.158519	180
145Kt A-B	0.334668	321	0.185128	315		0.511539	287		1.070727	129		0.165439	322
Hover A+B	0.228697	89	0.172602	102		0.228629	89		0.181253	291		0.153421	103
80Kt A+B	0.444824	35	0.233458	63		0.444938	35		0.928988	175		0.166951	71
120Kt A+B	0.401959	15	0.102478	137		0.402841	14		1.679193	173		0.171379	184
145Kt A+B	0.644317	356	0.075764	255		0.646459	356		1.799874	185		0.244248	229

Flight #	Vib Mag	Vib Phase	Pred Mag	Pred Phase	Yellow Wt	After Mag	After Phase	Yellow P/L	After Mag	After Phase	Yellow Tab	After Mag	After Phase
15													
Fpg100 A-B	0.363445	249	0.044457	32	80	1.083352	316	30	1.630054	130	20	0.411868	206
Hover A-B	0.177773	202	0.128494	41		0.427051	238		1.956539	145		0.276902	167
80Kt A-B	0.256493	215	0.109086	253		0.506661	240		0.831888	133		0.23179	192
120Kt A-B	0.409914	219	0.195748	244		0.672653	232		1.338673	146		0.406464	197
145Kt A-B	0.214618	163	0.18547	83		0.378148	215		1.586923	136		0.375719	153
Hover A+B	0.074173	173	0.152435	165		0.073728	173		0.387663	268		0.133231	212
80Kt A+B	0.304634	276	0.037687	283		0.305708	276		1.349217	201		0.487299	235
120Kt A+B	0.579386	275	0.144156	297		0.581379	275		2.060193	193		0.857859	233
145Kt A+B	0.479439	271	0.137422	89		0.482247	271		2.50061	194		1.010004	218

Flight #	Vib Mag	Vib Phase	Pred Mag	Pred Phase	Yellow Wt	After Mag	After Phase	Yellow P/L	After Mag	After Phase	Yellow Tab	After Mag	After Phase
16													
Fpg100 A-B	0.374782	269	0.090561	58	80	1.195644	318	30	1.526207	127	20	0.328622	221
Hover A-B	0.161809	285	0.158173	63		0.451571	267		1.735992	144		0.067048	203
80Kt A-B	0.222461	240	0.045509	248		0.506889	252		0.732074	129		0.157888	215
120Kt A-B	0.418754	261	0.24027	271		0.702885	257		1.037558	145		0.307763	244
145Kt A-B	0.04873	345	0.212789	42		0.294016	259		1.358156	131		0.126949	130
Hover A+B	0.163275	130	0.086611	142		0.162933	130		0.275524	261		0.151998	163
80Kt A+B	0.155919	152	0.113375	176		0.154722	152		1.429665	184		0.447117	183
120Kt A+B	0.416578	109	0.260885	98		0.414355	109		2.243364	167		0.748348	158
145Kt A+B	0.624346	102	0.279851	86		0.621235	102		2.606872	169		1.039969	153

Flight #	Vib Mag	Vib Phase	Pred Mag	Pred Phase	Yellow Wt	After Mag	After Phase	Yellow P/L	After Mag	After Phase	Yellow Tab	After Mag	After Phase
17													
Fpg100 A-B	0.031618	317	0.050796	59	80	1.024037	334	30	1.805875	120	20	0.258641	148
Hover A-B	0.117707	204	0.079119	36		0.383469	244		1.921829	144		0.227202	159
80Kt A-B	0.073185	186	0.041995	66		0.320983	248		0.864868	119		0.129634	134
120Kt A-B	0.076669	171	0.059912	59		0.311485	236		1.335737	130		0.206848	134
145Kt A-B	0.224682	199	0.117649	225		0.47158	228		1.503437	140		0.343935	174
Hover A+B	0.033688	339	0.069537	300		0.034126	339		0.419734	283		0.091715	265
80Kt A+B	0.232903	94	0.096333	66		0.231857	94		1.307397	178		0.352028	157
120Kt A+B	0.399486	99	0.084833	82		0.397408	99		2.178215	167		0.685962	156
145Kt A+B	0.574942	96	0.089234	116		0.571986	96		2.53441	170		0.961197	154

Flight #	Vib Mag	Vib Phase	Pred Mag	Pred Phase	Yellow Wt	After Mag	After Phase	Yellow P/L	After Mag	After Phase	Yellow Tab	After Mag	After Phase
18													
Fpg100 A-B	0.10891	151	0.050044	16	80	0.887043	336	30	1.933096	122	20	0.398909	148
Hover A-B	0.097986	189	0.056474	54		0.349833	243		1.932445	143		0.231435	150
80Kt A-B	0.058938	188	0.003668	189		0.315864	251		0.857654	119		0.120082	129
120Kt A-B	0.065231	187	0.023473	325		0.322076	240		1.314334	130		0.185505	136
145Kt A-B	0.119797	145	0.060929	39		0.290945	226		1.517209	133		0.28878	142
Hover A+B	0.115527	42	0.144143	29		0.115804	42		0.352808	295		0.046329	357
80Kt A+B	0.144347	147	0.099493	6		0.14311	147		1.415628	184		0.43109	182
120Kt A+B	0.450975	142	0.091338	63		0.448725	142		2.442037	171		0.931503	170
145Kt A+B	0.709512	146	0.080946	148		0.706326	146		3.034649	175		1.411913	170

Flight #	Vib Mag	Vib Phase	Pred Mag	Pred Phase	Yellow Wt	After Mag	After Phase	Yellow P/L	After Mag	After Phase	Yellow Tab	After Mag	After Phase
19													
Fpg100 A-B	0.065843	279	0.148752	218	80	1.031178	332	30	1.773744	121	20	0.25029	158
Hover A-B	0.198795	64	0.175332	18		0.119829	283		1.917394	135		0.308531	93
80Kt A-B	0.095744	76	0.077975	67		0.19798	263		0.914788	111		0.194438	89
120Kt A-B	0.226021	87	0.123039	62		0.097675	207		1.459156	122		0.366807	99
145Kt A-B	0.321385	81	0.255459	44		0.068969	143		1.621236	123		0.434272	100
Hover A+B	0.164591	216	0.056255	240		0.164279	216		0.497889	262		0.24661	225
80Kt A+B	0.588989	171	0.199789	198		0.58801	171		1.872481	183		0.890396	180
120Kt A+B	0.947801	168	0.314875	210		0.946059	169		3.000183	174		1.491208	177
145Kt A+B	1.537488	163	0.547287	187		1.534801	163		3.918124	175		2.292662	172

Flight #	Vib Mag	Vib Phase	Pred Mag	Pred Phase	Yellow Wt	After Mag	After Phase	Yellow P/L	After Mag	After Phase	Yellow Tab	After Mag	After Phase
20													
Fpg100 A-B	0.442209	204	0.064965	271	80	0.777295	310	30	1.934348	133	20	0.646767	182
Hover A-B	0.174997	177	0.077556	318		0.372328	230		2.010072	144		0.312077	154
80Kt A-B	0.138393	102	0.10312	24		0.171421	244		0.973705	113		0.24117	101
120Kt A-B	0.135376	119	0.133645	9		0.224545	223		1.413227	127		0.287996	118
145Kt A-B	0.341969	151	0.154564	112		0.417944	195		1.727227	136		0.509111	147
Hover A+B	0.049651	199	0.115483	126		0.04926	199		0.413426	272		0.128947	228
80Kt A+B	0.459304	223	0.103606	169		0.459367	223		1.70118	197		0.765271	212
120Kt A+B	0.678619	229	0.036912	41		0.679114	229		2.533648	189		1.183963	212
145Kt A+B	1.151947	229	0.134108	242		1.152754	229		3.341251	197		1.858797	213

Appendix C: AH-64A Database

Note: All data in this appendix was manually typed into Microsoft Excel spreadsheets.
The data was originally presented with a graphic user interface in the PC-GBS program.

Flight Log					
Flight #	Type	BUNO	Date	Time	Vib Category
1	AH-64A	86-08964	6/5/2003	153548	good
2	AH-64A	86-08962	11/14/2003	132815	good
3	AH-64A	86-08964	6/5/2003	145701	good
4	AH-64A	86-08963	8/11/2003	94214	good
5	AH-64A	91-00113	1/28/2005	35232	good
6	AH-64A	86-08962	1/29/2004	115335	Above
7	AH-64A	86-08962	10/18/2002	172058	Above
8	AH-64A	86-08962	5/5/2003	121031	Above
9	AH-64A	91-00113	1/15/2005	61607	Above
10	AH-64A	88-00282	8/6/2004	121059	Above
11	AH-64A	91-00113	1/15/2005	31415	Caution
12	AH-64A	86-08962	1/29/2004	105756	Caution
13	AH-64A	86-08963	1/19/2004	74156	Caution
14	AH-64A	86-08964	1/22/2003	162720	Caution
15	AH-64A	91-00113	1/14/2005	92415	Caution
16	AH-64A	86-08962	4/9/2003	160621	Exceed
17	AH-64A	86-08962	4/9/2003	171712	Exceed
18	AH-64A	86-08962	11/7/2003	102919	Exceed
19	AH-64A	86-08962	11/7/2003	145649	Exceed
20	AH-64A	86-08964	1/10/2002	141123	Exceed

Flight	1				2				3				4			
	Wt	P/L	8	6	4	Wt	P/L	8	6	4	Wt	P/L	8	6	4	4
1	-278	0	0	0	0	-113	-0.5	0	0	0	0	0	0	0	0	0
2	0	0	0	0	0	0	0	0	0	0	0	-0.75	0	0	0	0
3	0	0	0	1	0	-217	0	-1	0	0	0	0	1.5	0	0	0
4	0	0	0.5	0	0	0	0	0	-0.5	0	0	0	0	0	-0.5	0
5	-165	0	0	0	0	0	-0.75	0	0	0	0	0	0	0	0	0
6	0	0	0	0	0	0	0.75	-0.5	0	0	0	0	0.5	0	0	0
7	0	-1	0	1.5	0	113	0.5	0	0	0	0	0	0	0	0	0
8	-165	0	-0.5	0	0	165	0	0.5	0	0	0	0	-2	-0.5	0	0
9	0	0.5	0	-1.5	0	165	0	0	-0.5	0	0	0	0	0	0	0
10	-165	-1.75	0	0	0.5	165	0	0	0	0	0	0	0	0.5	0	0
11	0	0.5	0	0	1	0	0	0	0	0.5	0	0	0	0	1	0
12	113	2	0.5	0	0	-217	0	0	0	1.5	0	0	0	0	-0.75	3.5
13	0	0	0	0	0	0	0	1	0	0	0	0	0	0	-113	0
14	0	0	0	0	1	0	-3.75	0.5	0	0	0	0	2	0	0	0
15	0	0	2	0	0	113	0	0	0.5	0	0	-0.5	0	2	0	0
16	0	-5	0.5	0	0	0	0	-1	0	0	0	0	0	0	-0.75	0
17	0	-2.75	0	0	0	0	0	-1.5	0	0	0	0	-0.5	0	-1.75	0
18	0	0	0	2	0	0	0	0	0	0	0	0	0	0	0	2.5
19	0	0	0	-1.5	0	0	0	0	-2	0	0	-1	0	0	-0.5	0
20	226	0.5	0	0	0	278	0	0	2	0	0	0	0	0	-0.5	0

Batch	Vib Mag	Vib Phase	Pred Mag	Pred Phase	#1 Blade Wt	After Mag	After Phase	#1 Blade P/L	After Mag	After Phase	#1 Blade Tab 8	After Mag	After Phase	#1 Blade Tab 6	After Mag	After Phase	#1 Blade Tab 4	After Mag	After Phase
1																			
FPG100	0.116931	166	0.058835	298	113	0.183871	167	0.5	0.100682	160	0.5	0.116792	166	0.5	0.116792	166	0.5	0.116795	166
Hover Lat	0.085828	200	0.072847	250		0.138279	187		0.054198	121		0.077419	191		0.065493	181		0.049691	166
60K Vert	0.171535	168	0.087651	129		0.197414	178		0.181748	172		0.199012	190		0.232637	200		0.223584	209
80 K Vert	0.133674	192	0.097796	197		0.133198	191		0.14804	207		0.260505	225		0.317749	240		0.437768	246
100 K Vert	0.130108	184	0.070924	191		0.129969	184		0.152503	209		0.242586	230		0.338182	235		0.447965	244
120 K Vert	0.107955	160	0.035466	161		0.107573	159		0.134035	195		0.240239	226		0.334865	237		0.474209	247
140 K Vert	0.090145	177	0.042047	285		0.089394	177		0.173615	217		0.327282	229		0.447661	239		0.707141	232

Batch	Vib Mag	Vib Phase	Pred Mag	Pred Phase	#1 Blade Wt	After Mag	After Phase	#1 Blade P/L	After Mag	After Phase	#1 Blade Tab 8	After Mag	After Phase	#1 Blade Tab 6	After Mag	After Phase	#1 Blade Tab 4	After Mag	After Phase
2																			
FPG100	0.068736	225	0.057926	258	-113	0.064371	286	0.5	0.050399	235	0.5	0.068668	225	0.5	0.068665	225	0.5	0.06866	225
Hover Lat	0.156707	214	0.025258	295		0.124559	234		0.0781	189		0.145241	210		0.129379	207		0.108252	206
60K Vert	0.074744	147	0.023543	156		0.077553	115		0.080867	158		0.095927	198		0.13637	213		0.138529	229
80 K Vert	0.07762	163	0.095848	297		0.077284	163		0.077338	193		0.185331	227		0.247733	246		0.370291	250
100 K Vert	0.142985	130	0.01744	341		0.143007	129		0.104953	154		0.134508	209		0.221285	225		0.323671	241
120 K Vert	0.203573	145	0.074586	201		0.203259	145		0.198866	167		0.251108	202		0.319354	219		0.436353	235
140 K Vert	0.252516	134	0.114811	207		0.252145	134		0.235243	162		0.307974	193		0.377315	213		0.644924	216

Batch	Vib Mag	Vib Phase	Pred Mag	Pred Phase	#1 Blade Wt	After Mag	After Phase	#1 Blade P/L	After Mag	After Phase	#1 Blade Tab 8	After Mag	After Phase	#1 Blade Tab 6	After Mag	After Phase	#1 Blade Tab 4	After Mag	After Phase
3																			
FPG100	0.127352	110	0.068366	182	113	0.172082	130	0.5	0.129522	101	0.5	0.12727	110	0.5	0.127274	110	0.5	0.127281	110
Hover Lat	0.195151	81	0.09695	79		0.207929	98		0.280519	73		0.209477	81		0.224987	79		0.241423	75
60K Vert	0.022116	347	0.120537	318		0.035539	257		0.018137	301		0.074643	265		0.123691	256		0.150479	268
80 K Vert	0.182843	186	0.102055	266		0.182401	186		0.192333	198		0.293885	217		0.339646	232		0.454589	239
100 K Vert	0.051449	284	0.059642	338		0.051082	285		0.114793	275		0.226202	267		0.320065	260		0.445569	263
120 K Vert	0.16641	171	0.019174	213		0.165904	170		0.197348	193		0.293527	218		0.380032	230		0.510344	241
140 K Vert	0.20431	135	0.085837	30		0.204087	135		0.196528	170		0.290217	202		0.375584	220		0.644227	220

Batch	Vib Mag	Vib Phase	Pred Mag	Pred Phase	#1 Blade Wt	After Mag	After Phase	#1 Blade P/L	After Mag	After Phase	#1 Blade Tab 8	After Mag	After Phase	#1 Blade Tab 6	After Mag	After Phase	#1 Blade Tab 4	After Mag	After Phase
4																			
FPG100	0.120262	246	0.120246	246	113	0.150584	220	0.5	0.106258	253	0.5	0.120241	246	0.5	0.120237	246	-0.5	0.120228	246
Hover Lat	0.110412	31	0.118456	44		0.080099	62		0.198456	42		0.122131	36		0.138836	38		0.063927	15
60K Vert	0.143915	170	0.142603	208		0.171412	181		0.154653	174		0.175903	194		0.212914	205		0.20579	124
80 K Vert	0.143248	132	0.064338	205		0.143309	131		0.117474	145		0.156345	199		0.18711	230		0.481982	95
100 K Vert	0.243478	97	0.040356	33		0.243909	97		0.179934	100		0.085055	130		0.09754	195		0.637003	86
120 K Vert	0.153558	129	0.12044	243		0.153592	128		0.132392	159		0.185112	209		0.265718	229		0.596702	91
140 K Vert	0.290249	87	0.030551	37		0.290755	86		0.183411	100		0.114644	161		0.158572	218		0.926695	67

Batch	Vib Mag	Vib Phase	Pred Mag	Pred Phase	#1 Blade Wt	After Mag	After Phase	#1 Blade P/L	After Mag	After Phase	#1 Blade Tab 8	After Mag	After Phase	#1 Blade Tab 6	After Mag	After Phase	#1 Blade Tab 4	After Mag	After Phase
5																			
FPG100	0.076928	223	0.05257	304	113	0.128526	198	0.5	0.057982	231	0.5	0.076855	223	0.5	0.076852	223	0.5	0.076847	223
Hover Lat	0.053418	349	0.054062	64		0.005569	146		0.124774	32		0.057543	4		0.070255	15		0.090687	20
60K Vert	0.121979	162	0.083888	132		0.146294	177		0.131271	168		0.148736	193		0.185548	205		0.180917	217
80 K Vert	0.18709	180	0.127131	180		0.186691	180		0.192371	192		0.287682	213		0.329073	230		0.443026	238
100 K Vert	0.27539	200	0.189534	211		0.274885	199		0.306264	211		0.392837	223		0.485834	228		0.587399	236
120 K Vert	0.105057	185	0.051384	275		0.104407	185		0.156633	212		0.279717	232		0.379633	241		0.523171	249
140 K Vert	0.102098	163	0.077709	327		0.101485	163		0.167366	209		0.316634	225		0.434218	236		0.698403	230

Batch	Vib Mag	Vib Phase	Pred Mag	Pred Phase	#1 Blade Wt	After Mag	After Phase	#1 Blade P/L	After Mag	After Phase	#1 Blade Tab 8	After Mag	After Phase	#1 Blade Tab 6	After Mag	After Phase	#1 Blade Tab 4	After Mag	After Phase
6																			
FPG100	0.058034	328	0.085174	316	-113	0.123438	339	0.5	0.07238	342	0.5	0.058168	328	0.5	0.058166	328	0.5	0.058161	328
Hover Lat	0.145198	158	0.053947	220		0.088104	153		0.152501	123		0.148386	153		0.144443	146		0.138899	138
60K Vert	0.178742	169	0.132312	134		0.158992	156		0.18912	173		0.206693	190		0.240164	199		0.230777	209
80 K Vert	0.185945	203	0.040172	115		0.185349	203		0.206009	213		0.321763	226		0.378246	239		0.497114	244
100 K Vert	0.167916	185	0.154589	113		0.167401	185		0.188359	205		0.272053	225		0.365445	230		0.470505	240
120 K Vert	0.196544	188	0.164774	98		0.195789	188		0.243783	204		0.351761	222		0.441164	232		0.572332	241
140 K Vert	0.311266	225	0.017861	266		0.310391	225		0.424809	231		0.584243	234		0.707403	239		0.96529	234

Batch	Vib Mag	Vib Phase	Pred Mag	Pred Phase	#1 Blade Wt	After Mag	After Phase	#1 Blade P/L	After Mag	After Phase	#1 Blade Tab 8	After Mag	After Phase	#1 Blade Tab 6	After Mag	After Phase	#1 Blade Tab 4	After Mag	After Phase
7																			
FPG100	0.100501	282	0.067864	274	113	0.095982	243	0.5	0.099301	294	0.5	0.100566	282	0.5	0.100562	282	0.5	0.100555	282
Hover Lat	0.163468	89	0.064378	90		0.18448	107		0.245333	77		0.177366	87		0.191951	84		0.207052	80
60K Vert	0.159363	74	0.096368	171		0.124405	83		0.146135	77		0.085231	79		0.038594	101		0.018376	25
80 K Vert	0.160485	78	0.144015	258		0.160994	78		0.121549	74		0.018563	184		0.093068	275		0.215603	266
100 K Vert	0.159045	74	0.188453	221		0.159608	74		0.097028	66		0.028588	306		0.115149	258		0.240822	264
120 K Vert	0.475223	56	0.123231	40		0.47599	56		0.399609	54		0.271576	43		0.20052	22		0.201417	336
140 K Vert	0.321169	70	0.044154	289		0.321865	70		0.202355	73		0.053521	108		0.091956	249		0.352169	227

Batch	Vib Mag	Vib Phase	Pred Mag	Pred Phase	#1 Blade Wt	After Mag	After Phase	#1 Blade P/L	After Mag	After Phase	#1 Blade Tab 8	After Mag	After Phase	#1 Blade Tab 6	After Mag	After Phase	#1 Blade Tab 4	After Mag	After Phase
8																			
FPG100	0.181767	257	0.124307	306	113	0.195687	237	0.5	0.170826	263	0.5	0.181774	257	0.5	0.18177	257	0.5	0.181762	257
Hover Lat	0.140271	224	0.012827	253		0.17846	208		0.052589	205		0.127333	221		0.110383	220		0.088937	220
60K Vert	0.231821	167	0.217138	160		0.256369	175		0.241691	170		0.254755	184		0.283687	193		0.269402	200
80 K Vert	0.113337	141	0.023403	21		0.113304	140		0.094579	160		0.164788	212		0.210957	237		0.330057	245
100 K Vert	0.111833	99	0.03246	333		0.112247	98		0.050251	113		0.07791	237		0.175562	242		0.293635	253
120 K Vert	0.198608	109	0.073491	70		0.198909	108		0.147252	128		0.131022	189		0.193662	223		0.320978	243
140 K Vert	0.346395	149	0.188134	170		0.345975	148		0.351524	168		0.426549	190		0.483485	205		0.746699	211

Batch	Vib Mag	Vib Phase	Pred Mag	Pred Phase	#1 Blade Wt	After Mag	After Phase	#1 Blade P/L	After Mag	After Phase	#1 Blade Tab 8	After Mag	After Phase	#1 Blade Tab 6	After Mag	After Phase	#1 Blade Tab 4	After Mag	After Phase
9																			
FPG100	0.188258	234	0.092984	217	113	0.22474	219	0.5	0.171031	238	0.5	0.18821	234	0.5	0.188206	234	0.5	0.1882	234
Hover Lat	0.169459	304	0.113618	357		0.132513	287		0.162086	337		0.161245	308		0.157785	315		0.162152	322
60K Vert	0.199788	160	0.152296	133		0.222388	172		0.208802	166		0.219369	182		0.248224	193		0.234358	202
80 K Vert	0.314941	162	0.256443	142		0.314709	160		0.305119	168		0.354066	189		0.354584	204		0.439663	218
100 K Vert	0.42366	176	0.101127	180		0.423303	176		0.42799	185		0.474049	199		0.546207	206		0.614516	217
120 K Vert	0.178907	130	0.164599	44		0.178922	130		0.15658	156		0.195793	202		0.268312	223		0.394085	240
140 K Vert	0.121618	115	0.179962	12		0.12171	115		0.100504	180		0.228055	219		0.341277	235		0.606805	229

Batch	Vib Mag	Vib Phase	Pred Mag	Pred Phase	#1 Blade Wt	After Mag	After Phase	#1 Blade P/L	After Mag	After Phase	#1 Blade Tab 8	After Mag	After Phase	#1 Blade Tab 6	After Mag	After Phase	#1 Blade Tab 4	After Mag	After Phase
10																			
FPG100	0.02973	151	0.066929	71	113	0.09612	163	0.5	0.023176	106	0.5	0.029594	151	-0.5	0.029592	151	0.5	0.029599	151
Hover Lat	0.208752	70	0.020881	60		0.209642	86		0.299246	65		0.23428	70		0.17728	71		0.258828	66
60K Vert	0.187317	257	0.093792	284		0.223984	252		0.200559	255		0.261962	255		0.067599	280		0.336206	258
80 K Vert	0.055764	227	0.058781	199		0.055172	227		0.089836	244		0.219491	245		0.211393	93		0.424208	258
100 K Vert	0.152948	179	0.174757	144		0.152568	179		0.168604	202		0.250803	224		0.283257	108		0.451062	241
120 K Vert	0.224711	204	0.11342	175		0.223947	204		0.285504	215		0.408362	228		0.262655	118		0.637406	243
140 K Vert	0.266139	256	0.104149	211		0.265507	257		0.384814	253		0.545129	250		0.155362	59		0.920487	243

Batch	Vib Mag	Vib Phase	Pred Mag	Pred Phase	#1 Blade Wt	After Mag	After Phase	#1 Blade P/L	After Mag	After Phase	#1 Blade Tab 8	After Mag	After Phase	#1 Blade Tab 6	After Mag	After Phase	#1 Blade Tab 4	After Mag	After Phase
11																			
FPG100	0.155697	242	0.121463	236	113	0.187112	222	-0.5	0.172175	237	0.5	0.155666	242	0.5	0.155662	242	0.5	0.155656	242
Hover Lat	0.218824	302	0.053623	37		0.182246	289		0.26922	283		0.210001	305		0.205291	310		0.207494	316
60K Vert	0.472251	137	0.186364	159		0.475917	142		0.470557	135		0.45173	146		0.48054	153		0.413171	155
80 K Vert	0.55443	140	0.147788	208		0.5544	140		0.580023	137		0.517773	158		0.464296	167		0.477673	182
100 K Vert	0.744927	138	0.196002	190		0.744966	138		0.788168	134		0.66166	151		0.659843	159		0.626993	170
120 K Vert	0.583765	120	0.22742	302		0.58392	120		0.636888	114		0.462564	140		0.413339	153		0.37252	176
140 K Vert	0.580582	111	0.215469	251		0.580734	111		0.671374	104		0.442179	139		0.382261	157		0.559348	182

Batch	Vib Mag	Vib Phase	Pred Mag	Pred Phase	#1 Blade Wt	After Mag	After Phase	#1 Blade P/L	After Mag	After Phase	#1 Blade Tab 8	After Mag	After Phase	#1 Blade Tab 6	After Mag	After Phase	#1 Blade Tab 4	After Mag	After Phase
12																			
FPG100	0.049782	314	0.132554	283	113	0.039056	216	0.5	0.060658	332	0.5	0.049902	314	0.5	0.049899	314	-0.5	0.049902	314
Hover Lat	0.261302	183	0.073662	134		0.317608	180		0.217448	163		0.256119	180		0.246148	176		0.29822	190
60K Vert	0.32757	118	0.122269	167		0.317984	125		0.324451	121		0.285814	130		0.269119	140		0.452605	106
80 K Vert	0.23601	117	0.271751	249		0.236219	116		0.201884	122		0.167127	161		0.137325	196		0.585714	95
100 K Vert	0.400815	87	0.093329	32		0.40131	87		0.336209	87		0.224528	92		0.142525	109		0.798054	84
120 K Vert	0.747712	70	0.237599	28		0.748407	70		0.66981	70		0.52819	69		0.42224	65		1.225449	74
140 K Vert	0.364869	67	0.11905	267		0.365596	67		0.245663	67		0.086497	78		0.052093	272		1.022364	61

Batch	Vib Mag	Vib Phase	Pred Mag	Pred Phase	#1 Blade Wt	After Mag	After Phase	#1 Blade P/L	After Mag	After Phase	#1 Blade Tab 8	After Mag	After Phase	#1 Blade Tab 6	After Mag	After Phase	#1 Blade Tab 4	After Mag	After Phase
13																			
FPG100	0.137813	250	0.07271	242	113	0.162154	226	0.5	0.125001	257	0.5	0.137803	250	0.5	0.137799	250	0.5	0.137792	250
Hover Lat	0.057329	273	0.04486	346		0.06955	219		0.058708	18		0.04204	280		0.034797	302		0.039166	335
60K Vert	0.09722	275	0.161231	184		0.128036	261		0.107375	268		0.167252	263		0.21608	259		0.242892	266
80 K Vert	0.140983	317	0.214978	179		0.140984	318		0.169691	307		0.258399	281		0.353432	283		0.470037	277
100 K Vert	0.496776	343	0.155533	322		0.497008	343		0.515872	336		0.550931	325		0.578108	315		0.672895	307
120 K Vert	0.581443	342	0.141403	336		0.581852	342		0.582847	334		0.624403	321		0.688875	313		0.808119	306
140 K Vert	0.688503	336	0.127493	344		0.689028	336		0.698035	327		0.73064	314		0.825066	306		0.88368	289

Batch	Vib Mag	Vib Phase	Pred Mag	Pred Phase	#1 Blade Wt	After Mag	After Phase	#1 Blade P/L	After Mag	After Phase	#1 Blade Tab 8	After Mag	After Phase	#1 Blade Tab 6	After Mag	After Phase	#1 Blade Tab 4	After Mag	After Phase
14																			
FPG100	0.207505	298	0.064603	310	113	0.173548	280	-0.5	0.206539	292	0.5	0.207601	298	0.5	0.207597	298	0.5	0.20759	298
Hover Lat	0.683454	321	0.059474	317		0.631851	319		0.69808	313		0.678746	322		0.678691	324		0.685152	325
60K Vert	0.291504	164	0.211339	177		0.314171	171		0.282554	162		0.3094	178		0.333832	186		0.315249	192
80 K Vert	0.250215	139	0.139924	66		0.250201	139		0.27732	132		0.24122	178		0.230616	202		0.315958	221
100 K Vert	0.259832	113	0.264753	46		0.260118	113		0.319709	108		0.143394	154		0.171053	189		0.228997	222
120 K Vert	0.494931	146	0.070155	74		0.494724	146		0.517903	137		0.48093	172		0.491599	185		0.530063	202
140 K Vert	0.559829	137	0.074699	91		0.559571	137		0.608198	127		0.552221	167		0.553383	181		0.780427	193

Batch	Vib Mag	Vib Phase	Pred Mag	Pred Phase	#1 Blade Wt	After Mag	After Phase	#1 Blade P/L	After Mag	After Phase	#1 Blade Tab 8	After Mag	After Phase	#1 Blade Tab 6	After Mag	After Phase	#1 Blade Tab 4	After Mag	After Phase
15																			
FPG100	0.123747	231	0.057057	209	113	0.166498	210	0.5	0.105958	236	0.5	0.123691	231	0.5	0.123688	231	0.5	0.123682	231
Hover Lat	0.12058	340	0.120951	14		0.062788	334		0.170657	12		0.121462	347		0.129646	354		0.146341	0
60K Vert	0.192154	187	0.126067	112		0.22683	193		0.205867	189		0.238287	203		0.279266	210		0.276322	218
80 K Vert	0.326912	187	0.220933	149		0.326463	187		0.335157	193		0.426186	208		0.45491	220		0.557936	228
100 K Vert	0.54274	204	0.069744	174		0.542189	204		0.575611	210		0.657579	218		0.746397	221		0.836961	228
120 K Vert	0.240951	174	0.240769	63		0.240405	174		0.271962	190		0.35808	211		0.435871	223		0.555876	235
140 K Vert	0.179458	206	0.237107	14		0.178552	206		0.282057	222		0.438631	229		0.558847	237		0.821925	232

Batch	Vib Mag	Vib Phase	Pred Mag	Pred Phase	#1 Blade Wt	After Mag	After Phase	#1 Blade P/L	After Mag	After Phase	#1 Blade Tab 8	After Mag	After Phase	#1 Blade Tab 6	After Mag	After Phase	#1 Blade Tab 4	After Mag	After Phase
16																			
FPG100	0.311844	357	0.180622	318	113	0.245719	359	0.5	0.330824	358	0.5	0.31198	357	0.5	0.311981	357	0.5	0.31198	357
Hover Lat	0.695	70	0.246018	218		0.690681	75		0.784188	68		0.709591	70		0.726191	70		0.744296	69
60K Vert	0.255071	176	0.076453	142		0.284171	182		0.266742	178		0.28735	190		0.320248	197		0.3088	204
80 K Vert	0.162979	190	0.16985	89		0.162509	190		0.175748	203		0.28365	221		0.335353	236		0.452963	242
100 K Vert	0.3304	229	0.227316	96		0.329789	229		0.383336	235		0.489671	240		0.587511	241		0.701583	246
120 K Vert	0.642435	166	0.679946	105		0.641974	166		0.657062	173		0.692817	185		0.723634	193		0.776441	205
140 K Vert	1.612921	235	0.62767	241		1.612099	235		1.730033	236		1.890659	236		2.014101	238		2.271375	236

Batch	Vib Mag	Vib Phase	Pred Mag	Pred Phase	#1 Blade Wt	After Mag	After Phase	#1 Blade P/L	After Mag	After Phase	#1 Blade Tab 8	After Mag	After Phase	#1 Blade Tab 6	After Mag	After Phase	#1 Blade Tab 4	After Mag	After Phase
17																			
FPG100	0.157059	11	0.10917	315	113	0.098459	26	0.5	0.177518	12	0.5	0.157183	11	0.5	0.157184	11	0.5	0.157185	11
Hover Lat	0.432138	103	0.208548	221		0.460417	109		0.498495	95		0.444502	102		0.456112	100		0.466151	98
60K Vert	0.366045	137	0.22409	108		0.369637	143		0.368098	139		0.346466	148		0.345399	157		0.312227	160
80 K Vert	0.19705	159	0.110409	359		0.159485	159		0.151606	174		0.226234	207		0.260898	228		0.37319	238
100 K Vert	0.192427	184	0.141118	62		0.19201	184		0.210482	202		0.289173	221		0.380587	227		0.481975	237
120 K Vert	0.746078	150	0.547388	114		0.745815	150		0.738267	156		0.731419	167		0.728896	176		0.736438	188
140 K Vert	1.035895	235	0.666506	260		1.035075	235		1.153214	236		1.314037	237		1.438741	239		1.694521	236

Batch	Vib Mag	Vib Phase	Pred Mag	Pred Phase	#1 Blade Wt	After Mag	After Phase	#1 Blade P/L	After Mag	After Phase	#1 Blade Tab 8	After Mag	After Phase	#1 Blade Tab 6	After Mag	After Phase	#1 Blade Tab 4	After Mag	After Phase
18																			
FPG100	0.239721	42	0.239662	42	113	0.206238	57	0.5	0.259357	40	0.5	0.239797	42	0.5	0.2398	42	0.5	0.239805	42
Hover Lat	0.308792	283	0.112868	266		0.287895	273		0.256906	299		0.296643	285		0.286212	287		0.2798	292
60K Vert	1.342822	127	0.557385	140		1.337391	128		1.341781	127		1.305818	129		1.285603	131		1.247222	132
80 K Vert	1.262397	128	0.401148	340		1.262495	128		1.231964	129		1.17803	135		1.095036	137		1.034667	143
100 K Vert	2.152217	132	0.414499	150		2.152318	132		2.106725	133		2.042775	136		2.010602	138		1.929183	141
120 K Vert	2.272505	128	0.157378	141		2.272541	128		2.233769	130		2.156429	133		2.087569	135		1.982885	139
140 K Vert	2.205741	131	0.611424	264		2.205678	131		2.158372	134		2.114862	138		2.038818	141		2.108201	149

Batch	Vib Mag	Vib Phase	Pred Mag	Pred Phase	#1 Blade Wt	After Mag	After Phase	#1 Blade P/L	After Mag	After Phase	#1 Blade Tab 8	After Mag	After Phase	#1 Blade Tab 6	After Mag	After Phase	#1 Blade Tab 4	After Mag	After Phase
19																			
FPG100	0.164325	125	0.079066	111	113	0.217753	137	0.5	0.160776	118	0.5	0.164217	125	0.5	0.16422	125	-0.5	0.164219	125
Hover Lat	0.430017	175	0.115959	203		0.487524	174		0.391272	164		0.426441	174		0.417871	171		0.46122	181
60K Vert	0.423048	194	0.098588	252		0.459482	197		0.437574	195		0.471508	201		0.510449	205		0.384808	174
80 K Vert	0.414549	196	0.143595	24		0.414047	196		0.428354	201		0.526792	211		0.558809	221		0.432868	143
100 K Vert	0.416661	197	0.219134	325		0.416153	197		0.443265	205		0.519401	215		0.606057	220		0.425181	141
120 K Vert	0.859669	194	0.20682	208		0.858961	194		0.906617	198		0.992231	205		1.054709	210		0.798171	160
140 K Vert	0.668493	213	0.146644	276		0.667592	213		0.770888	217		0.920613	222		1.027591	227		0.294741	137

Batch	Vib Mag	Vib Phase	Pred Mag	Pred Phase	#1 Blade Wt	After Mag	After Phase	#1 Blade P/L	After Mag	After Phase	#1 Blade Tab 8	After Mag	After Phase	#1 Blade Tab 6	After Mag	After Phase	#1 Blade Tab 4	After Mag	After Phase
20																			
FPG100	0.144012	292	0.041371	115	113	0.12063	265	0.5	0.145789	301	0.5	0.144098	292	0.5	0.144094	292	0.5	0.144087	292
Hover Lat	0.141529	219	0.040576	65		0.183162	204		0.058847	193		0.129321	215		0.112888	213		0.091483	212
60K Vert	0.70392	348	0.148341	18		0.681708	346		0.694142	347		0.693702	342		0.687902	338		0.72144	337
80 K Vert	0.96919	356	0.067199	342		0.969558	356		0.971437	354		0.941132	346		0.991996	342		1.015132	335
100 K Vert	0.908439	351	0.087184	170		0.908741	351		0.917788	347		0.928175	340		0.926903	334		0.988817	327
120 K Vert	1.39741	349	0.180572	341		1.397896	349		1.386565	345		1.391672	340		1.421293	335		1.491641	330
140 K Vert	1.45824	339	0.160983	218		1.458802	339		1.45629	335		1.457185	328		1.520578	324		1.480971	313

Batch	Vib Mag	Vib Phase	Pred Mag	Pred Phase	#1 Blade Wt	After Mag	After Phase	After P/L	After Mag	After Phase	#1 Blade Tab 8	After Mag	After Phase	#1 Blade Tab 6	After Mag	After Phase	#1 Blade Tab 4	After Mag	After Phase
1																			
FPG100	0.116931	166	0.058835	298	1017	0.71337	169	12	0.344675	34	5	0.116923	166	5	0.116908	166	5	0.116913	166
Hover Lat	0.085828	200	0.072847	250		0.590163	171		1.856367	58		0.117796	106		0.260573	74		0.451984	57
60K Vert	0.171535	168	0.087651	129		0.489369	208		0.475601	194		0.816862	236		1.315563	239		1.496725	260
80 K Vert	0.133674	192	0.097796	197		0.13367	192		0.786202	252		1.779134	248		2.569398	261		3.821504	252
100 K Vert	0.130108	184	0.070924	191		0.130135	184		1.240264	257		1.858129	258		2.80207	253		4.041442	258
120 K Vert	0.107955	160	0.035466	161		0.107972	160		1.536802	240		2.25438	250		3.303877	254		4.832154	259
140 K Vert	0.090145	177	0.042047	285		0.090179	177		2.377982	241		2.914765	242		4.182457	249		6.676825	237

Batch	Vib Mag	Vib Phase	Pred Mag	Pred Phase	#1 Blade Wt	After Mag	After Phase	After P/L	After Mag	After Phase	#1 Blade Tab 8	After Mag	After Phase	#1 Blade Tab 6	After Mag	After Phase	#1 Blade Tab 4	After Mag	After Phase
2																			
FPG100	0.068736	225	0.057926	258	1017	0.637501	174	12	0.369998	18	5	0.06877	225	5	0.068641	225	5	0.068641	225
Hover Lat	0.156707	214	0.025258	295		0.633707	177		1.780738	58		0.09821	146		0.193111	83		0.376208	58
60K Vert	0.074744	147	0.023543	156		0.397342	214		0.373734	198		0.75969	243		1.260388	243		1.464157	256
80 K Vert	0.07762	163	0.095848	297		0.077646	163		0.722592	256		1.711935	249		2.511393	262		3.762075	261
100 K Vert	0.142985	130	0.01744	341		0.14307	130		1.114642	257		1.732849	259		2.676177	254		3.916322	258
120 K Vert	0.203573	145	0.074586	201		0.20361	145		1.505177	236		2.204178	248		3.247396	253		4.768844	258
140 K Vert	0.252516	134	0.114811	207		0.252607	134		2.271931	237		2.802599	239		4.052395	247		6.579211	236

Batch	Vib Mag	Vib Phase	Pred Mag	Pred Phase	#1 Blade Wt	After Mag	After Phase	After P/L	After Mag	After Phase	#1 Blade Tab 8	After Mag	After Phase	#1 Blade Tab 6	After Mag	After Phase	#1 Blade Tab 4	After Mag	After Phase
3																			
FPG100	0.127352	110	0.068366	182	1017	0.671905	160	12	0.455518	39	5	0.12731	110	5	0.12742	110	5	0.127425	110
Hover Lat	0.195151	81	0.09695	79		0.565733	147		2.102551	58		0.344023	77		0.506131	69		0.698256	59
60K Vert	0.022116	347	0.120537	318		0.363147	228		0.314726	211		0.76638	250		1.26434	247		1.489629	260
80 K Vert	0.182843	186	0.102055	266		0.182844	186		0.795979	249		1.791738	247		2.570546	260		3.823673	259
100 K Vert	0.051449	284	0.059642	338		0.05136	284		1.255083	264		1.873559	263		2.803361	256		4.053417	260
120 K Vert	0.16641	171	0.019174	213		0.166411	171		1.57769	238		2.285292	249		3.330772	253		4.854124	258
140 K Vert	0.20431	135	0.085837	30		0.2044	135		2.286325	238		2.818814	240		4.07375	247		6.590927	236

Batch	Vib Mag	Vib Phase	Pred Mag	Pred Phase	#1 Blade Wt	After Mag	After Phase	After P/L	After Mag	After Phase	#1 Blade Tab 8	After Mag	After Phase	#1 Blade Tab 6	After Mag	After Phase	#1 Blade Tab 4	After Mag	After Phase
4																			
FPG100	0.120262	246	0.120246	246	1017	0.636977	180	12	0.355318	9	5	0.120305	246	5	0.120162	246	5	0.12016	246
Hover Lat	0.110412	31	0.118456	44		0.444821	157		0.2028791	55		0.245869	54		0.41875	54		0.629032	48
60K Vert	0.143915	170	0.142603	208		0.472844	211		0.454264	197		0.813757	238		1.314798	240		1.503214	253
80 K Vert	0.143248	132	0.064338	205		0.143299	132		0.648876	252		1.644455	248		2.436049	262		3.690161	260
100 K Vert	0.243478	97	0.040356	33		0.243565	97		0.975788	259		1.596196	260		2.538946	254		3.784738	259
120 K Vert	0.153558	129	0.12044	243		0.153615	129		1.466056	238		2.179239	250		3.229531	254		4.579831	259
140 K Vert	0.290249	87	0.030551	37		0.290344	87		2.081695	239		2.617923	242		3.885601	249		6.391989	237

Batch	Vib Mag	Vib Phase	Pred Mag	Pred Phase	#1 Blade Wt	After Mag	After Phase	After P/L	After Mag	After Phase	#1 Blade Tab 8	After Mag	After Phase	#1 Blade Tab 6	After Mag	After Phase	#1 Blade Tab 4	After Mag	After Phase
5																			
FPG100	0.076928	223	0.05257	304	1017	0.649588	175	12	0.365107	18	5	0.076961	223	5	0.076833	223	5	0.076833	223
Hover Lat	0.053418	349	0.054062	64		0.46741	167		1.964095	55		0.16771	53		0.341972	52		0.555073	46
60K Vert	0.121979	162	0.083888	132		0.447155	211		0.428468	196		0.794981	239		1.299291	241		1.493431	254
80 K Vert	0.18709	180	0.127131	180		0.187099	180		0.785047	248		1.789285	246		2.572251	260		3.835695	259
100 K Vert	0.27539	200	0.189534	211		0.275394	200		1.364347	252		1.98375	255		2.943133	252		4.184375	257
120 K Vert	0.105057	185	0.051384	275		0.105037	185		1.592405	240		2.319458	251		3.378897	254		4.921206	259
140 K Vert	0.102098	163	0.077709	327		0.102155	163		2.381063	240		2.92209	242		4.199339	249		6.719731	237

Batch	Vib Mag	Vib Phase	Pred Mag	Pred Phase	#1 Blade Wt	After Mag	After Phase	After P/L	After Mag	After Phase	#1 Blade Tab 8	After Mag	After Phase	#1 Blade Tab 6	After Mag	After Phase	#1 Blade Tab 4	After Mag	After Phase
6																			
FPG100	0.058034	328	0.085174	316	1017	0.543826	171	12	0.46924	17	5	0.058055	328	5	0.058025	328	5	0.05802	328
Hover Lat	0.145198	158	0.053947	220		0.659995	165		1.898592	60		0.21359	114		0.332585	87		0.498936	67
60K Vert	0.178742	169	0.132312	134		0.496528	208		0.483151	194		0.821841	236		1.320115	238		1.499671	252
80 K Vert	0.185945	203	0.040172	115		0.185928	203		0.824393	251		1.837547	248		2.622165	260		3.874937	260
100 K Vert	0.167916	185	0.154589	113		0.167942	185		1.255086	255		1.872162	257		2.819199	253		4.056128	258
120 K Vert	0.196544	188	0.164774	98		0.196521	188		1.639719	238		2.346771	249		3.391516	253		4.913641	258
140 K Vert	0.311266	225	0.017861	266		0.311219	225		2.63983	241		3.176988	242		4.443387	248		6.943069	237

Batch	Vib Mag	Vib Phase	Pred Mag	Pred Phase	#1 Blade Wt	After Mag	After Phase	After P/L	After Mag	After Phase	#1 Blade Tab 8	After Mag	After Phase	#1 Blade Tab 6	After Mag	After Phase	#1 Blade Tab 4	After Mag	After Phase
7																			
FPG100	0.100501	282	0.067864	274	1017	0.564717	178	12	0.426542	9	5	0.100545	282	5	0.100423	282	5	0.100419	282
Hover Lat	0.163468	89	0.064378	90		0.573132	151		2.066057	58		0.31012	80		0.46978	70		0.660264	60
60K Vert	0.159363	74	0.096368	171		0.247616	207		0.248759	180		0.61214	247		1.124233	245		1.332035	260
80 K Vert	0.160485	78	0.144015	258		0.160544	78		0.570793	263		1.550812	252		2.367776	264		3.616577	262
100 K Vert	0.159045	74	0.188453	221		0.159116	74		1.051279	264		1.670382	263		2.60203	256		3.852746	260
120 K Vert	0.475223	56	0.123231	40		0.475298	56		1.053928	247		1.811342	258		2.875036	259		4.424664	262
140 K Vert	0.321169	70	0.044154	289		0.32125	70		2.024632	241		2.563408	243		3.840002	250		6.329074	237

Batch	Vib Mag	Vib Phase	Pred Mag	Pred Phase	#1 Blade Wt	After Mag	After Phase	After P/L	After Mag	After Phase	#1 Blade Tab 8	After Mag	After Phase	#1 Blade Tab 6	After Mag	After Phase	#1 Blade Tab 4	After Mag	After Phase
8																			
FPG100	0.181767	257	0.124307	306	1017	0.630141	186	12	0.359302	358	5	0.181812	257	5	0.18167	257	5	0.181667	257
Hover Lat	0.140271	224	0.012827	253		0.603691	178		1.787935	57		0.068145	139		0.18884	73		0.384182	53
60K Vert	0.231821	167	0.217138	160		0.5342	203		0.52823	191		0.836657	232		1.331732	236		1.498411	250
80 K Vert	0.113337	141	0.023403	21		0.113382	141		0.679028	253		1.670947	248		2.464538	262		3.71558	260
100 K Vert	0.111833	99	0.03246	333		0.11192	99		1.099109	261		1.71762	261		2.653163	255		3.898038	259
120 K Vert	0.198608	109	0.073491	70		0.198682	109		1.38758	238		2.098823	250		3.14729	254		4.675208	259
140 K Vert	0.346395	149	0.188134	170		0.346471	149		2.342231	234		2.867989	237		4.103662	245		6.650371	235

Batch	Vib Mag	Vib Phase	Pred Mag	Pred Phase	#1 Blade Wt	After Mag	After Phase	#1 Blade P/L	After Mag	After Phase	#1 Blade Tab 8	After Mag	After Phase	#1 Blade Tab 6	After Mag	After Phase	#1 Blade Tab 4	After Mag	After Phase
9																			
FPG100	0.188258	234	0.092984	217	-1017	0.550165	331	12	0.293456	3	5	0.188297	234	5	0.188159	234	5	0.188158	234
Hover Lat	0.169459	304	0.113618	357		0.654834	337		1.885267	51		0.144642	1		0.288027	29		0.50561	32
60K Vert	0.199788	162	0.152296	133		0.337019	77		0.494892	191		0.815849	234		1.316933	237		1.492412	251
80 K Vert	0.314941	160	0.255443	142		0.314943	160		0.742689	237		1.742701	242		2.490916	257		3.754189	257
100 K Vert	0.42366	176	0.101127	180		0.423669	176		1.316413	244		1.92248	249		2.891322	248		4.114307	254
120 K Vert	0.178907	130	0.164599	44		0.178925	130		1.470797	237		2.183362	249		3.238267	253		4.775866	258
140 K Vert	0.121618	115	0.179962	12		0.121667	115		2.287389	240		2.828334	242		4.106228	249		6.625158	237

Batch	Vib Mag	Vib Phase	Pred Mag	Pred Phase	#1 Blade Wt	After Mag	After Phase	#1 Blade P/L	After Mag	After Phase	#1 Blade Tab 8	After Mag	After Phase	#1 Blade Tab 6	After Mag	After Phase	#1 Blade Tab 4	After Mag	After Phase
10																			
FPG100	0.02973	151	0.066929	71	1017	0.628754	168	12	0.41729	26	5	0.02971	151	5	0.029734	151	5	0.02974	151
Hover Lat	0.208752	70	0.020881	60		0.534902	144		2.140504	57		0.359976	70		0.527995	64		0.727151	56
60K Vert	0.187317	257	0.093792	284		0.544493	236		0.476873	225		0.960376	250		1.461695	247		1.686846	259
80 K Vert	0.055764	227	0.058781	199		0.055725	227		0.781828	259		1.771714	251		2.587656	263		3.845902	261
100 K Vert	0.152948	179	0.174757	144		0.152982	179		1.242964	256		1.864559	257		2.817194	253		4.063365	258
120 K Vert	0.224711	204	0.11342	175		0.224666	204		1.710399	239		2.425865	249		3.478489	253		5.011434	258
140 K Vert	0.266139	256	0.104149	211		0.266052	256		2.615599	244		3.160133	245		4.450511	250		6.934935	239

Batch	Vib Mag	Vib Phase	Pred Mag	Pred Phase	#1 Blade Wt	After Mag	After Phase	#1 Blade P/L	After Mag	After Phase	#1 Blade Tab 8	After Mag	After Phase	#1 Blade Tab 6	After Mag	After Phase	#1 Blade Tab 4	After Mag	After Phase
11																			
FPG100	0.155697	242	0.121463	236	1017	0.664868	182	12	0.330303	5	5	0.155739	242	5	0.155597	242	-5	0.155784	242
Hover Lat	0.218824	302	0.053623	37		0.397526	190		1.862913	50		0.170182	346		0.287575	19		0.634362	250
60K Vert	0.472251	137	0.186364	159		0.616731	175		0.663001	166		0.752348	212		1.214193	224		1.796736	92
80 K Vert	0.55443	140	0.147788	208		0.554476	140		0.652036	215		1.602311	233		2.28559	252		4.128343	88
100 K Vert	0.744927	138	0.196002	190		0.745008	138		0.99787	225		1.547226	239		2.515065	241		4.4906	88
120 K Vert	0.583765	120	0.22742	302		0.583831	120		1.301713	222		1.923328	240		2.947209	248		5.358638	84
140 K Vert	0.580582	111	0.215469	251		0.580684	111		2.022041	230		2.543051	234		3.772827	244		7.062186	62

Batch	Vib Mag	Vib Phase	Pred Mag	Pred Phase	#1 Blade Wt	After Mag	After Phase	#1 Blade P/L	After Mag	After Phase	#1 Blade Tab 8	After Mag	After Phase	#1 Blade Tab 6	After Mag	After Phase	#1 Blade Tab 4	After Mag	After Phase
12																			
FPG100	0.049782	314	0.132554	283	1017	0.556746	172	12	0.452411	17	5	0.049813	314	5	0.049749	314	5	0.049743	314
Hover Lat	0.261302	183	0.073662	134		0.771312	172		1.782661	63		0.249049	148		0.287576	112		0.400633	80
60K Vert	0.32757	118	0.122269	167		0.419771	177		0.466535	163		0.61298	224		1.09867	232		1.252698	249
80 K Vert	0.23601	117	0.271751	249		0.236089	117		0.554077	247		1.550468	246		2.331051	261		3.583693	260
100 K Vert	0.400815	87	0.093329	32		0.400896	87		0.808371	260		1.427405	261		2.36663	254		3.610127	259
120 K Vert	0.747712	70	0.237599	28		0.747794	70		0.782247	238		1.512189	255		2.571789	258		4.116228	262
140 K Vert	0.364869	67	0.11905	267		0.364946	67		1.97686	242		2.51566	244		3.793243	250		6.276681	237

Batch	Vib Mag	Vib Phase	Pred Mag	Pred Phase	#1 Blade Wt	After Mag	After Phase	#1 Blade P/L	After Mag	After Phase	#1 Blade Tab 8	After Mag	After Phase	#1 Blade Tab 6	After Mag	After Phase	#1 Blade Tab 4	After Mag	After Phase
13																			
FPG100	0.137813	250	0.07271	242	-1017	0.591773	336	12	0.354906	6	5	0.137857	250	5	0.137714	250	5	0.137712	250
Hover Lat	0.057329	273	0.04486	346		0.534632	341		1.880372	55		0.099419	59		0.271805	55		0.482186	46
60K Vert	0.09722	275	0.161231	184		0.320874	32		0.379489	222		0.857496	251		1.354666	248		1.58301	260
80 K Vert	0.140983	317	0.214978	179		0.140961	317		0.817955	270		1.772937	256		2.612197	266		3.856018	264
100 K Vert	0.496776	343	0.155533	322		0.496753	343		1.377977	283		1.964511	277		2.826306	266		4.095887	267
120 K Vert	0.581443	342	0.141403	336		0.581464	342		1.550214	265		2.344493	267		3.406279	266		4.966219	267
140 K Vert	0.688503	336	0.127493	344		0.688483	336		2.39525	259		2.933731	258		4.255909	259		6.569587	244

Batch	Vib Mag	Vib Phase	Pred Mag	Pred Phase	#1 Blade Wt	After Mag	After Phase	#1 Blade P/L	After Mag	After Phase	#1 Blade Tab 8	After Mag	After Phase	#1 Blade Tab 6	After Mag	After Phase	#1 Blade Tab 4	After Mag	After Phase
14																			
FPG100	0.207505	298	0.064603	310	1017	0.494967	188	12	0.496379	358	5	0.207544	298	5	0.207447	298	5	0.207442	298
Hover Lat	0.683454	321	0.059474	317		0.316308	275		1.984219	36		0.647189	333		0.701351	347		0.859956	358
60K Vert	0.291504	164	0.211339	177		0.576302	199		0.578328	188		0.852091	228		1.342255	234		1.494097	248
80 K Vert	0.250215	139	0.139924	66		0.250282	139		0.63109	242		1.626916	244		2.390288	259		3.643475	259
100 K Vert	0.259632	113	0.264753	46		0.259921	113		0.991798	255		1.60832	257		2.55476	252		3.790211	258
120 K Vert	0.494931	146	0.070155	74		0.494966	146		1.535719	225		2.164499	240		3.178154	248		4.670109	254
140 K Vert	0.559829	137	0.074699	91		0.559917	137		2.257887	229		2.769734	233		3.973231	243		6.552264	233

Batch	Vib Mag	Vib Phase	Pred Mag	Pred Phase	#1 Blade Wt	After Mag	After Phase	#1 Blade P/L	After Mag	After Phase	#1 Blade Tab 8	After Mag	After Phase	#1 Blade Tab 6	After Mag	After Phase	#1 Blade Tab 4	After Mag	After Phase
15																			
FPG100	0.123747	231	0.057057	209	1017	0.669136	178	12	0.332452	12	5	0.123784	231	5	0.123649	231	5	0.123648	231
Hover Lat	0.12058	340	0.120951	14		0.401281	169		1.975651	53		0.192415	32		0.361088	42		0.578974	40
60K Vert	0.192154	187	0.126067	112		0.541959	212		0.51804	200		0.885042	237		1.388495	239		1.572257	252
80 K Vert	0.326912	187	0.220933	149		0.326913	187		0.880188	241		1.8839	243		2.638854	257		3.903277	257
100 K Vert	0.54274	204	0.069744	174		0.542736	204		1.572956	246		2.181455	250		3.149264	248		4.373304	254
120 K Vert	0.240951	174	0.240769	63		0.240947	174		1.63408	236		2.335333	247		3.384948	252		4.91589	257
140 K Vert	0.179458	206	0.237107	14		0.179443	206		2.506387	240		3.047442	242		4.323606	248		6.856359	237

Batch	Vib Mag	Vib Phase	Pred Mag	Pred Phase	#1 Blade Wt	After Mag	After Phase	#1 Blade P/L	After Mag	After Phase	#1 Blade Tab 8	After Mag	After Phase	#1 Blade Tab 6	After Mag	After Phase	#1 Blade Tab 4	After Mag	After Phase
16																			
FPG100	0.311844	357	0.180622	318	1017	0.290842	160	12	0.726018	12	5	0.311844	357	5	0.311885	357	5	0.311881	357
Hover Lat	0.695	70	0.246018	218		0.815969	109		2.604943	60		0.845349	70		1.01099	67		1.201418	62
60K Vert	0.255071	176	0.076453	142		0.574333	205		0.563606	194		0.881057	232		1.375856	236		1.540114	249
80 K Vert	0.162979	190	0.16985	89		0.162976	190		0.797915	250		1.792347	248		2.576306	261		3.82874	260
100 K Vert	0.3304	229	0.227316	96		0.330359	229		1.492981	256		2.109756	257		3.055078	253		4.291877	258
120 K Vert	0.642435	166	0.679946	105		0.642443	166		1.776704	223		2.382105	237		3.378499	245		4.850572	252
140 K Vert	1.612921	235	0.62767	241		1.61286	235		3.944329	239		4.479083	241		5.729424	246		8.24691	237

Batch	Vib Mag	Vib Phase	Pred Mag	Pred Phase	#1 Blade Wt	After Mag	After Phase	After P/L	After Mag	After Phase	#1 Blade Tab 8	After Mag	After Phase	#1 Blade Tab 6	After Mag	After Phase	#1 Blade Tab 4	After Mag	After Phase
17																			
FPG100	0.157059	11	0.10917	315	-1017	0.744235	354	12	0.586898	20	5	0.157047	11	5	0.15712	11	5	0.157117	11
Hover Lat	0.432138	103	0.208548	221		0.509532	37		2.242161	64		0.565447	95		0.702542	85		0.859898	74
60K Vert	0.366045	137	0.22409	108		0.516297	90		0.566934	170		0.721072	220		1.197664	229		1.32922	245
80 K Vert	0.159705	159	0.110409	359		0.159708	159		0.713587	249		1.708776	247		2.489405	260		3.741624	260
100 K Vert	0.192427	184	0.141118	62		0.192428	184		1.259784	254		1.875682	256		2.82405	252		4.058306	257
120 K Vert	0.746078	150	0.547388	114		0.746071	150		1.653973	217		2.214718	234		3.192674	243		4.651221	251
140 K Vert	1.035895	235	0.666506	260		1.035848	235		3.369772	240		3.905998	242		5.164913	247		7.669677	238

Batch	Vib Mag	Vib Phase	Pred Mag	Pred Phase	#1 Blade Wt	After Mag	After Phase	After P/L	After Mag	After Phase	#1 Blade Tab 8	After Mag	After Phase	#1 Blade Tab 6	After Mag	After Phase	#1 Blade Tab 4	After Mag	After Phase
18																			
FPG100	0.239721	42	0.239662	42	1017	0.490548	146	12	0.663856	29	5	0.239689	42	5	0.239814	42	5	0.239814	42
Hover Lat	0.308792	283	0.112868	266		0.470407	203		1.730708	48		0.198256	307		0.225785	354		0.413629	15
60K Vert	1.342822	127	0.557385	140		1.340143	143		1.430539	140		1.146603	161		1.318412	183		1.150848	199
80 K Vert	1.262397	128	0.401148	340		1.26245	128		0.922089	163		1.443848	206		1.836622	236		3.034757	248
100 K Vert	2.152217	132	0.414499	150		2.152301	132		1.638028	166		1.695274	187		2.356669	207		3.165442	228
120 K Vert	2.272505	128	0.157378	141		2.272562	128		2.125804	169		2.100131	190		2.634756	213		3.747995	233
140 K Vert	2.205741	131	0.611424	264		2.205834	131		2.562974	189		2.864925	199		3.646851	218		6.358806	219

Batch	Vib Mag	Vib Phase	Pred Mag	Pred Phase	#1 Blade Wt	After Mag	After Phase	After P/L	After Mag	After Phase	#1 Blade Tab 8	After Mag	After Phase	#1 Blade Tab 6	After Mag	After Phase	#1 Blade Tab 4	After Mag	After Phase
19																			
FPG100	0.164325	125	0.079066	111	1017	0.724795	160	12	0.42829	45	5	0.164289	125	5	0.164372	125	5	0.164377	125
Hover Lat	0.430017	175	0.115959	203		0.943842	171		1.75484	68		0.418835	155		0.416282	131		0.45179	103
60K Vert	0.423048	194	0.098588	252		0.768904	209		0.748911	200		1.074593	230		1.568039	234		1.712854	246
80 K Vert	0.414549	196	0.143595	24		0.41454	196		0.977026	239		1.970159	242		2.707347	256		3.959875	256
100 K Vert	0.416661	197	0.219134	325		0.416668	197		1.432307	247		2.039001	251		2.996231	249		4.214903	255
120 K Vert	0.859669	194	0.20682	208		0.859638	194		2.178943	226		2.798768	238		3.794526	244		5.25992	251
140 K Vert	0.668493	213	0.146644	276		0.668466	213		2.939964	236		3.469499	238		4.708879	245		7.250772	236

Batch	Vib Mag	Vib Phase	Pred Mag	Pred Phase	#1 Blade Wt	After Mag	After Phase	After P/L	After Mag	After Phase	#1 Blade Tab 8	After Mag	After Phase	#1 Blade Tab 6	After Mag	After Phase	#1 Blade Tab 4	After Mag	After Phase
20																			
FPG100	0.144012	292	0.041371	115	1017	0.531057	182	12	0.455483	4	5	0.144053	292	5	0.143947	292	5	0.143942	292
Hover Lat	0.141529	219	0.040576	65		0.613787	177		1.790217	57		0.081535	139		0.195186	77		0.385914	55
60K Vert	0.70392	348	0.148341	18		0.587388	316		0.495224	323		0.94485	295		1.311113	278		1.652236	284
80 K Vert	0.96919	356	0.067199	342		0.969178	356		1.165633	318		1.745501	285		2.66641	285		3.8202	277
100 K Vert	0.908439	351	0.067184	170		0.908393	351		1.534647	299		2.058194	288		2.831165	275		4.095589	273
120 K Vert	1.39741	349	0.180572	341		1.397406	349		1.781012	293		2.538465	286		3.536542	279		5.077285	276
140 K Vert	1.45824	339	0.160983	218		1.458178	339		2.607763	276		3.105973	272		4.419725	269		6.503921	251

Appendix D: AH-64D Database

Note: All data in this appendix was manually typed into Microsoft Excel spreadsheets. The data was originally presented with a graphic user interface in the PC-GBS program.

Flight Log

Flight #	Type	BUNO	Date	Time	Vib Category
1	AH-64D	00-05184	6/8/2005	25649	good
2	AH-64D	01-05276	9/29/2005	50641	good
3	AH-64D	01-05283	10/14/2005	81022	good
4	AH-64D	96-05024	9/15/2005	44633	good
5	AH-64D	99-05134	10/18/2005	95536	good
6	AH-64D	96-05024	9/15/2005	40530	above
7	AH-64D	99-05134	10/18/2005	40724	above
8	AH-64D	00-05184	8/20/2005	102558	above
9	AH-64D	01-05283	10/13/2005	101630	above
10	AH-64D	96-05024	9/7/2005	72518	above
11	AH-64D	00-05184	8/20/2005	105108	caution
12	AH-64D	01-05283	10/13/2005	95431	caution
13	AH-64D	01-05276	9/29/2005	43748	caution
14	AH-64D	01-05277	10/18/2005	55723	caution
15	AH-64D	01-05277	11/22/2005	25833	caution
16	AH-64D	01-05283	10/13/2005	92020	exceed
17	AH-64D	96-05134	6/9/2005	23649	exceed
18	AH-64D	01-05276	9/29/2005	21844	exceed
19	AH-64D	01-05277	10/18/2005	31631	exceed
20	AH-64D	01-05277	10/18/2005	43503	exceed

Flight #	1					2					3					4				
	Wt	P/L	8	6	4	Wt	P/L	8	6	4	Wt	P/L	8	6	4	Wt	P/L	8	6	4
1	0	0	0	-2	0	-165	0	-1.5	0	0	0	0	-3	0	0	0	0	0	-0.5	0
2	-217	0	0	0	0	113	0.5	-0.5	0	0	0	1.25	-1	0	0	0	0	0	0	0
3	-391	-0.5	0	0	0	0	-1.5	0	0	0.5	0	0	0	0	0	0	0	0	0	0
4	0	-1	3	0	0	0	0.5	0.5	0	0	0	0	0	0	0.5	0	0	0	0	0
5	-113	-0.5	0	0	0	113	-1	0	0.5	0	0	0	0	-0.5	0	0	0	0	0	0
6	0	-1.75	4	0	0	217	2	-0.5	0	0	0	0	0	2	0	0	0	0	1	0
7	0	-0.75	-0.5	0	0	0	-1.5	0	0	0	0	0	0	-1	0	0	0	-1	0	0
8	-165	0	0	0	-1	-278	0	-2	0	0	0	0	-3	0	0	0	0	0	0	-0.5
9	0	0	0	0	-1.5	0	0	0	0	-0.5	0	1.75	-5	0	0	0	0	-3	0	0
10	443	0	5	0	0	0	1.5	1.5	0	0	0	0	0	0	1.5	0	0	0	0	1
11	0	0	0	-2	0	0	0	-3.5	0	0	0	-0.5	-2	0	0	0	-1.25	0	-1	0
12	-113	0	0	0	0.5	-113	0	0	0	0.5	0	1.25	-1.5	0	0	0	1.75	1	0	0
13	-278	-1.25	2	0	0	-165	-0.75	0	0	0	0	0	0	0	0	0	0	1	0	0
14	-226	0	2	0	0	113	0	3	0	0	0	0	0	0	0.5	0	0	0	0	0.5
15	339	0	0	0	0	-452	-0.75	0	0	0	0	0.5	-1	0	0	0	0	-0.5	0	0
16	504	0	0	2.5	0	-391	0	0	0	1.5	0	-2.5	0	0	-0.5	0	0	0	0	0
17	330	2	0	0	0	113	-1	0	0	0	0	0	-3.5	0	0	0	0	-1	0	0
18	-278	0	0	1	0	-165	0	0	0	0	0	1	0	0	0	0	1.5	0	2	0
19	0	0	1	0	0	0	0	2.5	0	0	0	0	0	0	1.5	0	0	0	0	1
20	-330	0	0.5	0	0	113	0	2.5	0	0	0	0	0	0	0	0	0	0	0	0

Full Soln

Flight #	Vib Mag	Vib Phase	Pred Mag	Pred Phase	#1 Blade Wt	After Mag	After Phase	#1 Blade P/L	After Mag	After Phase	#1 Blade Tab 8	After Mag	After Phase	#1 Blade Tab 6	After Mag	After Phase	#1 Blade Tab 4	After Mag	After Phase
1																			
FPG100	0.147334	119	0.108185	152	113	0.191353	131	0.5	0.143753	110	0.5	0.147333	119	0.5	0.147333	119	0.5	0.147333	119
Hover Lat	0.121139	85	0.046326	92		0.135004	108		0.193567	74		0.121134	85		0.121134	85		0.121134	85
60K Vert	0.232054	249	0.118116	252		0.276389	242		0.247826	251		0.310213	252		0.393931	258		0.55586	253
80 K Vert	0.033979	260	0.158664	340		0.07598	226		0.065325	266		0.119514	261		0.178009	261		0.402824	259
100 K Vert	0.06676	71	0.098376	15		0.038643	126		0.015256	27		0.029224	276		0.096079	280		0.262238	259
120 K Vert	0.143341	130	0.138725	57		0.152142	149		0.115214	169		0.11779	177		0.147234	210		0.289905	231
140 K Vert	0.195829	135	0.027307	195		0.192823	150		0.186908	172		0.189556	182		0.193395	205		0.408414	225

Flight #	Vib Mag	Vib Phase	Pred Mag	Pred Phase	#1 Blade Wt	After Mag	After Phase	#1 Blade P/L	After Mag	After Phase	#1 Blade Tab 8	After Mag	After Phase	#1 Blade Tab 6	After Mag	After Phase	#1 Blade Tab 4	After Mag	After Phase
2																			
FPG100	0.137854	188	0.073521	207	113	0.189821	181	0.5	0.115876	186	0.5	0.137855	188	0.5	0.137855	188	0.5	0.137855	188
Hover Lat	0.175692	88	0.071707	4		0.189312	104		0.2458	79		0.175687	88		0.175687	88		0.175687	88
60K Vert	0.182888	166	0.092035	171		0.223278	176		0.173883	172		0.190483	191		0.21657	216		0.373701	227
80 K Vert	0.026498	164	0.06653	352		0.073477	191		0.034177	226		0.086265	244		0.143192	251		0.367343	255
100 K Vert	0.057402	321	0.117364	7		0.068256	270		0.099561	292		0.131396	281		0.198468	282		0.358067	265
120 K Vert	0.054141	216	0.078936	77		0.105366	218		0.136959	241		0.153517	243		0.229885	249		0.392472	250
140 K Vert	0.185824	218	0.088054	192		0.234933	222		0.298056	230		0.325916	233		0.381346	241		0.618217	241

Flight #	Vib Mag	Vib Phase	Pred Mag	Pred Phase	#1 Blade Wt	After Mag	After Phase	#1 Blade P/L	After Mag	After Phase	#1 Blade Tab 8	After Mag	After Phase	#1 Blade Tab 6	After Mag	After Phase	#1 Blade Tab 4	After Mag	After Phase
3																			
FPG100	0.171603	217	0.10053	274	113	0.209493	204	0.5	0.151074	220	0.5	0.171605	217	0.5	0.171605	217	0.5	0.171605	217
Hover Lat	0.099243	40	0.096774	82		0.075542	70		0.175026	47		0.09924	40		0.09924	40		0.09924	40
60K Vert	0.273403	280	0.086036	223		0.297454	270		0.29289	280		0.351019	276		0.441	276		0.585511	267
80 K Vert	0.269403	345	0.187158	36		0.232512	337		0.281118	339		0.292306	328		0.319775	318		0.473454	294
100 K Vert	0.132743	244	0.110519	116		0.182504	236		0.187595	249		0.225086	250		0.284257	257		0.45937	253
120 K Vert	0.146512	259	0.10108	54		0.188739	249		0.237273	258		0.254159	258		0.333368	259		0.494864	256
140 K Vert	0.189846	257	0.083129	81		0.237927	253		0.310233	253		0.342313	254		0.412341	259		0.64178	252

Flight #	Vib Mag	Vib Phase	Pred Mag	Pred Phase	#1 Blade Wt	After Mag	After Phase	#1 Blade P/L	After Mag	After Phase	#1 Blade Tab 8	After Mag	After Phase	#1 Blade Tab 6	After Mag	After Phase	#1 Blade Tab 4	After Mag	After Phase
4																			
FPG100	0.126137	304	0.141861	284	113	0.089944	281	0.5	0.134861	313	0.5	0.126138	304	0.5	0.126138	304	0.5	0.126138	304
Hover Lat	0.196119	85	0.022262	94		0.206201	100		0.26764	77		0.196114	85		0.196114	85		0.196114	85
60K Vert	0.089737	54	0.058701	235		0.045478	81		0.079266	43		0.043804	351		0.110246	299		0.24367	264
80 K Vert	0.11473	353	0.085996	262		0.076126	332		0.124386	338		0.141473	316		0.181489	300		0.37878	277
100 K Vert	0.270319	74	0.189401	119		0.230157	83		0.214213	72		0.176664	72		0.123414	56		0.059833	268
120 K Vert	0.183881	13	0.044767	212		0.139859	4		0.163925	344		0.164973	338		0.20046	315		0.308083	287
140 K Vert	0.227382	1	0.144649	230		0.202109	349		0.210016	329		0.224628	321		0.287701	311		0.429774	280

Flight #	Vib Mag	Vib Phase	Pred Mag	Pred Phase	#1 Blade Wt	After Mag	After Phase	#1 Blade P/L	After Mag	After Phase	#1 Blade Tab 8	After Mag	After Phase	#1 Blade Tab 6	After Mag	After Phase	#1 Blade Tab 4	After Mag	After Phase
5																			
FPG100	0.044327	193	0.064589	96	113	0.096721	176	0.5	0.022159	190	0.5	0.044328	193	0.5	0.044328	193	0.5	0.044328	193
Hover Lat	0.166397	336	0.038314	351		0.117276	330		0.194145	360		0.166399	336		0.166399	336		0.166399	336
60K Vert	0.129734	52	0.051041	138		0.081921	64		0.119504	44		0.074612	17		0.105896	321		0.213242	271
80 K Vert	0.092257	64	0.075882	120		0.062204	96		0.066179	51		0.027288	357		0.061735	287		0.28043	264
100 K Vert	0.079734	353	0.06781	317		0.054143	310		0.096884	317		0.118612	301		0.183397	294		0.329886	271
120 K Vert	0.060907	2	0.053246	329		0.037098	305		0.094323	294		0.107796	289		0.182456	278		0.335828	265
140 K Vert	0.105472	105	0.027734	164		0.082274	133		0.075665	188		0.090126	208		0.134575	241		0.371501	241

Flight #	Vib Mag	Vib Phase	Pred Mag	Pred Phase	#1 Blade Wt	After Mag	After Phase	#1 Blade P/L	After Mag	After Phase	#1 Blade Tab 8	After Mag	After Phase	#1 Blade Tab 6	After Mag	After Phase	#1 Blade Tab 4	After Mag	After Phase
6																			
FPG100	0.031513	158	0.049738	171	113	0.087114	161	0.5	0.01926	114	0.5	0.031514	158	0.5	0.031514	158	0.5	0.031514	158
Hover Lat	0.320981	103	0.058997	13		0.34375	111		0.379482	95		0.320976	103		0.320976	103		0.320976	103
60K Vert	0.221451	206	0.066935	99		0.274098	207		0.225426	211		0.272705	220		0.330591	233		0.495818	236
80 K Vert	0.37899	183	0.196929	178		0.427116	186		0.380389	188		0.405113	195		0.432536	202		0.589656	221
100 K Vert	0.190015	296	0.103515	4		0.206751	281		0.239403	288		0.271359	284		0.338409	283		0.491673	271
120 K Vert	0.147873	232	0.152566	99		0.198203	229		0.233729	241		0.250236	242		0.325782	247		0.488001	248
140 K Vert	0.234462	256	0.103033	176		0.282758	252		0.355111	253		0.387194	254		0.456971	258		0.686944	252

Flight #	Vib Mag	Vib Phase	Pred Mag	Pred Phase	#1 Blade Wt	After Mag	After Phase	#1 Blade P/L	After Mag	After Phase	#1 Blade Tab 8	After Mag	After Phase	#1 Blade Tab 6	After Mag	After Phase	#1 Blade Tab 4	After Mag	After Phase
7																			
FPG100	0.038476	29	0.076006	102	113	0.040309	119	0.5	0.060286	24	0.5	0.038475	29	0.5	0.038475	29	0.5	0.038475	29
Hover Lat	0.288189	355	0.027742	9		0.236734	356		0.331986	7		0.28819	355		0.28819	355		0.28819	355
60K Vert	0.212138	71	0.028569	169		0.174015	82		0.196605	67		0.135287	63		0.078653	23		0.115074	266
80 K Vert	0.182933	78	0.091276	141		0.15816	94		0.152435	75		0.097717	76		0.039857	68		0.185537	260
100 K Vert	0.070521	110	0.062634	253		0.076097	153		0.033258	162		0.049444	212		0.095802	253		0.272563	249
120 K Vert	0.118454	71	0.085874	339		0.07903	90		0.029293	53		0.014761	29		0.071589	272		0.230925	257
140 K Vert	0.195892	123	0.010565	187		0.182609	138		0.162735	161		0.159991	173		0.154331	201		0.368882	226

Flight #	Vib Mag	Vib Phase	Pred Mag	Pred Phase	#1 Blade Wt	After Mag	After Phase	#1 Blade P/L	After Mag	After Phase	#1 Blade Tab 8	After Mag	After Phase	#1 Blade Tab 6	After Mag	After Phase	#1 Blade Tab 4	After Mag	After Phase
8																			
FPG100	0.156643	117	0.036682	204	113	0.199384	129	0.5	0.153756	109	0.5	0.156642	117	-0.5	0.156642	117	0.5	0.156642	117
Hover Lat	0.199922	100	0.063588	71		0.22192	113		0.282828	88		0.199917	100		0.199917	100		0.199917	100
60K Vert	0.364091	228	0.146294	268		0.41524	226		0.374718	231		0.431881	234		0.265431	203		0.6684	241
80 K Vert	0.298852	224	0.078456	225		0.347547	221		0.32052	228		0.370254	232		0.203835	199		0.636284	244
100 K Vert	0.264106	202	0.072095	260		0.317044	204		0.296339	211		0.324935	216		0.248338	166		0.526489	232
120 K Vert	0.173487	197	0.102035	317		0.221757	202		0.233746	217		0.247389	219		0.184495	134		0.465021	227
140 K Vert	0.328146	196	0.170363	261		0.369025	201		0.415785	209		0.436293	213		0.305715	155		0.698041	228

Flight #	Vib Mag	Vib Phase	Pred Mag	Pred Phase	#1 Blade Wt	After Mag	After Phase	#1 Blade P/L	After Mag	After Phase	#1 Blade Tab 8	After Mag	After Phase	#1 Blade Tab 6	After Mag	After Phase	#1 Blade Tab 4	After Mag	After Phase
9																			
FPG100	0.034841	54	0.054794	172	113	0.055371	126	-0.5	0.022366	93	0.5	0.03484	54	0.5	0.03484	54	0.5	0.03484	54
Hover Lat	0.300408	45	0.066673	347		0.273443	54		0.224777	41		0.300405	45		0.300405	45		0.300405	45
60K Vert	0.15752	266	0.060204	145		0.193493	253		0.139306	263		0.237735	265		0.326528	268		0.481307	259
80 K Vert	0.326126	304	0.142892	37	37	0.321754	295		0.299192	307		0.393515	296		0.442857	291		0.642777	280
100 K Vert	0.255525	302	0.056053	117		0.264715	290		0.215257	312		0.330358	291		0.396682	289		0.539741	276
120 K Vert	0.385712	310	0.060288	47		0.38892	302		0.339966	322		0.457325	299		0.523245	294		0.651772	284
140 K Vert	0.486233	314	0.041995	81		0.498567	309		0.453358	329		0.569873	300		0.643029	298		0.796904	284

Flight #	Vib Mag	Vib Phase	Pred Mag	Pred Phase	#1 Blade Wt	After Mag	After Phase	#1 Blade P/L	After Mag	After Phase	#1 Blade Tab 8	After Mag	After Phase	#1 Blade Tab 6	After Mag	After Phase	#1 Blade Tab 4	After Mag	After Phase
10																			
FPG100	0.13623	343	0.072815	214	113	0.080572	342	-0.5	0.118188	337	0.5	0.13623	343	0.5	0.13623	343	0.5	0.13623	343
Hover Lat	0.139338	60	0.071208	22		0.130294	82		0.061588	64		0.139334	60		0.139334	60		0.139334	60
60K Vert	0.397807	194	0.218458	247		0.448525	196		0.399192	191		0.432435	204		0.466852	215		0.620184	222
80 K Vert	0.296432	192	0.02039	221		0.346696	194		0.293024	186		0.336469	206		0.373325	214		0.558826	230
100 K Vert	0.138551	44	0.177066	339		0.085054	49		0.186653	55		0.081309	3		0.113285	327		0.225044	276
120 K Vert	0.202343	71	0.014499	337		0.160854	81		0.292856	73		0.09546	66		0.030118	16		0.147194	260
140 K Vert	0.190663	75	0.151446	255		0.143489	81		0.31162	72		0.039708	92		0.038355	291		0.263283	247

Flight #	Vib Mag	Vib Phase	Pred Mag	Pred Phase	#1 Blade Wt	After Mag	After Phase	#1 Blade P/L	After Mag	After Phase	#1 Blade Tab 8	After Mag	After Phase	#1 Blade Tab 6	After Mag	After Phase	#1 Blade Tab 4	After Mag	After Phase
11																			
FPG100	0.154671	111	0.098763	101	-113	0.128037	91	0.5	0.154092	103	0.5	0.15467	111	0.5	0.15467	111	0.5	0.15467	111
Hover Lat	0.193828	107	0.208516	45		0.177391	92		0.251428	93		0.193823	107		0.193823	107		0.193823	107
60K Vert	0.253349	230	0.068638	114		0.203732	235		0.264686	234		0.323232	238		0.397217	246		0.563415	245
80 K Vert	0.551916	231	0.29081	254		0.50658	234		0.575935	233		0.627196	235		0.68037	237		0.894473	242
100 K Vert	0.138373	172	0.125204	95		0.105909	152		0.149806	195		0.171964	205		0.198461	225		0.368624	235
120 K Vert	0.197703	154	0.257816	93		0.183022	139		0.198772	180		0.204034	185		0.233964	204		0.36473	223
140 K Vert	0.162766	177	0.035089	55		0.143071	159		0.233752	206		0.253442	212		0.290292	227		0.523097	233

Flight #	Vib Mag	Vib Phase	Pred Mag	Pred Phase	#1 Blade Wt	After Mag	After Phase	#1 Blade P/L	After Mag	After Phase	#1 Blade Tab 8	After Mag	After Phase	#1 Blade Tab 6	After Mag	After Phase	#1 Blade Tab 4	After Mag	After Phase
12																			
FPG100	0.018759	292	0.040318	222	113	0.046069	181	0.5	0.030752	338	0.5	0.01876	292	-0.5	0.01876	292	0.5	0.01876	292
Hover Lat	0.316144	22	0.043536	89		0.273239	103		0.382543	29		0.316143	22		0.316143	22		0.316143	22
60K Vert	0.306206	93	0.206619	222		0.284593	108		0.287162	92		0.227679	97		0.474939	92		0.09559	186
80 K Vert	0.5631	97	0.200269	166		0.549772	102		0.531405	97		0.481249	100		0.702704	94		0.240632	125
100 K Vert	0.65862	86	0.213387	69		0.624948	90		0.601953	86		0.56526	87		0.816481	86		0.337776	95
120 K Vert	0.573725	124	0.180247	179		0.570705	129		0.516805	131		0.507777	133		0.717935	113		0.431897	161
140 K Vert	0.710215	114	0.15668	193		0.684896	118		0.633204	122		0.608735	124		0.904459	106		0.492819	153

Flight #	Vib Mag	Vib Phase	Pred Mag	Pred Phase	#1 Blade Wt	After Mag	After Phase	#1 Blade P/L	After Mag	After Phase	#1 Blade Tab 8	After Mag	After Phase	#1 Blade Tab 6	After Mag	After Phase	#1 Blade Tab 4	After Mag	After Phase
13																			
FPG100	0.102177	135	0.038712	226	113	0.153439	145	0.5	0.0934	123	0.5	0.102177	135	0.5	0.102177	135	0.5	0.102177	135
Hover Lat	0.258375	73	0.054741	107		0.256592	85		0.333994	70		0.258371	73		0.258371	73		0.258371	73
60K Vert	0.268254	134	0.132165	319		0.284499	145		0.251087	137		0.285221	150		0.187468	173		0.293202	205
80 K Vert	0.431669	140	0.031991	220		0.456175	146		0.410709	144		0.394111	151		0.378266	159		0.410541	192
100 K Vert	0.486692	147	0.037732	176		0.508753	153		0.465488	153		0.460012	158		0.426101	165		0.486626	186
120 K Vert	0.479786	143	0.05673	28		0.494423	149		0.452357	154		0.449664	156		0.434073	166		0.477488	186
140 K Vert	0.627742	146	0.065442	249		0.630496	151		0.616582	158		0.609306	161		0.573903	167		0.67869	187

Flight #	Vib Mag	Vib Phase	Pred Mag	Pred Phase	#1 Blade Wt	After Mag	After Phase	#1 Blade P/L	After Mag	After Phase	#1 Blade Tab 8	After Mag	After Phase	#1 Blade Tab 6	After Mag	After Phase	#1 Blade Tab 4	After Mag	After Phase
14																			
FPG100	0.151411	185	0.029644	164	-113	0.101767	196	0.5	0.129653	183	0.5	0.151412	185	-0.5	0.151412	185	0.5	0.151412	185
Hover Lat	0.123406	233	0.072491	299		0.108894	258		0.046142	225		0.123409	233		0.123409	233		0.123409	233
60K Vert	0.090014	310	0.00489	102		0.110425	338		0.10833	306		0.156534	288		0.114097	61		0.385021	267
80 K Vert	0.205333	323	0.10971	358		0.234069	334		0.227144	317		0.257454	306		0.188806	6		0.495047	281
100 K Vert	0.145414	341	0.059339	129		0.182499	355		0.16553	322		0.183101	311		0.180917	38		0.371821	280
120 K Vert	0.313365	349	0.057369	33		0.348079	355		0.322187	332		0.326067	329		0.365528	20		0.453571	299
140 K Vert	0.556559	343	0.067668	325		0.574088	348		0.557006	331		0.569585	328		0.572905	6		0.700799	303

Flight #	Vib Mag	Vib Phase	Pred Mag	Pred Phase	#1 Blade Wt	After Mag	After Phase	#1 Blade P/L	After Mag	After Phase	#1 Blade Tab 8	After Mag	After Phase	#1 Blade Tab 6	After Mag	After Phase	#1 Blade Tab 4	After Mag	After Phase
15																			
FPG100	0.159404	22	0.132313	216	113	0.121522	39	0.5	0.181499	21	-0.5	0.159403	22	0.5	0.159403	22	0.5	0.159403	22
Hover Lat	0.395231	33	0.033657	80		0.358502	39		0.46738	37		0.395228	33		0.395228	33		0.395228	33
60K Vert	0.314577	75	0.084023	258		0.278354	83		0.298011	73		0.39398	77		0.158281	59		0.011474	283
80 K Vert	0.311538	81	0.09342	224		0.285966	89		0.280596	79		0.397064	81		0.167506	80		0.057954	252
100 K Vert	0.62077	72	0.246967	53		0.577788	75		0.564844	71		0.714442	73		0.471007	67		0.293732	67
120 K Vert	0.421864	99	0.064539	148		0.397941	105		0.339711	105		0.522884	94		0.25447	113		0.173541	153
140 K Vert	0.34276	131	0.251832	225		0.333922	140		0.309785	152		0.437909	114		0.266018	172		0.41445	204

Flight #	Vib Mag	Vib Phase	Pred Mag	Pred Phase	#1 Blade Wt	After Mag	After Phase	#1 Blade P/L	After Mag	After Phase	#1 Blade Tab 8	After Mag	After Phase	#1 Blade Tab 6	After Mag	After Phase	#1 Blade Tab 4	After Mag	After Phase
16																			
FPG100	0.028967	192	0.231616	202	-113	0.033461	318	0.5	0.006911	181	0.5	0.028968	192	0.5	0.028968	192	0.5	0.028968	192
Hover Lat	0.047862	355	0.182607	89		0.099408	353		0.108638	34		0.047863	355		0.047863	355		0.047863	355
60K Vert	1.377877	52	0.316962	222		1.427667	51		1.366626	51		1.310357	50		1.250651	47		1.090039	45
80 K Vert	1.679968	47	0.239062	192		1.727462	46		1.658248	46		1.610597	45		1.56362	44		1.383281	39
100 K Vert	2.238233	49	0.368912	41		2.291158	49		2.19064	49		2.156752	48		2.117927	47		1.952002	45
120 K Vert	2.293396	52	0.104699	107		2.343457	51		2.211074	51		2.195576	51		2.128639	49		1.978369	48
140 K Vert	2.39225	54	0.418802	178		2.443165	54		2.274128	53		2.245773	53		2.195425	51		1.962461	50

Flight #	Vib Mag	Vib Phase	Pred Mag	Pred Phase	#1 Blade Wt	After Mag	After Phase	#1 Blade P/L	After Mag	After Phase	#1 Blade Tab 8	After Mag	After Phase	#1 Blade Tab 6	After Mag	After Phase	#1 Blade Tab 4	After Mag	After Phase
17																			
FPG100	0.092967	302	0.089895	100	113	0.062222	267	0.5	0.10171	315	0.5	0.092968	302	0.5	0.092968	302	0.5	0.092968	302
Hover Lat	0.37259	293	0.087192	62		0.348146	286		0.334658	304		0.372595	293		0.372595	293		0.372595	293
60K Vert	0.567993	59	0.152849	258		0.521534	62		0.554882	58		0.490065	55		0.432761	48		0.273959	39
80 K Vert	0.793623	341	0.05944	341		0.752262	62		0.76729	59		0.714919	57		0.661748	55		0.462307	44
100 K Vert	0.956517	64	0.053318	310		0.908716	65		0.90283	62		0.866043	62		0.815867	59		0.64065	57
120 K Vert	1.146847	64	0.111113	298		1.100343	65		1.058222	63		1.041632	63		0.96727	61		0.807517	59
140 K Vert	1.842375	67	0.162883	100		1.792516	68		1.720776	67		1.689411	67		1.626215	66		1.390128	66

Flight #	Vib Mag	Vib Phase	Pred Mag	Pred Phase	#1 Blade Wt	After Mag	After Phase	#1 Blade P/L	After Mag	After Phase	#1 Blade Tab 8	After Mag	After Phase	#1 Blade Tab 6	After Mag	After Phase	#1 Blade Tab 4	After Mag	After Phase
18																			
FPG100	0.014752	243	0.088017	297	113	0.059969	177	0.5	0.016441	334	0.5	0.014754	243	0.5	0.014754	243	0.5	0.014754	243
Hover Lat	0.276315	39	0.088382	57		0.244634	48		0.351071	43		0.276313	39		0.276313	39		0.276313	39
60K Vert	0.787207	165	0.133241	329		0.824281	168		0.777118	166		0.779395	171		0.759373	177		0.845619	188
80 K Vert	0.981633	164	0.186699	194		1.020928	166		0.971582	166		0.973823	169		0.973521	172		1.015906	185
100 K Vert	1.166197	161	0.203814	134		1.198428	163		1.156855	164		1.157444	166		1.129472	169		1.180738	177
120 K Vert	1.104326	164	0.093986	300		1.13428	166		1.105208	169		1.106767	170		1.10612	174		1.153982	182
140 K Vert	1.265135	162	0.171415	343		1.280445	164		1.281025	167		1.278853	169		1.251699	172		1.354879	182

Flight #	Vib Mag	Vib Phase	Pred Mag	Pred Phase	#1 Blade Wt	After Mag	After Phase	#1 Blade P/L	After Mag	After Phase	#1 Blade Tab 8	After Mag	After Phase	#1 Blade Tab 6	After Mag	After Phase	#1 Blade Tab 4	After Mag	After Phase
19																			
FPG100	0.105432	164	0.105433	164	113	0.161091	164	0.5	0.087162	157	0.5	0.105433	164	0.5	0.105433	164	0.5	0.105433	164
Hover Lat	0.064069	345	0.064069	345		0.013731	323		0.115107	26		0.064071	345		0.064071	345		0.064071	345
60K Vert	0.680677	243	0.151942	28		0.726722	240		0.694932	244		0.756052	245		0.833614	248		0.992665	247
80 K Vert	0.892178	234	0.130403	110		0.937375	232		0.916911	235		0.968572	236		1.021946	237		1.235218	241
100 K Vert	0.813141	241	0.027601	170		0.862776	239		0.866387	242		0.903243	243		0.956118	245		1.133321	245
120 K Vert	0.812045	238	0.088086	134		0.860826	237		0.898857	240		0.915262	240		0.989164	242		1.150014	243
140 K Vert	0.894919	244	0.170182	56		0.94531	244		1.016376	245		1.047388	245		1.11064	248		1.346317	246

Flight #	Vib Mag	Vib Phase	Pred Mag	Pred Phase	#1 Blade Wt	After Mag	After Phase	#1 Blade P/L	After Mag	After Phase	#1 Blade Tab 8	After Mag	After Phase	#1 Blade Tab 6	After Mag	After Phase	#1 Blade Tab 4	After Mag	After Phase
20																			
FPG100	0.16654	170	0.034084	78	113	0.221847	169	0.5	0.146704	167	0.5	0.166541	170	-0.5	0.166541	170	0.5	0.166541	170
Hover Lat	0.13765	209	0.054673	319		0.175512	199		0.07352	178		0.131767	209		0.131767	209		0.131767	209
60K Vert	0.243486	358	0.101851	126		0.201918	349		0.250542	353		0.25078	339		0.289039	33		0.364906	297
80 K Vert	0.412842	340	0.085991	322		0.377989	335		0.426283	336		0.43789	329		0.410177	0		0.595256	302
100 K Vert	0.512283	334	0.118731	310		0.489345	328		0.532942	328		0.544603	324		0.468526	351		0.668691	305
120 K Vert	0.511324	349	0.077926	62		0.480046	345		0.514108	339		0.515833	337		0.547088	9		0.596486	314
140 K Vert	0.836586	343	0.074918	18		0.822611	340		0.832692	335		0.84281	333		0.837946	358		0.932391	314

Full Soln

Flight #	Vib Mag	Vib Phase	Pred Mag	Pred Phase	#1 Blade Wt	After Mag	After Phase	#1 Blade P/L	After Mag	After Phase	#1 Blade Tab 8	After Mag	After Phase	#1 Blade Tab 6	After Mag	After Phase	#1 Blade Tab 4	After Mag	After Phase
1																			
FFG100	0.147334	119	0.108185	152	1017	0.613976	153	12	0.516736	32	5	0.147334	119	5	0.147334	119	5	0.147334	119
Hover Lat	0.121139	85	0.046326	92		0.487154	157		1.97084	59		0.121136	85		0.121136	85		0.121136	85
60K Vert	0.232054	249	0.118116	252		0.675933	224		0.667282	274		1.025064	260		1.902408	268		3.469777	256
80 K Vert	0.033979	260	0.158664	340		0.480176	208		0.792524	273		0.886707	262		1.469799	261		3.711092	259
100 K Vert	0.06676	71	0.098376	15		0.434676	211		1.290038	263		0.871592	259		1.509811	269		3.209629	257
120 K Vert	0.143341	130	0.138725	57		0.481239	202		2.087897	253		0.995949	249		1.775446	255		3.393944	253
140 K Vert	0.195829	135	0.027307	195		0.46234	211		2.838781	244		1.454654	243		2.114723	256		4.439963	248

Flight #	Vib Mag	Vib Phase	Pred Mag	Pred Phase	#1 Blade Wt	After Mag	After Phase	#1 Blade P/L	After Mag	After Phase	#1 Blade Tab 8	After Mag	After Phase	#1 Blade Tab 6	After Mag	After Phase	#1 Blade Tab 4	After Mag	After Phase
2																			
FFG100	0.137854	188	0.073521	207	1017	0.627036	168	12	0.394766	18	5	0.137855	188	5	0.137855	188	5	0.137855	188
Hover Lat	0.175692	89	0.071707	4		0.515893	151		2.01495	60		0.175689	89		0.175689	89		0.175689	89
60K Vert	0.182888	166	0.092035	171		0.617368	200		0.408627	264		0.796996	250		1.648836	264		3.243327	253
80 K Vert	0.026498	164	0.06653	352		0.480202	203		0.75082	271		0.849293	260		1.431996	260		3.672725	259
100 K Vert	0.057402	321	0.117364	7		0.476788	223		1.388594	264		0.967702	262		1.611941	270		3.307327	258
120 K Vert	0.054141	216	0.078936	77		0.513844	219		2.212799	255		1.16778	254		1.903401	258		3.518763	254
140 K Vert	0.185824	218	0.088054	192		0.636715	231		3.068859	246		1.687253	247		2.361814	257		4.675271	249

Flight #	Vib Mag	Vib Phase	Pred Mag	Pred Phase	#1 Blade Wt	After Mag	After Phase	#1 Blade P/L	After Mag	After Phase	#1 Blade Tab 8	After Mag	After Phase	#1 Blade Tab 6	After Mag	After Phase	#1 Blade Tab 4	After Mag	After Phase
3																			
FFG100	0.171603	217	0.10053	274	1017	0.616925	176	12	0.376155	6	5	0.171604	217	5	0.171604	217	5	0.171604	217
Hover Lat	0.099243	40	0.096774	82		0.404036	161		1.956399	57		0.09924	40		0.09924	40		0.09924	40
60K Vert	0.273403	280	0.086036	223		0.631219	236		0.740752	284		1.063685	268		1.954359	272		3.489215	258
80 K Vert	0.269403	345	0.187158	36		0.307008	239		0.882398	290		0.924316	278		1.490378	272		3.706158	263
100 K Vert	0.132743	244	0.110519	116		0.608079	222		1.483653	260		1.067493	257		1.696737	267		3.408682	256
120 K Vert	0.146512	259	0.10708	54		0.579821	229		2.31688	256		1.220532	256		2.009215	259		3.62194	255
140 K Vert	0.189846	257	0.083129	81		0.637074	242		3.090508	248		1.714695	251		2.409335	260		4.703198	251

Flight #	Vib Mag	Vib Phase	Pred Mag	Pred Phase	#1 Blade Wt	After Mag	After Phase	#1 Blade P/L	After Mag	After Phase	#1 Blade Tab 8	After Mag	After Phase	#1 Blade Tab 6	After Mag	After Phase	#1 Blade Tab 4	After Mag	After Phase
4																			
FFG100	0.126137	304	0.141861	284	1017	0.409063	174	12	0.58362	4	5	0.126137	304	5	0.126137	304	5	0.126137	304
Hover Lat	0.196119	85	0.022262	94		0.515384	149		2.038546	60		0.196117	85		0.196117	85		0.196117	85
60K Vert	0.089737	54	0.058701	235		0.393628	207		0.419738	296		0.72142	267		1.612445	272		3.153787	257
80 K Vert	0.11473	353	0.085996	262		0.367034	214		0.787329	281		0.857027	269		1.435859	266		3.668092	261
100 K Vert	0.270319	74	0.189401	119		0.322556	185		1.08892	264		0.669016	261		1.313718	271		3.007427	257
120 K Vert	0.183881	13	0.044767	212		0.306325	235		2.093798	261		1.003385	265		1.794474	264		3.393623	258
140 K Vert	0.227382	1	0.144649	230		0.374188	265		2.82174	251		1.462387	259		2.191576	266		4.444047	253

Flight #	Vib Mag	Vib Phase	Pred Mag	Pred Phase	#1 Blade Wt	After Mag	After Phase	After P/L	After Mag	After Phase	#1 Blade Tab 8	After Mag	After Phase	#1 Blade Tab 6	After Mag	After Phase	#1 Blade Tab 4	After Mag	After Phase
5																			
FFG100	0.044327	193	0.064589	96	1017	0.538325	165	12	0.48681	16	5	0.044328	193	5	0.044328	193	5	0.044328	193
Hover Lat	0.166397	336	0.038314	351		0.305586	179		1.89479	53		0.166396	336		0.166396	336		0.166396	336
60K Vert	0.129734	52	0.051041	138		0.355792	205		0.407792	302		0.691348	269		1.584705	274		3.118788	257
80 K Vert	0.092257	64	0.075882	120		0.393316	196		0.679607	277		0.764662	264		1.347121	262		3.586263	260
100 K Vert	0.079734	353	0.06781	317		0.433228	223		1.359302	265		0.93707	264		1.586273	271		3.275602	258
120 K Vert	0.060907	2	0.053246	329		0.413133	225		2.155202	258		1.059035	259		1.849935	260		3.459453	256
140 K Vert	0.105472	105	0.02734	164		0.39707	224		2.823399	246		1.442139	248		2.126249	259		4.431952	250

Flight #	Vib Mag	Vib Phase	Pred Mag	Pred Phase	#1 Blade Wt	After Mag	After Phase	After P/L	After Mag	After Phase	#1 Blade Tab 8	After Mag	After Phase	#1 Blade Tab 6	After Mag	After Phase	#1 Blade Tab 4	After Mag	After Phase
6																			
FFG100	0.031513	158	0.049738	171	1017	0.530811	163	12	0.5064	18	5	0.031514	158	5	0.031514	158	5	0.031514	158
Hover Lat	0.320981	103	0.058997	13		0.655439	144		2.099317	64		0.320979	103		0.320979	103		0.320979	103
60K Vert	0.221451	206	0.066935	99		0.694907	210		0.548633	263		0.934366	252		1.786632	264		3.377255	253
80 K Vert	0.17899	183	0.196929	178		0.824239	195		0.849021	247		1.000542	240		1.558529	248		3.784949	254
100 K Vert	0.190015	296	0.103515	4		0.554483	236		1.519723	266		1.097318	265		1.747282	271		3.431583	259
120 K Vert	0.147873	232	0.152566	99		0.604639	223		2.304896	255		1.210337	253		1.994773	257		3.610034	254
140 K Vert	0.234462	256	0.103033	176		0.68167	243		3.137599	248		1.760744	251		2.456431	260		4.751693	251

Flight #	Vib Mag	Vib Phase	Pred Mag	Pred Phase	#1 Blade Wt	After Mag	After Phase	After P/L	After Mag	After Phase	#1 Blade Tab 8	After Mag	After Phase	#1 Blade Tab 6	After Mag	After Phase	#1 Blade Tab 4	After Mag	After Phase
7																			
FFG100	0.038476	29	0.076006	102	1017	0.473569	160	12	0.56845	16	5	0.038476	29	5	0.038476	29	5	0.038476	29
Hover Lat	0.288189	355	0.027742	9		0.177133	164		2.013531	50		0.288188	355		0.288188	355		0.288188	355
60K Vert	0.212138	71	0.028569	169		0.336511	189		0.321649	309		0.592895	268		1.484996	273		3.023351	256
80 K Vert	0.182933	78	0.091276	141		0.381138	182		0.583497	278		0.669214	262		1.251569	262		3.490151	259
100 K Vert	0.070521	110	0.062634	253		0.473127	208		1.295069	261		0.879018	256		1.509763	267		3.220853	256
120 K Vert	0.118454	71	0.085874	339		0.363582	210		2.053882	256		0.95695	256		1.746484	259		3.35961	255
140 K Vert	0.195892	123	0.010565	187		0.422995	210		2.801027	244		1.417772	244		2.081958	257		4.402621	248

Flight #	Vib Mag	Vib Phase	Pred Mag	Pred Phase	#1 Blade Wt	After Mag	After Phase	After P/L	After Mag	After Phase	#1 Blade Tab 8	After Mag	After Phase	#1 Blade Tab 6	After Mag	After Phase	#1 Blade Tab 4	After Mag	After Phase
8																			
FFG100	0.156643	117	0.036682	204	1017	0.618578	153	12	0.522911	33	5	0.156644	117	5	0.156644	117	5	0.156644	117
Hover Lat	0.199922	100	0.063588	71		0.56037	151		2.015099	61		0.19992	100		0.19992	100		0.19992	100
60K Vert	0.364091	228	0.146294	268		0.831049	219		0.728244	261		1.115346	253		1.967847	263		3.562783	253
80 K Vert	0.298852	224	0.078456	225		0.747612	212		0.980008	260		1.103298	252		1.68086	255		3.918368	257
100 K Vert	0.264106	202	0.072095	260		0.74603	211		1.503443	253		1.103303	247		1.694711	260		3.432921	253
120 K Vert	0.173487	197	0.102035	317		0.623868	214		2.266279	252		1.174585	249		1.952716	254		3.573283	253
140 K Vert	0.328146	196	0.170363	261		0.740809	219		3.122397	243		1.740379	242		2.382435	253		4.716481	247

Flight #	Vib Mag	Vib Phase	Pred Mag	Pred Phase	#1 Blade Wt	After Mag	After Phase	After P/L	After Mag	After Phase	#1 Blade Tab 8	After Mag	After Phase	#1 Blade Tab 6	After Mag	After Phase	#1 Blade Tab 4	After Mag	After Phase
9																			
FFG100	0.034841	54	0.054794	172	1017	0.489224	159	12	0.558642	18	5	0.034841	54	5	0.034841	54	5	0.034841	54
Hover Lat	0.300408	45	0.066673	347		0.376978	131		2.156984	56		0.300405	45		0.300405	45		0.300405	45
60K Vert	0.15752	266	0.060204	145		0.592608	225		0.61946	281		0.957465	270		1.844419	270		3.398896	257
80 K Vert	0.326126	304	0.142892	37		0.518856	243		1.063263	282		1.115837	273		1.690857	269		3.91788	263
100 K Vert	0.255525	302	0.056053	117		0.565221	243		1.560436	268		1.13773	268		1.792528	273		3.462104	260
120 K Vert	0.385712	310	0.060288	47		0.598553	260		2.415997	263		1.336429	269		2.123185	267		3.706767	260
140 K Vert	0.486233	314	0.041995	81		0.728676	277		3.125411	255		1.793082	264		2.537836	269		4.750996	256

Flight #	Vib Mag	Vib Phase	Pred Mag	Pred Phase	#1 Blade Wt	After Mag	After Phase	After P/L	After Mag	After Phase	#1 Blade Tab 8	After Mag	After Phase	#1 Blade Tab 6	After Mag	After Phase	#1 Blade Tab 4	After Mag	After Phase
10																			
FFG100	0.13623	343	0.072815	214	1017	0.363113	163	12	0.649681	9	5	0.136229	343	5	0.136229	343	5	0.136229	343
Hover Lat	0.139338	60	0.071208	22		0.434118	154		2.00265	58		0.139335	60		0.139335	60		0.139335	60
60K Vert	0.397807	194	0.218458	247		0.862465	204		0.600805	245		1.009194	242		1.818069	258		3.441731	250
80 K Vert	0.296432	192	0.02039	221		0.752162	200		0.858157	253		0.997167	245		1.566887	251		3.802865	255
100 K Vert	0.138551	44	0.177066	339		0.351384	213		1.250758	266		0.828708	264		1.479365	272		3.164122	258
120 K Vert	0.202343	71	0.014499	337		0.305409	199		1.967304	257		0.871903	257		1.660786	260		3.271088	255
140 K Vert	0.190863	75	0.151446	255		0.283656	223		2.715913	247		1.336817	250		2.031336	261		4.326764	250

Flight #	Vib Mag	Vib Phase	Pred Mag	Pred Phase	#1 Blade Wt	After Mag	After Phase	After P/L	After Mag	After Phase	#1 Blade Tab 8	After Mag	After Phase	#1 Blade Tab 6	After Mag	After Phase	#1 Blade Tab 4	After Mag	After Phase
11																			
FFG100	0.154671	111	0.098763	101	1017	0.607094	151	12	0.538393	32	5	0.154671	111	5	0.154671	111	5	0.154671	111
Hover Lat	0.193828	107	0.208516	45		0.575384	154		1.994249	62		0.193826	107		0.193826	107		0.193826	107
60K Vert	0.253349	230	0.068638	114		0.720112	218		0.643948	267		1.019405	256		1.883528	266		3.466069	254
80 K Vert	0.551916	231	0.29081	254		0.985013	219		1.226416	256		1.357682	250		1.932975	253		4.171658	256
100 K Vert	0.138373	172	0.125204	95		0.595046	207		1.362661	256		0.95573	250		1.56406	263		3.29089	254
120 K Vert	0.197703	154	0.257816	93		0.568935	201		2.134323	251		1.049204	245		1.819639	253		3.438823	252
140 K Vert	0.162766	177	0.035089	55		0.559271	221		2.964859	244		1.581697	245		2.245811	256		4.567345	249

Flight #	Vib Mag	Vib Phase	Pred Mag	Pred Phase	#1 Blade Wt	After Mag	After Phase	After P/L	After Mag	After Phase	#1 Blade Tab 8	After Mag	After Phase	#1 Blade Tab 6	After Mag	After Phase	#1 Blade Tab 4	After Mag	After Phase
12																			
FFG100	0.018759	292	0.040318	222	1017	0.487429	165	12	0.533438	13	5	0.018758	292	5	0.018758	292	5	0.018758	292
Hover Lat	0.316144	22	0.043536	89		0.262874	131		2.129428	201		0.316142	22		0.316142	22		0.316142	22
60K Vert	0.306206	93	0.206619	222		0.423921	173		0.184701	309		0.49905	258		1.377586	270		2.944718	254
80 K Vert	0.5631	97	0.200269	166		0.609848	143		0.200956	262		0.344356	236		0.906406	252		3.144341	256
100 K Vert	0.65862	86	0.213387	69		0.507623	133		0.701209	258		0.296037	243		0.917765	270		2.631345	254
120 K Vert	0.573725	124	0.180247	179		0.697093	165		1.832715	243		0.809984	224		1.512737	243		3.126156	247
140 K Vert	0.710215	114	0.15668	193		0.610873	154		2.474549	235		1.126468	224		1.676019	247		4.033182	244

Flight #	Vib Mag	Vib Phase	Pred Mag	Pred Phase	#1 Blade Wt	After Mag	After Phase	After P/L	After Mag	After Phase	#1 Blade Tab 8	After Mag	After Phase	#1 Blade Tab 6	After Mag	After Phase	#1 Blade Tab 4	After Mag	After Phase
13																			
FFG100	0.102177	135	0.038712	226	-1017	0.412218	350	12	0.489469	26	5	0.102178	135	5	0.102178	135	5	0.102178	135
Hover Lat	0.258375	73	0.054741	107		0.589919	18		2.11916	59		0.258373	73		0.258373	73		0.258373	73
60K Vert	0.268254	134	0.132165	319		0.492153	64		0.263072	258		0.66287	245		1.501677	263		3.103997	252
80 K Vert	0.431669	140	0.031991	220		0.475503	80		0.56269	239		0.728561	231		1.268225	244		3.487614	253
100 K Vert	0.486692	147	0.037732	176		0.551746	91		1.232227	241		0.881825	228		1.384616	251		3.148081	248
120 K Vert	0.479786	143	0.05673	28		0.580824	93		2.034071	244		0.995098	229		1.714059	244		3.329703	247
140 K Vert	0.627742	146	0.065442	249		0.77154	110		2.85528	235		1.50512	226		2.046888	244		4.407455	243

Flight #	Vib Mag	Vib Phase	Pred Mag	Pred Phase	#1 Blade Wt	After Mag	After Phase	After P/L	After Mag	After Phase	#1 Blade Tab 8	After Mag	After Phase	#1 Blade Tab 6	After Mag	After Phase	#1 Blade Tab 4	After Mag	After Phase
14																			
FFG100	0.151411	185	0.029644	164	1017	0.642475	168	12	0.383416	20	5	0.151412	185	5	0.151412	185	5	0.151412	185
Hover Lat	0.123406	233	0.072491	299		0.532874	183		1.739173	58		0.123408	233		0.123408	233		0.123408	233
60K Vert	0.090014	310	0.00489	102		0.471448	223		0.552498	290		0.863193	268		1.754667	272		3.291134	257
80 K Vert	0.205333	323	0.10971	358		0.405159	231		0.905709	283		0.968048	272		1.543995	268		3.772933	262
100 K Vert	0.145414	341	0.059339	129		0.420634	232		1.391812	268		0.96869	267		1.624461	273		3.298029	259
120 K Vert	0.313365	349	0.057369	33		0.357648	262		2.182367	264		1.105105	272		1.891171	268		3.475488	260
140 K Vert	0.556559	343	0.067668	325		0.603728	297		2.902509	258		1.599429	271		2.358995	274		4.529297	258

Flight #	Vib Mag	Vib Phase	Pred Mag	Pred Phase	#1 Blade Wt	After Mag	After Phase	After P/L	After Mag	After Phase	#1 Blade Tab 8	After Mag	After Phase	#1 Blade Tab 6	After Mag	After Phase	#1 Blade Tab 4	After Mag	After Phase
15																			
FFG100	0.159404	22	0.132313	216	1017	0.389294	148	12	0.689722	17	5	0.159404	22	5	0.159404	22	5	0.159404	22
Hover Lat	0.395231	33	0.033657	80		0.314081	114		2.228934	53		0.395228	33		0.395228	33		0.395228	33
60K Vert	0.314577	75	0.084023	258		0.327047	171		0.258957	326		0.489416	269		1.383424	274		2.927262	256
80 K Vert	0.311538	81	0.09342	224		0.384779	163		0.460454	282		0.541351	262		1.124446	261		3.366004	259
100 K Vert	0.62077	72	0.246967	53		0.367592	124		0.753733	270		0.330567	271		0.995378	278		2.663455	258
120 K Vert	0.421864	99	0.064539	148		0.436091	164		1.789977	251		0.705713	242		1.474958	253		3.09663	252
140 K Vert	0.34276	131	0.251832	225		0.499519	194		2.77427	241		1.394543	238		2.023356	253		4.362711	247

Flight #	Vib Mag	Vib Phase	Pred Mag	Pred Phase	#1 Blade Wt	After Mag	After Phase	After P/L	After Mag	After Phase	#1 Blade Tab 8	After Mag	After Phase	#1 Blade Tab 6	After Mag	After Phase	#1 Blade Tab 4	After Mag	After Phase
16																			
FFG100	0.028967	192	0.231616	202	1017	0.524522	165	-12	0.559692	195	5	0.028967	192	5	0.028967	192	5	0.028967	192
Hover Lat	0.047862	355	0.182607	89		0.415192	171		1.839456	239		0.047861	355		0.047861	355		0.047861	355
60K Vert	1.377877	52	0.316962	22		0.94613	62		1.69225	65		0.81349	21		1.052624	325		2.054993	272
80 K Vert	1.679968	47	0.239062	192		1.266613	55		2.289961	61		1.094652	20		0.96237	348		2.423569	281
100 K Vert	2.238233	49	0.368912	41		1.767245	53		3.45886	62		1.494346	31		1.420551	5		1.652357	295
120 K Vert	2.293396	52	0.104699	107		1.846837	55		4.360773	64		1.385235	33		1.054603	359		1.640317	289
140 K Vert	2.39225	54	0.418802	178		1.93551	53		5.261899	61		1.023949	29		1.077247	346		2.329504	268

Flight #	Vib Mag	Vib Phase	Pred Mag	Pred Phase	#1 Blade Wt	After Mag	After Phase	After P/L	After Mag	After Phase	#1 Blade Tab 8	After Mag	After Phase	#1 Blade Tab 6	After Mag	After Phase	#1 Blade Tab 4	After Mag	After Phase
17																			
FPG100	0.092967	302	0.089895	100	1017	0.432903	171	12	0.565322	6	5	0.092966	302	5	0.092966	302	5	0.092966	302
Hover Lat	0.37259	293	0.087192	62		0.414249	221		1.680376	47		0.372592	293		0.372592	293		0.372592	293
60K Vert	0.567993	59	0.152849	258		0.262782	115		0.425864	5		0.364411	303		1.233813	284		2.696789	260
80 K Vert	0.793623	60	0.05944	341		0.494193	92		0.447284	351		0.316432	330		0.755104	284		2.939101	260
100 K Vert	0.956517	64	0.053318	310		0.571461	87		0.541152	296		0.251614	345		0.812423	298		2.356474	262
120 K Vert	1.146847	64	0.111113	298		0.752199	78		1.076764	269		0.240956	357		0.80715	280		2.360142	260
140 K Vert	1.842375	67	0.162683	100		1.397944	71		1.063117	247		0.3271	53		0.599606	305		2.680325	253

Flight #	Vib Mag	Vib Phase	Pred Mag	Pred Phase	#1 Blade Wt	After Mag	After Phase	After P/L	After Mag	After Phase	#1 Blade Tab 8	After Mag	After Phase	#1 Blade Tab 6	After Mag	After Phase	#1 Blade Tab 4	After Mag	After Phase
18																			
FPG100	0.014752	243	0.088017	297	-1017	0.497093	341	12	0.521332	14	5	0.014753	243	5	0.014753	243	5	0.014753	243
Hover Lat	0.276315	39	0.088382	57		0.68027	9		2.125537	55		0.276313	39		0.276313	39		0.276313	39
60K Vert	0.787207	165	0.133241	329		0.578397	128		0.672668	201		1.034628	215		1.655006	243		3.314815	242
80 K Vert	0.981633	164	0.186699	194		0.701621	139		1.022665	208		1.209916	208		1.629651	225		3.712291	244
100 K Vert	1.166197	161	0.203814	134		0.970153	137		1.614575	217		1.396547	203		1.659238	226		3.373827	237
120 K Vert	1.104326	164	0.093986	300		0.923527	140		2.403988	229		1.520253	209		2.0928	227		3.633725	237
140 K Vert	1.265135	162	0.171415	343		1.217888	141		3.264288	224		2.011586	211		2.38808	229		4.723119	235

Flight #	Vib Mag	Vib Phase	Pred Mag	Pred Phase	#1 Blade Wt	After Mag	After Phase	After P/L	After Mag	After Phase	#1 Blade Tab 8	After Mag	After Phase	#1 Blade Tab 6	After Mag	After Phase	#1 Blade Tab 4	After Mag	After Phase
19																			
FPG100	0.105432	164	0.105433	164	1017	0.604825	163	12	0.444271	23	5	0.105433	164	5	0.105433	164	5	0.105433	164
Hover Lat	0.064069	345	0.064069	345		0.399274	172		1.881951	56		0.064068	345		0.064069	345		0.064069	345
60K Vert	0.680677	243	0.151942	28		1.115787	230		1.068535	260		1.454674	254		2.307009	263		3.90171	254
80 K Vert	0.892178	234	0.130403	110		1.31363	224		1.554797	252		1.693232	247		2.264174	251		4.498195	254
100 K Vert	0.813141	241	0.027601	170		1.272377	232		2.136197	254		1.730929	250		2.327366	259		4.069109	254
120 K Vert	0.812045	238	0.088086	134		1.256579	231		2.953173	251		1.864044	248		2.638302	252		4.25884	252
140 K Vert	0.894919	244	0.170182	56		1.348435	241		3.799389	247		2.418942	248		3.09081	256		5.40823	249

Flight #	Vib Mag	Vib Phase	Pred Mag	Pred Phase	#1 Blade Wt	After Mag	After Phase	After P/L	After Mag	After Phase	#1 Blade Tab 8	After Mag	After Phase	#1 Blade Tab 6	After Mag	After Phase	#1 Blade Tab 4	After Mag	After Phase
20																			
FPG100	0.16654	170	0.034084	78	1017	0.66482	165	12	0.38668	26	5	0.166541	170	5	0.166541	170	5	0.166541	170
Hover Lat	0.131765	209	0.054673	319		0.57336	179		1.748388	60		0.131768	209		0.131768	209		0.131768	209
60K Vert	0.243486	358	0.101851	126		0.306404	238		0.594251	309		0.817962	281		1.714221	279		3.19789	260
80 K Vert	0.412842	340	0.085991	322		0.333571	265		0.996388	296		1.018585	285		1.569091	276		3.765117	265
100 K Vert	0.512283	334	0.118731	310		0.517838	277		1.595395	280		1.18193	284		1.850408	283		3.434278	265
120 K Vert	0.511324	349	0.077926	62		0.414505	291		2.204894	269		1.161919	282		1.927833	274		3.480526	263
140 K Vert	0.836586	343	0.074918	18		0.823055	311		2.937574	264		1.703414	280		2.470647	280		4.554678	261

Appendix E: UH-60 Matlab Code

Note: The Matlab codes contained in this appendix were each used to perform one or more specific functions in the course of this research. There are several instances where parts of the code have been commented out with the % symbol. In order to reproduce all of the analysis of this thesis, some lines of code may need to be un-commented and other lines commented out.

```
% Capt Nathan A Miller
% This program creates MAT data files from imported Excel database
% Ensure that the two databases are imported into matlab prior to
running

function Excel_to_Mat
global data
global data2
clc

n = length(data2(:,1));
for j=1:n
% Read Vibration Magnitude and Phase as well as prediction magnitude
% and phase from Excel File and assign to data matrix

UH60VIBES(j,1) = data(2+(j-1)*13,2);
UH60VIBES(j,2) = data(2+(j-1)*13,3);
UH60VIBES(j,3) = data(2+(j-1)*13,4);
UH60VIBES(j,4) = data(2+(j-1)*13,5);
UH60VIBES(j,5) = data(3+(j-1)*13,2);
UH60VIBES(j,6) = data(3+(j-1)*13,3);
UH60VIBES(j,7) = data(3+(j-1)*13,4);
UH60VIBES(j,8) = data(3+(j-1)*13,5);
UH60VIBES(j,9) = data(4+(j-1)*13,2);
UH60VIBES(j,10) = data(4+(j-1)*13,3);
UH60VIBES(j,11) = data(4+(j-1)*13,4);
UH60VIBES(j,12) = data(4+(j-1)*13,5);
UH60VIBES(j,13) = data(8+(j-1)*13,2);
UH60VIBES(j,14) = data(8+(j-1)*13,3);
UH60VIBES(j,15) = data(8+(j-1)*13,4);
UH60VIBES(j,16) = data(8+(j-1)*13,5);
UH60VIBES(j,17) = data(5+(j-1)*13,2);
UH60VIBES(j,18) = data(5+(j-1)*13,3);
UH60VIBES(j,19) = data(5+(j-1)*13,4);
UH60VIBES(j,20) = data(5+(j-1)*13,5);
UH60VIBES(j,21) = data(9+(j-1)*13,2);
UH60VIBES(j,22) = data(9+(j-1)*13,3);
UH60VIBES(j,23) = data(9+(j-1)*13,4);
UH60VIBES(j,24) = data(9+(j-1)*13,5);
UH60VIBES(j,25) = data(6+(j-1)*13,2);
UH60VIBES(j,26) = data(6+(j-1)*13,3);
UH60VIBES(j,27) = data(6+(j-1)*13,4);
UH60VIBES(j,28) = data(6+(j-1)*13,5);
```

```

UH60VIBES(j,29) = data(10+(j-1)*13,2);
UH60VIBES(j,30) = data(10+(j-1)*13,3);
UH60VIBES(j,31) = data(10+(j-1)*13,4);
UH60VIBES(j,32) = data(10+(j-1)*13,5);
UH60VIBES(j,33) = data(7+(j-1)*13,2);
UH60VIBES(j,34) = data(7+(j-1)*13,3);
UH60VIBES(j,35) = data(7+(j-1)*13,4);
UH60VIBES(j,36) = data(7+(j-1)*13,5);
end
save UH60VIBES.mat UH60VIBES

UH60_VMEP_Adjustments = zeros(n,12);
for j=1:n
    for k=1:12
        UH60_VMEP_Adjustments(j,k) = data2(j,k+1);
    end
end
save UH60_VMEP_Adjustments.mat UH60_VMEP_Adjustments

UH60_Coeff_Data = zeros(n,57);
for j=1:n
    UH60_Coeff_Data(j,1)=data(2+(j-1)*13,6);
    UH60_Coeff_Data(j,20)=data(2+(j-1)*13,9);    % Records manual
    adjustment
    UH60_Coeff_Data(j,39)=data(2+(j-1)*13,12);    % that produces delta
    vibes
    for k=1:3
        UH60_Coeff_Data(j,[2 3]+(k-1)*19) = data(2+(j-1)*13,[7 8]+(k-1)*3);    % FPG100(A-B)
        UH60_Coeff_Data(j,[4 5]+(k-1)*19) = data(3+(j-1)*13,[7 8]+(k-1)*3);    % 0 Kts(A-B)
        UH60_Coeff_Data(j,[6 7]+(k-1)*19) = data(4+(j-1)*13,[7 8]+(k-1)*3);    % 80 Kts(A-B)
        UH60_Coeff_Data(j,[8 9]+(k-1)*19) = data(8+(j-1)*13,[7 8]+(k-1)*3);    % 80 Kts(A+B)
        UH60_Coeff_Data(j,[10 11]+(k-1)*19) = data(5+(j-1)*13,[7 8]+(k-1)*3);    % 120 Kts(A-B)
        UH60_Coeff_Data(j,[12 13]+(k-1)*19) = data(9+(j-1)*13,[7 8]+(k-1)*3);    % 120 Kts(A+B)
        UH60_Coeff_Data(j,[14 15]+(k-1)*19) = data(6+(j-1)*13,[7 8]+(k-1)*3);    % 145 Kts(A-B)
        UH60_Coeff_Data(j,[16 17]+(k-1)*19) = data(10+(j-1)*13,[7 8]+(k-1)*3);    % 145 Kts(A+B)
        UH60_Coeff_Data(j,[18 19]+(k-1)*19) = data(7+(j-1)*13,[7 8]+(k-1)*3);    % 0 Kts(A+B)    Non
        AVA quantity
    end
    UH60_Coeff_Data(j,[58 59]) = data(2+(j-1)*13,[15 16]);
    UH60_Coeff_Data(j,[60 61]) = data(3+(j-1)*13,[15 16]);
    UH60_Coeff_Data(j,[62 63]) = data(4+(j-1)*13,[15 16]);
    UH60_Coeff_Data(j,[64 65]) = data(8+(j-1)*13,[15 16]);
    UH60_Coeff_Data(j,[66 67]) = data(5+(j-1)*13,[15 16]);
    UH60_Coeff_Data(j,[68 69]) = data(9+(j-1)*13,[15 16]);
    UH60_Coeff_Data(j,[70 71]) = data(6+(j-1)*13,[15 16]);
    UH60_Coeff_Data(j,[72 73]) = data(10+(j-1)*13,[15 16]);
    UH60_Coeff_Data(j,[74 75]) = data(7+(j-1)*13,[15 16]);
end
save UH60_Coeff_Data.mat UH60_Coeff_Data

%%%%%%%%%%%%%%

```



```

% Capt Nathan A Miller
% Thesis work
% This program loads vibe data and calculates an AVA adjustment matrix

function Vibs2AVA_ADJ

load UH60VIBES.mat
n = length(UH60VIBES(:,1));

for j=1:n
mag = UH60VIBES(j,[1 5 9 13 17 21 25 29])';
phase = UH60VIBES(j,[2 6 10 14 18 22 26 30])';
vibsCmplx = mag.*(cos( phase*pi/180 ) + i*sin( phase*pi/180 ) );

pmag = UH60VIBES(j,[3 7 11 15 19 23 27 31])';
pphase = UH60VIBES(j,[4 8 12 16 20 24 28 32])';
pvibsCmplx = pmag.*(cos( pphase*pi/180 ) + i*sin( pphase*pi/180 ) );

delvib = -vibsCmplx + pvibsCmplx;

adj(j) = LinearUH60( delvib );
end

for k=1:n
    magnitude(k,:) = adj(k).mag';
    Phase(k,:) = adj(k).phase';
end
AVAadj.mag = magnitude;
AVAadj.phase = Phase;
save AVAadj.mat AVAadj

%%%%%%%%%%%%%%%%%%%%%%%%%%%%%%%%%%%%%%%%%%%%%%%%%%%%%%%%%%%%%%%%%%%%%%%%%%%%%%

% Capt Miller
% This function converts a complex vibset into an adjustment set based
%on the AVA sensitivity coefficients.

function adj = LinearUH60( vibsCmplx )

% Matrix of coefficient magnitudes
mag = [0.00993, 0.0, 0.0;      % FPG100 (A - B)
       0.0, 0.0460, 0.0162;   % 0 kts (A - B)
       0.0, 0.0289, 0.0105;   % 80 kts (A - B)
       0.0, 0.0410, 0.0296;   % 80 kts (A + B)
       0.0, 0.0369, 0.0113;   % 120 kts (A - B)
       0.0, 0.0516, 0.0413;   % 120 kts (A + B)
       0.0, 0.0460, 0.0180;   % 145 kts (A - B)
       0.0, 0.0660, 0.0530];  % 145 kts (A + B)

% Matrix of coefficient phases (deg)
phase = [338.0, 0.0, 0.0;    % FPG100 (A - B)
         0.0, 147.3, 146.7;  % 0 kts (A - B)
         0.0, 126.7, 122.4;  % 80 kts (A - B)
         0.0, 196.2, 196.2;  % 80 kts (A + B)
         0.0, 138.0, 136.7;  % 120 kts (A - B)

```

```

        0.0, 189.6, 191.7;    % 120 kts (A + B)
        0.0, 147.0, 139.0;    % 145 kts (A - B)
        0.0, 192.7, 192.0];    % 145 kts (A + B)
% Convert the coefficients to complex numbers
A = mag.*(cos( phase*pi/180 ) + i*sin( phase*pi/180 ) );

% Calculate the adjustments
adjCmplx = A\vibsCmplx;
% Convert the adjustments to magnitude and phase
adj.mag = abs( adjCmplx );
adj.phase = angle( adjCmplx )*180/pi;

%%%%%%%%%%%%%%%%%%%%%%%%%%%%%%%%%%%%%%%%%%%%%%%%%%%%%%%%%%%%%%%%%%%%%%%%

% Capt Nathan A Miller
% Converts VMEP adjustments into magnitude and phase of adjustments.

function VMEP_2_MagPhase

load UH60_VMEP_Adjustments.mat
n = length(UH60_VMEP_Adjustments(:,1));

a=UH60_VMEP_Adjustments;
clear UH60_VMEP_Adjustments

for j=1:n
    %           Yellow   Blue   Red   Blck
    adjcplx(j,1) = +a(j,1)-i*a(j,4)-a(j,7)+i*a(j,10); % Weight Adj
    adjcplx(j,2) = +a(j,2)-i*a(j,5)-a(j,8)+i*a(j,11); % P/L Adj
    adjcplx(j,3) = +a(j,3)-i*a(j,6)-a(j,9)+i*a(j,12); % Tab Adj
end
VMEPadj.mag=abs(adjcplx);
VMEPadj.phase = angle(adjcplx)*180/pi;

save VMEPadj.mat VMEPadj

%%%%%%%%%%%%%%%%%%%%%%%%%%%%%%%%%%%%%%%%%%%%%%%%%%%%%%%%%%%%%%%%%%%%%%%%

% Capt Miller
% This program converts the coefficient matrix data into actual
% coefficient matrices. The program loads the raw vibe data from
% UH60Vibes.mat and computes a delta vibe from the predicted vibe
values
% stored in UH60_Coeff_Data.mat. The coefficient matrix is computed
% column by column. Once computed, the coefficient matrix operates on
a
% vibe set to produce a linear adjustment set.

function VMEP_Coefficient_Matrix

load UH60VIBES.mat
load UH60_Coeff_Data.mat

n=length(UH60VIBES(:,1))
for j=1:n

```

```

        wt = UH60_Coeff_Data(j,1);
        pl = UH60_Coeff_Data(j,20);
        tab = UH60_Coeff_Data(j,39);
        for k=1:9 % loops over the 8 flight conditons, FPG100(A-B),
Hover(A-B),
        % 80Kts(A-B)(A+B), 120Kts(A-B)(A+B),145Kts(A-B)(A+B) and
finally
        % the VMEP specific Hover(A+B)condition as #9
        vibmag=UH60VIBES(j,1+4*(k-1));
        vibphase=UH60VIBES(j,2+4*(k-1));
        vibcmplx=vibmag*(cos( vibphase*pi/180 ) + ...
            i*sin( vibphase*pi/180 ) );
        pvibwtmag=UH60_Coeff_Data(j,2+2*(k-1));
        pvibwtphase=UH60_Coeff_Data(j,3+2*(k-1));
        pvibwtcmplx=pvibwtmag*(cos( pvibwtphase*pi/180 ) + ...
            i*sin( pvibwtphase*pi/180 ) );
        pvibplmag=UH60_Coeff_Data(j,21+2*(k-1));
        pvibplphase=UH60_Coeff_Data(j,22+2*(k-1));
        pvibplcmplx=pvibplmag*(cos( pvibplphase*pi/180 ) + ...
            i*sin( pvibplphase*pi/180 ) );
        pvibtabmag=UH60_Coeff_Data(j,40+2*(k-1));
        pvibtabphase=UH60_Coeff_Data(j,41+2*(k-1));
        pvibtabcmplx=pvibtabmag*(cos( pvibtabphase*pi/180 ) + ...
            i*sin( pvibtabphase*pi/180 ) );
        dvibwt=pvibwtcmplx-vibcmplx;
        dvibpl=pvibplcmplx-vibcmplx;
        dvibtab=pvibtabcmplx-vibcmplx;
        A(k,1)=dvibwt/wt;
        A(k,2)=dvibpl/pl;
        A(k,3)=dvibtab/tab;
    end
    Coeff{j}=A;
end

%%%%%%%%%%%%%%%%%%%%%%%%%%%%%%%%%%%%%%%%%%%%%%%%%%%%%%%%%%%%%%%%%%%%%%%%%%

% Capt Miller
% This program creates polar plots of the ad hoc coefficient
% adjustments as well as the VMEP and AVA adjustments. It also
% calculates the maximum difference between the VMEP adjustments and
% the ad hoc adjustments.

clear;clc;close all;

load Coeff.mat
load UH60VIBES.mat
load VMEPadj.mat

% Runs the Least Squares Coefficient function to generate the LSC
% matrix from the Coeff cell.
[LSC, standard]=Least_Squares_Coeff(Coeff);
r=0

```

```

for z=1:5
    r=r+1;
    vib_num=z;
    b=1 ;% Sets beginning Coefficient Matrix to consider
    e=length(Coeff); % Sets ending Coefficient Matrix to consider
                        %(set to length(Coeff) to do all)
    % Convert Pre-Adjustment vibe data into complex array
    for j=1:length(Coeff)
        mag = UH60VIBES(j,[1 5 9 13 17 21 25 29 33])';
        phase = UH60VIBES(j,[2 6 10 14 18 22 26 30 34])';
        vibsCmplx = mag.*(cos( phase*pi/180 ) + i*sin( phase*pi/180 ) );
        pmag = UH60VIBES(j,[3 7 11 15 19 23 27 31 35])';
        pphase = UH60VIBES(j,[4 8 12 16 20 24 28 32 36])';
        pvibsCmplx = pmag.*(cos( pphase*pi/180 ) + i*sin( pphase*pi/180 )
    );
        vibset(:,j) = -vibsCmplx+pvibsCmplx;
    end

    % Select discrete vibe set to use for comparison
    discrete_vib=vibset(:,vib_num);

    for j=1:length(Coeff)
        adj(:,j)=Coeff{j}\vibset(:,j);
        % adj(:,j)=Coeff{j}\discrete_vib;
        Cmag(:,j) = abs(adj(:,j)); % Calculate real-number Mag and
        Cphase(:,j) = (angle(adj(:,j)))*180/pi; % Phase values for later
    use
    end

    VMEP2AVA.mag = Cmag'; % Stores Mag and Phase data to disk
    VMEP2AVA.phase = Cphase';
    save VMEP2AVA.mat VMEP2AVA

    % Calculate the Least Squares Method adjustment
    A = LSC.mag.*(cos( LSC.phase*pi/180 ) + i*sin( LSC.phase*pi/180 ) );
    LS_adj=A\discrete_vib;

    AVA_adj=LinearUH60( discrete_vib(1:8)- pvibsCmplx(1:8));
    %AVA_adj=LinearUH60( discrete_vib(1:8));
    VMEPmag=VMEPadj.mag(vib_num,:);
    VMEPphase=VMEPadj.phase(vib_num,:);

    % Determine the max magnitude so we can normalize our adjustments for
    % use in plotting on a single graph
    for k=1:3

        M=max(VMEPmag(k), abs(LS_adj(k)));
        Max(k)=max(M,AVA_adj.mag(k));
    end

    subplot(2,3,r)
    polar(0,1,'.w')
    hold;

    % Plot PCR adjustments

```

```

polar(VMEPphase(1)*pi/180,VMEPmag(1)/Max(1),'*r')
polar(angle(adj(1,z)),abs(adj(1,z))/Max(1),'ro')
% polar(angle(LS_adj(1)),abs(LS_adj(1))/Max(1),'sr')
% polar(AVA_adj.phase(1)*pi/180,AVA_adj.mag(1)/Max(1), 'or')

% Plot Tab adjustments
polar(VMEPphase(2)*pi/180,VMEPmag(2)/Max(2),'*k')
polar(angle(adj(2,z)),abs(adj(2,z))/Max(2),'ok')
% polar(angle(LS_adj(2)),abs(LS_adj(2))/Max(2),'sk')
% polar(AVA_adj.phase(2)*pi/180, AVA_adj.mag(2)/Max(2), 'ok')

% Plot Tab adjustments
polar(VMEPphase(3)*pi/180,VMEPmag(3)/Max(3),'*b')
polar(angle(adj(3,z)),abs(adj(3,z))/Max(3),'ob')
% polar(angle(LS_adj(3)),abs(LS_adj(3))/Max(3),'sb')
% polar(AVA_adj.phase(3)*pi/180, AVA_adj.mag(3)/Max(3), 'ob')
title('Red-wt, Black-PCR, Blue-Tab')
% figure(2)
% subplot(1,3,1)
% polar(angle(adj(1,b:e)),abs(adj(1,b:e)),'xr')
% title('Weight')
% subplot(1,3,2)
% polar(angle(adj(2,b:e)),abs(adj(2,b:e)),'xr')
% title('PCR')
% subplot(1,3,3)
%% polar(angle(adj(3,b:e)),abs(adj(3,b:e)),'xr')
% title('Trim Tab')
end
VMEPcplx = VMEPadj.mag.*(cos(VMEPadj.phase*pi/180) + ...
    i*sin(VMEPadj.phase*pi/180));
for j=1:20
    diff(j,:)=abs(VMEPcplx(j,:) - (A\vibset(:,j))).'
end
max(diff)
figure(2)
polar(AVA_adj.phase(2)*pi/180,AVA_adj.mag(2),'or')
hold on
polar(VMEPphase(2)*pi/180,VMEPmag(2),'*r')

%%%%%%%%%%%%%%%%%%%%%%%%%%%%%%%%%%%%%%%%%%%%%%%%%%%%%%%%%%%%%%%%%%%%%%%%

% Capt Miller
% This function creates a single coefficient matrix from N coefficient
% matrices by summing the squares of the N coefficient matrix
% components
% and then taking the square root. It also calculates the standard
% deviation of all ad hoc coefficients from their mean value.

function [LSC, standard]=Least_Squares_Coeff(Coeff)

numcoeff=length(Coeff);
numrows=length(Coeff{1}(:,1));
numcollumns=length(Coeff{1}(1,:));

```

```

C=zeros(numrows,numcollumns);

for j=1:numcoeff
    A.mag=abs(Coeff{ j});
    A.phase=angle(Coeff{ j});
    C=C+(A.mag.^2).*(cos( A.phase ) + i*sin( A.phase ) );
end

LSC.mag=sqrt(abs(C)/numcoeff);
LSC.phase=angle(C)*180/pi;
for j=1:numrows
    for k=1:numcollumns
        if LSC.phase(j,k) < 0
            LSC.phase(j,k) = LSC.phase(j,k)+360;
        end
    end
end

LSCcmplx = LSC.mag.*(cos(LSC.phase*pi/180)+i*sin(LSC.phase*pi/180));
for j=1:numcoeff

    diff{ j}=abs(Coeff{ j}-LSCcmplx);

end
for j=1:numrows
    for k=1:numcollumns
        for l=1:numcoeff
            temp(l)=diff{ l}(j,k);
        end
        standard(j,k) = std(temp);
    end
end

%%%%%%%%%%%%%%%%%%%%%%%%%%%%%%%%%%%%%%%%%%%%%%%%%%%%%%%%%%%%%%%%%%%%%%%%%%

% Capt Miller

% This program will maesure the difference between the VMEP adjustment
and
% the ad hoc adjustment for each flight. Intent is to determine
% if the minus zero produces any differences in adjustments.

clear;clc;close all;

load Coeff.mat
load UH60VIBES.mat
load UH60_Coeff_Data.mat
load VMEPadj.mat

n=20
[LSC, standard]=Least_Squares_Coeff(Coeff)
for j=1:n

    mag = UH60VIBES(j,[1 5 9 13 17 21 25 29 33])';
    phase = UH60VIBES(j,[2 6 10 14 18 22 26 30 34])';

```

```

vibsCmplx = mag.*(cos( phase*pi/180 ) + i*sin( phase*pi/180 ) );
pmag = UH60VIBES(j,[3 7 11 15 19 23 27 31 35]);
pphase = UH60VIBES(j,[4 8 12 16 20 24 28 32 36]);
pvibsCmplx = pmag.*(cos( pphase*pi/180 ) + i*sin( pphase*pi/180 )
);

vibset(:,j) = -vibsCmplx+pvibsCmplx;
end

VMEPcplx = VMEPadj.mag.*(cos(VMEPadj.phase*pi/180) + ...
i*sin(VMEPadj.phase*pi/180));

A = LSC.mag.*(cos( LSC.phase*pi/180 ) + i*sin( LSC.phase*pi/180 ) );

for j=1:10
    tmp{2*j-1,:}=Coeff{2*j};% tmp(odd) = A(even)
    tmp{2*j,:}=Coeff{2*j-1};% tmp(even) = A(odd)
end
%clear Coeff; % Do not rem out if you wish to swap around
%Coeff=tmp; % ad hoc matrices
for j=1:n

    %adj(j,:)=A\vibset(:,j); % This one for plotting RMS ad hoc
    adj(j,:)=Coeff{j}\vibset(:,j);%This one for plotting individual ad
hocs
end
for type=1:3
    %figure(type)
    subplot(1,3,type)
    polar(angle(adj(1:n,type)),abs(adj(1:n,type)),'ko')
    hold on
    polar(angle(VMEPcplx(1:n,type)),abs(VMEPcplx(1:n,type)),'k+')
end
for j=1:20
    diff(j,:)=abs(VMEPcplx(j,:) - adj(j,:));
end
diff
max(diff)

%figure(1)
subplot(1,3,1)
title('Weight')
%legend('Ad Hoc Adjustment','Real Adjustment')
%figure(2)
subplot(1,3,2)
title('Pitch Link')
%legend('Ad Hoc Adjustment','Real Adjustment')
%figure(3)
subplot(1,3,3)
title('Trim Tab')
%legend('Ad Hoc Adjustment','Real Adjustment')

```

```

%%%%%%%%%%%%%%%%%%%%%%%%%%%%%%%%%%%%%%%%%%%%%%%%%%%%%%%%%%%%%%%%%%%%%%%%

```

```

% Capt Nathan A Miller
% Determining difference in AVA and VMEP methods using Histograms.

clear; clc;
load AVAadj.mat
load VMEPadj.mat

AVAcomplex = AVAadj.mag.*(cos( AVAadj.phase*pi/180 ) +...
    i*sin( AVAadj.phase*pi/180 ) );
VMEPcomplex = VMEPadj.mag.*(cos( VMEPadj.phase*pi/180 ) +...
    i*sin( VMEPadj.phase*pi/180 ) );
Magnitude_diff = abs(AVAcomplex - VMEPcomplex);

Rel_mag_diff = Magnitude_diff./AVAadj.mag;

for i=1:20
    if abs(AVAcomplex(i,2)) < 1/2
        % if abs(VMEPcomplex(i,2)) < 113/2
        Rel_mag_diff(i,2)=0;

        abs(AVAcomplex(i,2))
        abs(VMEPcomplex(i,2))
        %end
    end

    if abs(AVAcomplex(i,3)) < 2/2
        % if abs(VMEPcomplex(i,3)) < 0.5/2
        Rel_mag_diff(i,3)=0;

        abs(AVAcomplex(i,3))
        abs(VMEPcomplex(i,3))
        %end
    end
end
X = ([0 1 2 3 4 5 6 7 8 9]+0.5)/10;

for i=1:2
    [n(i,:),xout(i,:)]=hist(Rel_mag_diff(:,i+1),X);
    subplot(1,2,i);
    bar(xout(i,:)*100,n(i,:)/0.2,'k');
    AXIS([0 100 0 50])
    ylabel('Percentage of Total Flights Sampled')
end
subplot(1,2,1)
title('Pitch Link')

subplot(1,2,2)
title('Trim Tab')
text(-60,-3,'Percent Difference of PC-GBS Adjustments from AVA
Algorithm Adjustments')

%%%%%%%%%%%%%%%%%%%%%%%%%%%%%%%%%%%%%%%%%%%%%%%%%%%%%%%%%%%%%%%%%%%%%%%%

```



```

% Capt Miller Thesis
% This is a test program to determine if any mistakes were made
% during data entry. Any errors in vib data entry will appear as gross
% differences in the plotted ad hoc coefficients.

clear all; clf; clc; close all
load Coeff.mat
[LSC, standard]=Least_Squares_Coeff(Coeff);
[LSCgood, standardgood]=Least_Squares_Coeff(Coeff(1:5));
[LSCexd, standardexd]=Least_Squares_Coeff(Coeff(15:20));
b=1;
e=length(Coeff);
n=1;
FLG=-1 %positive for single fig
state=6;
for h=1:9
for j=b:e
    value(h,j+1-b,:)=Coeff{j}(h,:);
end
end
latvalue = value([1 2 3 5 7],:,:);
vertvalue = value([9 4 6 8],:,:);

for h=1:9
    max1(h)=max(abs(value(h,:,1)));
    max2(h)=max(abs(value(h,:,2)));
    max3(h)=max(abs(value(h,:,3)));
end
for h=1:5
    latmax1(h)=max(abs(latvalue(h,:,1)));
    latmax2(h)=max(abs(latvalue(h,:,2)));
    latmax3(h)=max(abs(latvalue(h,:,3)));
end
for h=1:4
    vertmax1(h)=max(abs(vertvalue(h,:,1)));
    vertmax2(h)=max(abs(vertvalue(h,:,2)));
    vertmax3(h)=max(abs(vertvalue(h,:,3)));
end
for h=1:9
%figure(h)
subplot(3,3,h)
%polar(angle(value(h,:,1)),abs(value(h,:,1))/max1(h),'bx')
%hold on
polar(angle(value(h,:,n)),abs(value(h,:,n)),'rx')
%figure(2)
%subplot(3,3,h)
%polar(angle(value(h,:,2)),abs(value(h,:,2))/max2(h),'rx')
%figure(3)
%subplot(3,3,h)
%polar(angle(value(h,:,3)),abs(value(h,:,3))/max3(h),'gx')
end
    subplot(3,3,1)
title('FPG100 A-B')
    subplot(3,3,2)
title('Hover A-B')

```

```

subplot(3,3,3)
title('80 Kts A-B')
subplot(3,3,4)
title('80 Kts A+B')
subplot(3,3,5)
title('120 Kts A-B')
subplot(3,3,6)
title('120 Kts A+B')
subplot(3,3,7)
title('145 Kts A-B')
subplot(3,3,8)
title('145 Kts A+B')
subplot(3,3,9)
title('Hover A+B')
if FLG>0
figure(1)
clf;
polar(angle(value(state(:,n))),abs(value(state(:,n))), 'rx')
end
figure(2)
for i=1:5
    temp = max(latmax1(i)*10,latmax2(i));
    maxval = max(temp,latmax3(i));
    subplot(2,3,i) % Each subplot is for a different lateral regime
    polar(0,maxval,'w.')
    hold on
    polar(angle(latvalue(i,:,1)),abs(latvalue(i,:,1))*10,'kx')
    polar(angle(latvalue(i,:,2)),abs(latvalue(i,:,2)), 'kd')
    polar(angle(latvalue(i,:,3)),abs(latvalue(i,:,3)), 'k^')
end

figure(3)
for i=1:4
    temp = max(vertmax1(i),vertmax2(i));
    maxval = max(temp,vertmax3(i));
    subplot(2,2,i) % Each subplot is for a different lateral regime
    polar(0,maxval,'w.')
    hold on
    polar(angle(vertvalue(i,:,1)),abs(vertvalue(i,:,1))*10,'kx')%%%%%%%%%%
    %%%%%%%%%%%
    polar(angle(vertvalue(i,:,2)),abs(vertvalue(i,:,2)), 'kd')
    polar(angle(vertvalue(i,:,3)),abs(vertvalue(i,:,3)), 'k^')
end

abs(LSCexd.mag-LSCgood.mag)./LSCgood.mag*100

figure(4)
i=5
polar(0,.06,'w.')
hold on
polar(angle(latvalue(i,:,1)),abs(latvalue(i,:,1))*10,'kx')
polar(angle(latvalue(i,:,2)),abs(latvalue(i,:,2)), 'kd')
polar(angle(latvalue(i,:,3)),abs(latvalue(i,:,3)), 'k^')

```

Appendix F: AH-64A Matlab Code

Note: The Matlab codes contained in this appendix were each used to perform one or more specific functions in the course of this research. There are several instances where parts of the code have been commented out with the % symbol. In order to reproduce all of the analysis of this thesis, some lines of code may need to be un-commented and other lines commented out.

```
% Capt Nathan A Miller
% This program creates MAT data files from imported Excel database
% Ensure that the two databases are imported into matlab prior to
running

function Excel_to_MAT
global data data2
n = length(data2(:,2))-2
% Read Vibration Magnitude and Phase as well as prediction magnitude
% and phase from Excel File and assign to data matrix
AH64A_Vibes = zeros(n,28);
for j=1:n
    for k=1:7

        AH64A_Vibes(j,1+4*(k-1)) = data(1+k+(j-1)*11,2);
        AH64A_Vibes(j,2+4*(k-1)) = data(1+k+(j-1)*11,3);
        AH64A_Vibes(j,3+4*(k-1)) = data(1+k+(j-1)*11,4);
        AH64A_Vibes(j,4+4*(k-1)) = data(1+k+(j-1)*11,5);
    end
end
save AH64A_Vibes.mat AH64A_Vibes
AH64A_VMEP_Adjustments = zeros(n,20);
for j=1:n
    for k=1:20
        AH64A_VMEP_Adjustments(j,k) = data2(j+2,k+1);
    end
end
save AH64A_VMEP_Adjustments.mat AH64A_VMEP_Adjustments
AH64A_Coeff_Data = zeros(n,75);
for j=1:n
    AH64A_Coeff_Data(j,1)=data(2+(j-1)*11,6);
    AH64A_Coeff_Data(j,16)=data(2+(j-1)*11,9); % Records manual adjustment
    AH64A_Coeff_Data(j,31)=data(2+(j-1)*11,12); % that produces delta vibes
    AH64A_Coeff_Data(j,46)=data(2+(j-1)*11,15);
    AH64A_Coeff_Data(j,61)=data(2+(j-1)*11,18);
    for k=1:7
        for z=1:5
            AH64A_Coeff_Data(j,2*k+15*(z-1)) = data(1+k+(j-1)*11,7+3*(z-1));
            AH64A_Coeff_Data(j,2*k+1+15*(z-1))=data(1+k+(j-1)*11,8+3*(z-1));
        end
    end
end
end
save AH64A_Coeff_Data.mat AH64A_Coeff_Data

%%%%%%%%%%%%%%%%%%%%%%%%%%%%%%%%%%%%%%%%%%%%%%%%%%%%%%%%%%%%%%%%%%%%%%%%%
```

```
% Capt Nathan A Miller
% Thesis work
% This program loads vibe data and calculates an AVA adjustment matrix
```

```
function Vibs2AVA_ADJ
```

```
load AH64A_Vibes.mat
n = length(AH64A_Vibes(:,1));
```

```
for j=1:n
```

```
mag = AH64A_Vibes(j,[1 5 9 13 17 21 25]);
phase = AH64A_Vibes(j,[2 6 10 14 18 22 26]);
vibsCmplx = mag.*(cos( phase*pi/180 ) + i*sin( phase*pi/180 ) );
pmag = AH64A_Vibes(j,[3 7 11 15 19 23 27]);
pphase = AH64A_Vibes(j,[4 8 12 16 20 24 28]);
pvibsCmplx = pmag.*(cos( pphase*pi/180 ) + i*sin( pphase*pi/180 ) );
delvib = -vibsCmplx + pvibsCmplx;
adj(j) = LinearAH64A( delvib );
```

```
end
```

```
for k=1:n
```

```
    magnitude(k,:) = adj(k).mag';
    Phase(k,:) = adj(k).phase';
```

```
end
```

```
AVAadj.mag = magnitude;
AVAadj.phase = Phase;
save AVAadj.mat AVAadj
```

```
%%%%%%%%%%%%%%%%%%%%%%%%%%%%%%%%%%%%%%%%%%%%%%%%%%%%%%%%%%%%%%%%%%%%%%%%%
```

```
% Capt Nathan A Miller
% Converts VMEP adjustments into magnitude and phase of adjustments.
```

```
function VMEP_2_MagPhase
```

```
load AH64A_VMEP_Adjustments.mat
n = length(AH64A_VMEP_Adjustments(:,1));
```

```
a=AH64A_VMEP_Adjustments;
clear AH64A_VMEP_Adjustments
```

```
for j=1:n
```

```
    %           blade #    1          2          3          4
    adjcplx(j,1) = +a(j,1)-i*a(j,6)-a(j,11)+i*a(j,16); % Weight Adj
    adjcplx(j,2) = +a(j,2)-i*a(j,7)-a(j,12)+i*a(j,17); % P/L Adj
    adjcplx(j,3) = +a(j,3)-i*a(j,8)-a(j,13)+i*a(j,18); % Tab Adj 8
    adjcplx(j,4) = +a(j,4)-i*a(j,9)-a(j,14)+i*a(j,19); % Tab Adj 6
    adjcplx(j,5) = +a(j,5)-i*a(j,10)-a(j,15)+i*a(j,20); % Tab Adj 4
```

```
end
```

```

VMEPadj.mag=abs(adjcmplx);
VMEPadj.phase = angle(adjcmplx)*180/pi;

save VMEPadj.mat VMEPadj

%%%%%%%%%%%%%%%%%%%%%%%%%%%%%%%%%%%%%%%%%%%%%%%%%%%%%%%%%%%%%%%%%%%%%%%%

% Capt Miller
% This program generates plots of the ad hoc adjustments

clear;clc;close all;

load Coeff.mat
load AH64A_Vibes.mat

for j=1:length(Coeff)
    mag = AH64A_Vibes(j,[1 5 9 13 17 21 25]);
    phase = AH64A_Vibes(j,[2 6 10 14 18 22 26]);
    vibsCmplx = mag.*(cos( phase*pi/180 ) + i*sin( phase*pi/180 ) );

    pmag = AH64A_Vibes(j,[3 7 11 15 19 23 27]);
    pphase = AH64A_Vibes(j,[4 8 12 16 20 24 28]);
    pvibsCmplx = pmag.*(cos( pphase*pi/180 ) + i*sin( pphase*pi/180 )
);

    vib(:,j) = vibsCmplx;% - pvibsCmplx;

end
v=vib(:,1)
for j=1:length(Coeff)
    adj(:,j)=Coeff{j}\v;

    magnitude(:,j) = abs(adj(:,j));
    Faze(:,j) = (angle(adj(:,j)))*180/pi;

end

ava=LinearAH64A( v );
avaadj=ava.mag.*(cos( ava.phase*pi/180 ) + i*sin( ava.phase*pi/180
) );

VMEP2AVA.mag = magnitude';
VMEP2AVA.phase = Faze';
save VMEP2AVA.mat VMEP2AVA

figure(1)
if max(abs(ava.mag(1))) > max(abs(adj(1,:)))
    polar(ava.phase(1)*pi/180,ava.mag(1),'*r')
    hold
    polar(angle(adj(1,:)),abs(adj(1,:)))
else
    polar(angle(adj(1,:)),abs(adj(1,:)))
    hold
    polar(ava.phase(1)*pi/180,ava.mag(1),'*r')
end

```

```

ava.mag
ava.phase
figure(2)
    if max(abs(ava.mag(2))) > max(abs(adj(2,:)))
        polar(ava.phase(2)*pi/180,ava.mag(2),'*r')
        hold
        polar(angle(adj(2,:)),abs(adj(2,:)))
    else
        polar(angle(adj(2,:)),abs(adj(2,:)))
        hold
        polar(ava.phase(2)*pi/180,ava.mag(2),'*r')
    end

figure(3)
    if max(abs(ava.mag(3))) > max(abs(adj(3,:)))
        polar(ava.phase(3)*pi/180,ava.mag(3),'*r')
        hold
        polar(angle(adj(3,:)),abs(adj(3,:)))
    else
        polar(angle(adj(3,:)),abs(adj(3,:)))
        hold
        polar(ava.phase(3)*pi/180,ava.mag(3),'*r')
    end

figure(4)
    if max(abs(ava.mag(4))) > max(abs(adj(4,:)))
        polar(ava.phase(4)*pi/180,ava.mag(4),'*r')
        hold
        polar(angle(adj(4,:)),abs(adj(4,:)))
    else
        polar(angle(adj(4,:)),abs(adj(4,:)))
        hold
        polar(ava.phase(4)*pi/180,ava.mag(4),'*r')
    end

figure(5)
    if max(abs(ava.mag(5))) > max(abs(adj(5,:)))
        polar(ava.phase(5)*pi/180,ava.mag(5),'*r')
        hold
        polar(angle(adj(5,:)),abs(adj(5,:)))
    else
        polar(angle(adj(5,:)),abs(adj(5,:)))
        hold
        polar(ava.phase(5)*pi/180,ava.mag(5),'*r')
    end

%%%%%%%%%%%%%%%%%%%%%%%%%%%%%%%%%%%%%%%%%%%%%%%%%%%%%%%%%%%%%%%%%%%%%%%%

```

```

% Capt Miller
% This program converts the coefficient matrix data into actual
% coefficient matrices. The program loads the raw vibe data from
% AH64A_Vibes.mat and computes a delta vibe from the predicted vibe
% values stored in AH64A_Coeff_Data.mat. The coefficient matrix is
% computed column by column. Once computed, the coefficient matrix
% operates on a vibe set to produce a quasi-linear adjustment set.
% This process is repeated for each coefficient data set. The same
% vibe set is always used for comparison.

```

```

function VMEP_Coefficient_Matrix

```

```

load AH64A_Vibes.mat
load AH64A_Coeff_Data.mat
n=length(AH64A_Vibes(:,1));
for j=1:n

    wt = AH64A_Coeff_Data(j,1);
    pl = AH64A_Coeff_Data(j,16);
    tab8 = AH64A_Coeff_Data(j,31);
    tab6 = AH64A_Coeff_Data(j,46) ;
    tab4 = AH64A_Coeff_Data(j,61);

    for k=1:7 % loops over the 7 flight conditons, FPG100 through 140 Knots
        vibmag=AH64A_Vibes(j,1+4*(k-1));
        vibphase=AH64A_Vibes(j,2+4*(k-1));
        vibcmplx=vibmag*(cos( vibphase*pi/180 ) + ...
            i*sin( vibphase*pi/180 ) );

        pvibwtmag=AH64A_Coeff_Data(j,2+2*(k-1));
        pvibwtphase=AH64A_Coeff_Data(j,3+2*(k-1));
        pvibwtcmplx=pvibwtmag*(cos( pvibwtphase*pi/180 ) + ...
            i*sin( pvibwtphase*pi/180 ) );

        pvibplmag=AH64A_Coeff_Data(j,17+2*(k-1));
        pvibplphase=AH64A_Coeff_Data(j,18+2*(k-1));
        pvibplcmplx=pvibplmag*(cos( pvibplphase*pi/180 ) + ...
            i*sin( pvibplphase*pi/180 ) );

        pvibtab8mag=AH64A_Coeff_Data(j,32+2*(k-1));
        pvibtab8phase=AH64A_Coeff_Data(j,33+2*(k-1));
        pvibtab8cmplx=pvibtab8mag*(cos( pvibtab8phase*pi/180 ) + ...
            i*sin( pvibtab8phase*pi/180 ) );

        pvibtab6mag=AH64A_Coeff_Data(j,47+2*(k-1));
        pvibtab6phase=AH64A_Coeff_Data(j,48+2*(k-1));
        pvibtab6cmplx=pvibtab6mag*(cos( pvibtab6phase*pi/180 ) + ...
            i*sin( pvibtab6phase*pi/180 ) );

        pvibtab4mag=AH64A_Coeff_Data(j,62+2*(k-1));
        pvibtab4phase=AH64A_Coeff_Data(j,63+2*(k-1));
        pvibtab4cmplx=pvibtab4mag*(cos( pvibtab4phase*pi/180 ) + ...
            i*sin( pvibtab4phase*pi/180 ) );

        dvibwt=pvibwtcmplx-vibcmplx;
    end
end

```

```

dvibpl=pvibplcmplx-vibcmplx;
dvibtab8=pvibtab8cmplx-vibcmplx;
dvibtab6=pvibtab6cmplx-vibcmplx;
dvibtab4=pvibtab4cmplx-vibcmplx;

A(k,1)=dvibwt/wt;
A(k,2)=dvibpl/pl;
A(k,3)=dvibtab8/tab8;
A(k,4)=dvibtab6/tab6;
A(k,5)=dvibtab4/tab4;

end
Coeff{j}=A;

end
save Coeff.mat Coeff

%%%%%%%%%%%%%%%%%%%%%%%%%%%%%%%%%%%%%%%%%%%%%%%%%%%%%%%%%%%%%%%%%%%%%%%%%%%%%%

% Capt Miller Thesis
% This is a test program to determine if any mistakes were made
% during data entry.
clear; clf; clc;
load Coeff.mat
b=1
e=length(Coeff)
n=1
for h=1:7
    for j=b:e
        value(h,j+1-b,:)=Coeff{j}(h,:);
    end
end

for h=1:7
    max1(h)=max(abs(value(h,:,1)));
    max2(h)=max(abs(value(h,:,2)));
    max3(h)=max(abs(value(h,:,3)));
    max4(h)=max(abs(value(h,:,4)));
    max5(h)=max(abs(value(h,:,5)));
end

for h=1:7
%figure(h)
subplot(3,3,h)
%polar(angle(value(h,:,1)),abs(value(h,:,1))/max1(h),'bx')
polar(angle(value(h,:,n)),abs(value(h,:,n)),'rx')
%hold on
%figure(2)
%subplot(3,3,h)
%polar(angle(value(h,:,2)),abs(value(h,:,2))/max2(h),'rx')
%figure(3)
%subplot(3,3,h)
%polar(angle(value(h,:,3)),abs(value(h,:,3))/max3(h),'gx')
%polar(angle(value(h,:,4)),abs(value(h,:,4))/max4(h),'mx')
%polar(angle(value(h,:,5)),abs(value(h,:,5))/max5(h),'cx')

```



```

end
subplot(3,3,1)
title('FPG100 Lat')
subplot(3,3,2)
title('Hover Lat')
subplot(3,3,3)
title('60 Kts Vert')
subplot(3,3,4)
title('80 Kts Vert')
subplot(3,3,5)
title('100 Kts Vert')
subplot(3,3,6)
title('120 Kts Vert')
subplot(3,3,7)
title('140 Kts Vert')
%figure(1)
%clf;
%polar(angle(value(4,:,1)),abs(value(4,:,1)),'bx')

%%%%%%%%%%%%%%%%%%%%%%%%%%%%%%%%%%%%%%%%%%%%%%%%%%%%%%%%%%%%%%%%%%%%%%%%

% Capt Miller
% Rough plots of coeff matrix results

clear;clc;clf;

load Coeff.mat
load AH64A_Vibes.mat
load VMEPAdj.mat
[LSC, standard]=Least_Squares_Coeff(Coeff);
% Runs the Least Squares Coefficient function to
% generate the LSC matrix from the Coeff cell.
vib_num=20
b=1
e=length(Coeff)
for j=1:length(Coeff)
    mag = AH64A_Vibes(j,[1 5 9 13 17 21 25]);
    phase = AH64A_Vibes(j,[2 6 10 14 18 22 26]);
    vibsCmplx = mag.*(cos( phase*pi/180 ) + i*sin( phase*pi/180 ) );
    pmag = AH64A_Vibes(j,[3 7 11 15 19 23 27]);
    pphase = AH64A_Vibes(j,[4 8 12 16 20 24 28]);
    pvibsCmplx = pmag.*(cos( pphase*pi/180 ) + i*sin( pphase*pi/180 )
);
    vibset(:,j) = -vibsCmplx + pvibsCmplx;
end
discrete_vib=vibset(:,vib_num); % Select discrete vibe set to use for
comparison
for j=1:length(Coeff)
    adj(:,j)=Coeff{j}\discrete_vib;
    Cmag(:,j) = abs(adj(:,j));
    Cphase(:,j) = (angle(adj(:,j)))*180/pi;
end
VMEP2AVA.mag = Cmag';
VMEP2AVA.phase = Cphase';
save VMEP2AVA.mat VMEP2AVA

```

```

    % Calculate the Least Squares Method adjustment
    A = LSC.mag.*(cos( LSC.phase*pi/180 ) + i*sin( LSC.phase*pi/180 ) );
    LS_adj=A\discrete_vib;
    AVA_adj=LinearAH64A( discrete_vib );
    VMEPmag=VMEPadj.mag(vib_num,:);
    VMEPphase=VMEPadj.phase(vib_num,:);
    % Determine the max magnitude so we can normalize our adjustments for
    % use in plotting on a single graph
    for k=1:5
        Max1=max(max(Cmag(k,b:e)), AVA_adj.mag(k));
        %Max1=max(abs(AVA_adj.mag(k)));
        Max2=max(VMEPmag(k), abs(LS_adj(k)));
        Max(k)=max(Max1,Max2);
        %Max(k)=max(Cmag(k,b:e));
    end
    %figure(1)
    subplot(2,3,1)
    polar(0,1,'.w')
    hold
    % Plot weight adjustments
    % polar(Cphase(1,b:e)*pi/180,Cmag(1,b:e)/Max(1),'xr')
    polar(angle(LS_adj(1)),abs(LS_adj(1))/Max(1),'sr')
    polar(AVA_adj.phase(1)*pi/180,AVA_adj.mag(1)/Max(1),'or')
    polar(VMEPphase(1)*pi/180,VMEPmag(1)/Max(1),'*r')

    % Plot PCR adjustments
    % polar(Cphase(2,b:e)*pi/180,Cmag(2,b:e)/Max(2),'xk')
    polar(angle(LS_adj(2)),abs(LS_adj(2))/Max(2),'sk')
    polar(AVA_adj.phase(2)*pi/180,AVA_adj.mag(2)/Max(2),'ok')
    polar(VMEPphase(2)*pi/180,VMEPmag(2)/Max(2),'*k')

    % Plot tab 8 adjustments
    % polar(Cphase(3,b:e)*pi/180,Cmag(3,b:e)/Max(3),'xb')
    polar(angle(LS_adj(3)),abs(LS_adj(3))/Max(3),'sb')
    polar(AVA_adj.phase(3)*pi/180,AVA_adj.mag(3)/Max(3),'ob')
    polar(VMEPphase(3)*pi/180,VMEPmag(3)/Max(3),'*b')
    % Plot tab 6 adjustments
    % polar(Cphase(4,b:e)*pi/180,Cmag(4,b:e)/Max(4),'xg')
    polar(angle(LS_adj(4)),abs(LS_adj(4))/Max(4),'sg')
    polar(AVA_adj.phase(4)*pi/180,AVA_adj.mag(4)/Max(4),'og')
    polar(VMEPphase(4)*pi/180,VMEPmag(4)/Max(4),'*g')

    % Plot tab 4 adjustments
    % polar(Cphase(5,b:e)*pi/180,Cmag(5,b:e)/Max(5),'xm')
    polar(angle(LS_adj(5)),abs(LS_adj(5))/Max(5),'sm')
    polar(AVA_adj.phase(5)*pi/180,AVA_adj.mag(5)/Max(5),'om')
    polar(VMEPphase(5)*pi/180,VMEPmag(5)/Max(5),'*m')

    title('Red-Wt, Black-Pcr, Blue-Tab8, Green-Tab6, Magenta-Tab4')
    subplot(2,3,2)
    polar(Cphase(1,b:e)*pi/180,Cmag(1,b:e),'xr')
    title('Weight')
    subplot(2,3,3)
    polar(Cphase(2,b:e)*pi/180,Cmag(2,b:e),'xk')
    title('Pitch Link')

```



```

% Capt Miller
% This function creates a single coefficient matrix from N coefficient
% matrices by summing the squares of the N coefficient matrix
% components and then taking the square root.

function [LSC, standard]=Least_Squares_Coeff(Coeff)

numcoeff=length(Coeff);
numrows=length(Coeff{1}(:,1));
numcollumns=length(Coeff{1}(1,:));

C=zeros(numrows,numcollumns);

for j=1:numcoeff
    A.mag=abs(Coeff{j});
    A.phase=angle(Coeff{j});
    C=C+(A.mag.^2).*(cos( A.phase ) + i*sin( A.phase ) );
end

LSC.mag=sqrt(abs(C)/numcoeff);
LSC.phase=angle(C)*180/pi;
for j=1:numrows
    for k=1:numcollumns
        if LSC.phase(j,k) < 0
            LSC.phase(j,k) = LSC.phase(j,k)+360;
        end
    end
end

LSCcmplx = LSC.mag.*(cos(LSC.phase*pi/180)+i*sin(LSC.phase*pi/180));
for j=1:numcoeff

    diff{j}=abs(Coeff{j}-LSCcmplx);

end
for j=1:numrows
    for k=1:numcollumns
        for l=1:numcoeff
            temp(l)=diff{l}(j,k);
        end
        standard(j,k) = std(temp);
    end
end

%%%%%%%%%%%%%%%%%%%%%%%%%%%%%%%%%%%%%%%%%%%%%%%%%%%%%%%%%%%%%%%%%%%%%%%%

```

```

% Capt Miller

% This program will measure the difference between the VMEP adjustment
% and the ad hoc adjustment for each flight. This is done for normal
% ad hoc coefficients and ad hoc minus zero coefficients. Intent is to
% determine if the minus zero produces any differences in adjustments.

clear;clc;close all;

load Coeff.mat
load AH64A_Vibes.mat
load AH64A_Coeff_Data.mat
load VMEPAdj.mat
[LSC, standard]=Least_Squares_Coeff(Coeff);
n=20;
for j=1:length(Coeff)
    mag = AH64A_Vibes(j,[1 5 9 13 17 21 25]);
    phase = AH64A_Vibes(j,[2 6 10 14 18 22 26]);
    vibsCmplx = mag.*(cos( phase*pi/180 ) + i*sin( phase*pi/180 ) );
    pmag = AH64A_Vibes(j,[3 7 11 15 19 23 27]);
    pphase = AH64A_Vibes(j,[4 8 12 16 20 24 28]);
    pvibsCmplx = pmag.*(cos( pphase*pi/180 ) + i*sin( pphase*pi/180 )
);
    vibset(:,j) = -vibsCmplx + pvibsCmplx;
end

for j=1:10
    tmp{2*j-1,:}=Coeff{2*j};% tmp(odd) = A(even)
    tmp{2*j,:}=Coeff{2*j-1};% tmp(even) = A(odd)
end
%clear Coeff;
%Coeff=tmp;

VMEPcplx = VMEPAdj.mag.*(cos(VMEPAdj.phase*pi/180) + ...
    i*sin(VMEPAdj.phase*pi/180))

A = LSC.mag.*(cos( LSC.phase*pi/180 ) + i*sin( LSC.phase*pi/180 ) );
for j=1:20

%adj(j,:)=A\vibset(:,j); % This one for plotting RMS ad hoc
adj(j,:)=Coeff{j}\vibset(:,j);%This one for plotting individual ad
hocs
end
for type=1:5
    % figure(type)
    subplot(2,3,type)
    polar(angle(adj(1:n,type)),abs(adj(1:n,type)),'ko')
    hold on
    polar(angle(VMEPcplx(1:n,type)),abs(VMEPcplx(1:n,type)),'k+')
end
for j=1:20
    diff(j,:)=abs(VMEPcplx(j,:) - adj(j,:));
end
diff
max(diff)

```

```

%figure(1)
subplot(2,3,1)
title('Weight')
%legend('Ad Hoc Adjustment','Actual Adjustment')
%figure(2)
subplot(2,3,2)
title('Pitch Link')
%legend('Ad Hoc Adjustment','Actual Adjustment')
%figure(3)
subplot(2,3,3)
title('Trim Tab 8-10')
%legend('Ad Hoc Adjustment','Actual Adjustment')
subplot(2,3,4)
title('Trim Tab 6-10')
subplot(2,3,5)
title('Trim Tab 4-10')

%%%%%%%%%%%%%%%%%%%%%%%%%%%%%%%%%%%%%%%%%%%%%%%%%%%%%%%%%%%%%%%%%%%%%%%%

% Capt Nathan A Miller
% This program determines the difference between the AVA algorithm and
the
% PC-GBS and creates a histogram of the results for each adjustment
type.

clear; clc;
load AVAadj.mat
load VMEPadj.mat

AVAcomplex = AVAadj.mag.*(cos( AVAadj.phase*pi/180 ) +...
    i*sin( AVAadj.phase*pi/180 ) );
VMEPcomplex = VMEPadj.mag.*(cos( VMEPadj.phase*pi/180 ) +...
    i*sin( VMEPadj.phase*pi/180 ) );
Magnitude_diff = abs(AVAcomplex - VMEPcomplex);

Rel_mag_diff = Magnitude_diff./max(VMEPadj.mag, AVAadj.mag);

for i=1:20
    if abs(AVAcomplex(i,1)) < 113/2
        if abs(VMEPcomplex(i,1)) < 113/2
            Rel_mag_diff(i,1)=0;

            abs(AVAcomplex(i,1));
            abs(VMEPcomplex(i,1));
        end
    end

    if abs(AVAcomplex(i,2)) < 0.5/2
        if abs(VMEPcomplex(i,2)) < 0.5/2
            Rel_mag_diff(i,2)=0;

            abs(AVAcomplex(i,2));
            abs(VMEPcomplex(i,2));
        end
    end
end

```

```

        if abs(AVAcomplex(i,3)) < 0.5/2
            if abs(VMEPcomplex(i,3)) < 0.5/2
                Rel_mag_diff(i,3)=0;
            end
        end
        if abs(AVAcomplex(i,4)) < 0.5/2
            if abs(VMEPcomplex(i,4)) < 0.5/2
                Rel_mag_diff(i,4)=0;
            end
        end
        if abs(AVAcomplex(i,5)) < 0.5/2
            if abs(VMEPcomplex(i,5)) < 0.5/2
                Rel_mag_diff(i,5)=0;
            end
        end
    end
end

X = ([0 1 2 3 4 5 6 7 8 9]+0.5)/10;
for i=1:5
    [n(i,:),xout(i,:)]=hist(Rel_mag_diff(:,i),X);
    subplot(1,5,i);
    bar(xout(i,:)*100,n(i,:)/0.2,'k');
    AXIS([0 100 0 100])
end
subplot(1,5,1)
title('Weight','FontSize',16)
ylabel('Percentage of Total Flights Sampled','FontSize',16)
subplot(1,5,2)
title('Pitch Link','FontSize',16)
subplot(1,5,3)
title('Tab 8-10','FontSize',16)
xlabel('Percent Difference of PC-GBS Adjustments from AVA Algorithm Adjustments','FontSize',16)
subplot(1,5,4)
title('Tab 6-10','FontSize',16)
subplot(1,5,5)
title('Tab 4-10','FontSize',16)

%%%%%%%%%%%%%%%%%%%%%%%%%%%%%%%%%%%%%%%%%%%%%%%%%%%%%%%%%%%%%%%%%%%%%%%%%%%%%%

% Capt Miller Thesis
% This is a test program to determine if any mistakes were made
% during data entry.
clear all; close all; clc;

load Coeff.mat
[LSC, standard]=Least_Squares_Coeff(Coeff);
[LSCgood, standardgood]=Least_Squares_Coeff(Coeff(1:5));
[LSCexd, standardexd]=Least_Squares_Coeff(Coeff(15:20));
b=1;
e=length(Coeff);
n=1;
for h=1:7
    for j=b:e
        value(h,j+1-b,:)=Coeff{j}(h,:);
    end
end

```

```

end

end
vertvalue = value(3:7, :, :);
latvalue = value(1:2, :, :);
for h=1:7
    max1(h)=max(abs(value(h, :, 1)));
    max2(h)=max(abs(value(h, :, 2)));
    max3(h)=max(abs(value(h, :, 3)));
    max4(h)=max(abs(value(h, :, 4)));
    max5(h)=max(abs(value(h, :, 5)));
end

for h=1:5
    vertmax1(h)=max(abs(vertvalue(h, :, 1)));
    vertmax2(h)=max(abs(vertvalue(h, :, 2)));
    vertmax3(h)=max(abs(vertvalue(h, :, 3)));
    vertmax4(h)=max(abs(vertvalue(h, :, 4)));
    vertmax5(h)=max(abs(vertvalue(h, :, 5)));
end
for h=1:2
    latmax1(h)=max(abs(latvalue(h, :, 1)));
    latmax2(h)=max(abs(latvalue(h, :, 2)));
    latmax3(h)=max(abs(latvalue(h, :, 3)));
    latmax4(h)=max(abs(latvalue(h, :, 4)));
    latmax5(h)=max(abs(latvalue(h, :, 5)));
end

for h=1:7
    subplot(3,3,h)
    %polar(angle(value(h, :, 1)),abs(value(h, :, 1))/max1(h), 'bx')
    polar(angle(value(h, :, n)),abs(value(h, :, n)), 'rx')
end

subplot(3,3,1)
title('FPG100 Lat')
subplot(3,3,2)
title('Hover Lat')
subplot(3,3,3)
title('60 Kts Vert')
subplot(3,3,4)
title('80 Kts Vert')
subplot(3,3,5)
title('100 Kts Vert')
subplot(3,3,6)
title('120 Kts Vert')
subplot(3,3,7)
title('140 Kts Vert')

figure(2)
for i=1:5
    temp1 = max(vertmax1(i),vertmax2(i));
    temp2 = max(vertmax3(i),vertmax4(i));
    temp3 = max(temp1,temp2);

```



```

maxval = max(temp3,vertmax5(i));

subplot(2,3,i)      % Each subplot is for a different lateral regime
polar(0,maxval,'w.')
hold on
polar(angle(vertvalue(i,:,1)),abs(vertvalue(i,:,1)),'kx')
polar(angle(vertvalue(i,:,2)),abs(vertvalue(i,:,2)),'kd')
polar(angle(vertvalue(i,:,3)),abs(vertvalue(i,:,3)),'k^')
polar(angle(vertvalue(i,:,4)),abs(vertvalue(i,:,4)),'kv')
polar(angle(vertvalue(i,:,5)),abs(vertvalue(i,:,5)),'kp')
end
figure(3)
for i=1:2
    temp1 = max(latmax1(i),latmax2(i));
    temp2 = max(latmax3(i),latmax4(i));
    temp3 = max(temp1,temp2);
    maxval = max(temp3,latmax5(i));
subplot(1,2,i)      % Each subplot is for a different lateral regime
polar(0,maxval,'w.')
hold on
polar(angle(latvalue(i,:,1)),abs(latvalue(i,:,1)*100),'kx')
polar(angle(latvalue(i,:,2)),abs(latvalue(i,:,2)),'kd')
polar(angle(latvalue(i,:,3)),abs(latvalue(i,:,3)),'k^')
polar(angle(latvalue(i,:,4)),abs(latvalue(i,:,4)),'kv')
polar(angle(latvalue(i,:,5)),abs(latvalue(i,:,5)),'kp')
end

figure(4)
polar(0,maxval,'w.')
hold on
polar(angle(latvalue(i,:,1)),abs(latvalue(i,:,1)*100),'ko')
polar(angle(latvalue(i,:,2)),abs(latvalue(i,:,2)),'kd')
polar(angle(latvalue(i,:,3)),abs(latvalue(i,:,3)),'k^')
polar(angle(latvalue(i,:,4)),abs(latvalue(i,:,4)),'kv')
polar(angle(latvalue(i,:,5)),abs(latvalue(i,:,5)),'kp')
title('Ad Hoc Coefficients for Hover(Lat) for AH-64A')

abs(LSCexd.mag-LSCgood.mag)./LSCgood.mag*100

%%%%%%%%%%%%%%%%%%%%%%%%%%%%%%%%%%%%%%%%%%%%%%%%%%%%%%%%%%%%%%%%%%%%%%%%

```

Appendix G: AH-64D Matlab Code

Note: The Matlab codes contained in this appendix were each used to perform one or more specific functions in the course of this research. There are several instances where parts of the code have been commented out with the % symbol. In order to reproduce all of the analysis of this thesis, some lines of code may need to be un-commented and other lines commented out.

```
% Capt Nathan A Miller
% This program creates MAT data files from imported Excel database
% Ensure that the two databases are imported into matlab prior to
running

function Excel_to_MAT
global data data2
n = length(data2(:,2))-2
% Read Vibration Magnitude and Phase as well as prediction magnitude
% and phase from Excel File and assign to data matrix
Longbow_Vibes = zeros(n,28);
for j=1:n
    for k=1:7
        Longbow_Vibes(j,1+4*(k-1)) = data(1+k+(j-1)*11,2);
        Longbow_Vibes(j,2+4*(k-1)) = data(1+k+(j-1)*11,3);
        Longbow_Vibes(j,3+4*(k-1)) = data(1+k+(j-1)*11,4);
        Longbow_Vibes(j,4+4*(k-1)) = data(1+k+(j-1)*11,5);
    end
end
save Longbow_Vibes.mat Longbow_Vibes
Longbow_VMEP_Adjustments = zeros(n,20);
for j=1:n
    for k=1:20
        Longbow_VMEP_Adjustments(j,k) = data2(j+2,k+1);
    end
end
save Longbow_VMEP_Adjustments.mat Longbow_VMEP_Adjustments
Longbow_Coeff_Data = zeros(n,75);
for j=1:n
    Longbow_Coeff_Data(j,1)=data(2+(j-1)*11,6);
    Longbow_Coeff_Data(j,16)=data(2+(j-1)*11,9); % Records manual adjustment
    Longbow_Coeff_Data(j,31)=data(2+(j-1)*11,12); % that produces delta vibes
    Longbow_Coeff_Data(j,46)=data(2+(j-1)*11,15);
    Longbow_Coeff_Data(j,61)=data(2+(j-1)*11,18);
    for k=1:7
        for z=1:5
            Longbow_Coeff_Data(j,2*k+15*(z-1)) = data(1+k+(j-1)*11,7+3*(z-1));
            Longbow_Coeff_Data(j,2*k+15*(z-1))=data(1+k+(j-1)*11,8+3*(z-1));
        end
        Longbow_Coeff_Data(j,74+2*k)=data(1+k+(j-1)*11,21);
        Longbow_Coeff_Data(j,75+2*k)=data(1+k+(j-1)*11,22);
    end
end
save Longbow_Coeff_Data.mat Longbow_Coeff_Data
%%%%%%%%%%%%%%%%%%%%%%%%%%%%%%%%%%%%%%%%%%%%%%%%%%%%%%%%%%%%%%%%%%%%%%%%%
```

```

% Capt Miller
% This program converts the coefficient matrix data into actual
% coefficient matrices. The program loads the raw vibe data from
% AH64A_Vibes.mat and computes a delta vibe from the predicted vibe
% values stored in AH64A_Coeff_Data.mat. The coefficient matrix is
% computed column by column. Once computed, the coefficient matrix
% operates on a vibe set to produce a quasi-linear adjustment set.
% This process is repeated for each coefficient data set. The same
% vibe set is always used for comparison.

function VMEP_Coefficient_Matrix
FLG=-1;
delta=0;
load Longbow_Vibes.mat
load Longbow_Coeff_Data.mat

n=length(Longbow_Vibes(:,1));
for j=1:n

    wt = Longbow_Coeff_Data(j,1);
    pl = Longbow_Coeff_Data(j,16);
    tab8 = Longbow_Coeff_Data(j,31);
    tab6 = Longbow_Coeff_Data(j,46) ;
    tab4 = Longbow_Coeff_Data(j,61);

    for k=1:7 % loops over the 7 flight conditons, FPG100 through 140 Knots
        vibmag=Longbow_Vibes(j,1+4*(k-1));
        vibphase=Longbow_Vibes(j,2+4*(k-1));
        vibcmplx=vibmag*(cos( vibphase*pi/180 ) + ...
            i*sin( vibphase*pi/180 ) );

        pvibwtmag=Longbow_Coeff_Data(j,2+2*(k-1));
        pvibwtphase=Longbow_Coeff_Data(j,3+2*(k-1));
        pvibwtcmplx=pvibwtmag*(cos( pvibwtphase*pi/180 ) + ...
            i*sin( pvibwtphase*pi/180 ) );

        pvibplmag=Longbow_Coeff_Data(j,17+2*(k-1));
        pvibplphase=Longbow_Coeff_Data(j,18+2*(k-1));
        pvibplcmplx=pvibplmag*(cos( pvibplphase*pi/180 ) + ...
            i*sin( pvibplphase*pi/180 ) );

        pvibtab8mag=Longbow_Coeff_Data(j,32+2*(k-1));
        pvibtab8phase=Longbow_Coeff_Data(j,33+2*(k-1));
        pvibtab8cmplx=pvibtab8mag*(cos( pvibtab8phase*pi/180 ) + ...
            i*sin( pvibtab8phase*pi/180 ) );

        pvibtab6mag=Longbow_Coeff_Data(j,47+2*(k-1));
        pvibtab6phase=Longbow_Coeff_Data(j,48+2*(k-1));
        pvibtab6cmplx=pvibtab6mag*(cos( pvibtab6phase*pi/180 ) + ...
            i*sin( pvibtab6phase*pi/180 ) );

        pvibtab4mag=Longbow_Coeff_Data(j,62+2*(k-1));
        pvibtab4phase=Longbow_Coeff_Data(j,63+2*(k-1));
        pvibtab4cmplx=pvibtab4mag*(cos( pvibtab4phase*pi/180 ) + ...

```

```

        i*sin( pvibtab4phase*pi/180 ) );
    if FLG > 0
        zeromag=Longbow_Coeff_Data(j,76+2*(k-1));
        zerophase=Longbow_Coeff_Data(j,77+2*(k-1));
        zerocmplx=zeromag*(cos( zerophase*pi/180 ) + ...
            i*sin( zerophase*pi/180 ) );
        delta=vibcmlpx-zerocmplx;

    end

    dvibwt=pvibwtcmlpx-vibcmlpx-delta;
    dvibpl=pvibplcmlpx-vibcmlpx-delta;
    dvibtab8=pvibtab8cmlpx-vibcmlpx-delta;
    dvibtab6=pvibtab6cmlpx-vibcmlpx-delta;
    dvibtab4=pvibtab4cmlpx-vibcmlpx-delta;

    A(k,1)=dvibwt/wt;
    A(k,2)=dvibpl/pl;
    A(k,3)=dvibtab8/tab8;
    A(k,4)=dvibtab6/tab6;
    A(k,5)=dvibtab4/tab4;

    end
    Coeff{j}=A;

end
save Coeff.mat Coeff

%%%%%%%%%%%%%%%%%%%%%%%%%%%%%%%%%%%%%%%%%%%%%%%%%%%%%%%%%%%%%%%%%%%%%%%%

% Capt Nathan A Miller
% Converts VMEP adjustments into magnitude and phase of adjustments.
function VMEP_2_MagPhase

    load Longbow_VMEP_Adjustments.mat

    n = length(Longbow_VMEP_Adjustments(:,1));
    a=Longbow_VMEP_Adjustments;
    clear Longbow_VMEP_Adjustments

    for j=1:n

        %
        %           1           2           3           4
        adjcmlpx(j,1) = +a(j,1)-i*a(j,6)-a(j,11)+i*a(j,16); % Weight Adj
        adjcmlpx(j,2) = +a(j,2)-i*a(j,7)-a(j,12)+i*a(j,17); % P/L Adj
        adjcmlpx(j,3) = +a(j,3)-i*a(j,8)-a(j,13)+i*a(j,18); % Tab Adj 8
        adjcmlpx(j,4) = +a(j,4)-i*a(j,9)-a(j,14)+i*a(j,19); % Tab Adj 6
        adjcmlpx(j,5) = +a(j,5)-i*a(j,10)-a(j,15)+i*a(j,20); % Tab Adj 4

    end

    VMEPadj.mag=abs(adjcmlpx);
    VMEPadj.phase = angle(adjcmlpx)*180/pi;

    save VMEPadj.mat VMEPadj

    %%%%%%%%%%%%%%%%%%%%%%%%%%%%%%%%%%%%%%%%%%%%%%%%%%%%%%%%%%%%%%%%%%%%%%%%%

```

```

% Capt Nathan A Miller
% Thesis work
% This program loads vibe data and calculates an AVA adjustment matrix

function Vibs2AVA_ADJ

load Longbow_Vibes.mat
n = length(Longbow_Vibes(:,1));

for j=1:n

mag = Longbow_Vibes(j,[1 5 9 13 17 21 25]);
phase = Longbow_Vibes(j,[2 6 10 14 18 22 26]);

vibsCmplx = mag.*(cos( phase*pi/180 ) + i*sin( phase*pi/180 ) );

pmag = Longbow_Vibes(j,[3 7 11 15 19 23 27]);
pphase = Longbow_Vibes(j,[4 8 12 16 20 24 28]);
pvibsCmplx = pmag.*(cos( pphase*pi/180 ) + i*sin( pphase*pi/180 ) );
delvib = -vibsCmplx + pvibsCmplx;

adj(j) = LinearLongbow( delvib );

end
for k=1:n
    magnitude(k,:) = adj(k).mag';
    Phase(k,:) = adj(k).phase';
end
AVAadj.mag = magnitude;
AVAadj.phase = Phase;
save AVAadj.mat AVAadj

%%%%%%%%%%%%%%%%%%%%%%%%%%%%%%%%%%%%%%%%%%%%%%%%%%%%%%%%%%%%%%%%%%%%%%%%%%

% Capt Miller
% This file computes ad hoc coefficients using all flights, only good
% flights, and only exceedence flights. These coefficients are then
% compared by producing adjustment sets for the 20 sampled flights.
% The differences in adjustments are then compared based on the "Good"
% flight ad hoc matrix and the "Exceed" flight ad hoc matrix. If the
two
% matrices produce adjustments that are within the tolerance of
mechanical
% limitations of the aircraft, then the adjustment types are
identical.

clear, close all, clc;
load Coeff.mat
load Longbow_Vibes.mat
[LSC, standard]=Least_Squares_Coeff(Coeff);
[LSCgood, standardgood]=Least_Squares_Coeff(Coeff(1:5));
[LSCexd, standardexd]=Least_Squares_Coeff(Coeff(15:20));

LSCgoodcplx = LSCgood.mag.*(cos(LSCgood.phase*pi/180) + ...
    i*sin(LSCgood.phase*pi/180));

```

```

LSCexdcplx = LSCexd.mag.*(cos(LSCexd.phase*pi/180) + ...
    i*sin(LSCexd.phase*pi/180));

for j=1:length(Coeff)
    mag = Longbow_Vibes(j,[1 5 9 13 17 21 25]);
    phase = Longbow_Vibes(j,[2 6 10 14 18 22 26]);
    vibsCmplx = mag.*(cos( phase*pi/180 ) + i*sin( phase*pi/180 ) );
    pmag = Longbow_Vibes(j,[3 7 11 15 19 23 27]);
    pphase = Longbow_Vibes(j,[4 8 12 16 20 24 28]);
    pvibsCmplx = pmag.*(cos( pphase*pi/180 ) + i*sin( pphase*pi/180 )
);
    vibset(:,j) = -vibsCmplx+pvibsCmplx;
end
for j=1:length(Coeff)
    discrete_vib=vibset(:,j);
    adjgood(j,:)=LSCgoodcplx\discrete_vib;
    adjexceed(j,:)=LSCexdcplx\discrete_vib;
end
diff = abs(adjgood-adjexceed)
maxdiff(1:5) = max(diff(:,1:5))

PctDiffCoeff = abs(LSCgoodcplx-LSCexdcplx)./abs(LSCgoodcplx)*100

%%%%%%%%%%%%%%%%%%%%%%%%%%%%%%%%%%%%%%%%%%%%%%%%%%%%%%%%%%%%%%%%%%%%%%%%%%

% Capt Miller
% This program plots AVA, VMEP, and ad hoc adjustments together for
% comparison. It also plots RMS of ad hoc.

clear;clc;clf;

load Coeff.mat
load Longbow_Vibes.mat
load VMEPadj.mat

% Runs the Least Squares Coefficient function to
% generate the LSC matrix from the Coeff cell.
[LSC, standard]=Least_Squares_Coeff(Coeff)
vib_num=16
b=1
e=length(Coeff)

for j=1:length(Coeff)
    mag = Longbow_Vibes(j,[1 5 9 13 17 21 25]);
    phase = Longbow_Vibes(j,[2 6 10 14 18 22 26]);
    vibsCmplx = mag.*(cos( phase*pi/180 ) + i*sin( phase*pi/180 ) );
    pmag = Longbow_Vibes(j,[3 7 11 15 19 23 27]);
    pphase = Longbow_Vibes(j,[4 8 12 16 20 24 28]);
    pvibsCmplx = pmag.*(cos( pphase*pi/180 ) + i*sin( pphase*pi/180 )
);
    vibset(:,j) = -vibsCmplx+pvibsCmplx;
end

discrete_vib=vibset(:,vib_num); % Select discrete vibe set to use for
comparison

```

```

for j=1:length(Coeff)
    adj(:,j)=Coeff{j}\discrete_vib;
    Cmag(:,j) = abs(adj(:,j));
    Cphase(:,j) = (angle(adj(:,j)))*180/pi;
end

VMEP2AVA.mag = Cmag';
VMEP2AVA.phase = Cphase';
save VMEP2AVA.mat VMEP2AVA

% Calculate the Least Squares Method adjustment
A = LSC.mag.*(cos( LSC.phase*pi/180 ) + i*sin( LSC.phase*pi/180 ) );
LS_adj=A\discrete_vib;

AVA_adj=LinearLongbow( discrete_vib );

VMEPmag=VMEPadj.mag(vib_num,:);
VMEPphase=VMEPadj.phase(vib_num,:);
% Determine the max magnitude so we can normalize our adjustments for
% use in plotting on a single graph
for k=1:5
    Max1=max(max(Cmag(k,b:e)), AVA_adj.mag(k));
    %Max1=max(abs(AVA_adj.mag(k)));
    Max2=max(VMEPmag(k), abs(LS_adj(k)));
    Max(k)=max(Max1,Max2);
    %Max(k)=max(Cmag(k,b:e));
end

figure(1)
subplot(2,3,1)
polar(0,1,'.w')
hold

% Plot weight adjustments
% polar(Cphase(1,b:e)*pi/180,Cmag(1,b:e)/Max(1),'xr')
polar(angle(LS_adj(1)),abs(LS_adj(1))/Max(1),'sr')
polar(AVA_adj.phase(1)*pi/180,AVA_adj.mag(1)/Max(1),'or')
polar(VMEPphase(1)*pi/180,VMEPmag(1)/Max(1),'*r')

% Plot PCR adjustments
% polar(Cphase(2,b:e)*pi/180,Cmag(2,b:e)/Max(2),'xk')
polar(angle(LS_adj(2)),abs(LS_adj(2))/Max(2),'sk')
polar(AVA_adj.phase(2)*pi/180,AVA_adj.mag(2)/Max(2),'ok')
polar(VMEPphase(2)*pi/180,VMEPmag(2)/Max(2),'*k')

% Plot tab 8 adjustments
% polar(Cphase(3,b:e)*pi/180,Cmag(3,b:e)/Max(3),'xb')
polar(angle(LS_adj(3)),abs(LS_adj(3))/Max(3),'sb')
polar(AVA_adj.phase(3)*pi/180,AVA_adj.mag(3)/Max(3),'ob')
polar(VMEPphase(3)*pi/180,VMEPmag(3)/Max(3),'*b')

% Plot tab 6 adjustments
% polar(Cphase(4,b:e)*pi/180,Cmag(4,b:e)/Max(4),'xg')

```

```

polar(angle(LS_adj(4)),abs(LS_adj(4))/Max(4),'sg')
polar(AVA_adj.phase(4)*pi/180,AVA_adj.mag(4)/Max(4),'og')
polar(VMEPphase(4)*pi/180,VMEPmag(4)/Max(4),'*g')

% Plot tab 4 adjustments
%   polar(Cphase(5,b:e)*pi/180,Cmag(5,b:e)/Max(5),'xm')
polar(angle(LS_adj(5)),abs(LS_adj(5))/Max(5),'sm')
polar(AVA_adj.phase(5)*pi/180,AVA_adj.mag(5)/Max(5),'om')
polar(VMEPphase(5)*pi/180,VMEPmag(5)/Max(5),'*m')

title('Red-Wt, Black-Pcr, Blue-Tab8, Green-Tab6, Magenta-Tab4')
subplot(2,3,2)
polar(Cphase(1,b:e)*pi/180,Cmag(1,b:e),'xr')
subplot(2,3,3)
polar(Cphase(2,b:e)*pi/180,Cmag(2,b:e),'xk')
subplot(2,3,4)
polar(Cphase(3,b:e)*pi/180,Cmag(3,b:e),'xb')
subplot(2,3,5)
polar(Cphase(4,b:e)*pi/180,Cmag(4,b:e),'xg')
subplot(2,3,6)
polar(Cphase(5,b:e)*pi/180,Cmag(5,b:e),'xm')

VMEPcplx = VMEPadj.mag.*(cos(VMEPadj.phase*pi/180) + ...
    i*sin(VMEPadj.phase*pi/180));
for j=1:20
    diff(j,:)=abs(VMEPcplx(j,:) - (A\vibset(:,j))).')

    end
    max(diff)
figure(2)

polar(0,1,'.w')
hold

% Plot weight adjustments

polar(AVA_adj.phase(1)*pi/180,AVA_adj.mag(1)/Max(1),'or')
polar(VMEPphase(1)*pi/180,VMEPmag(1)/Max(1),'*r')

% Plot PCR adjustments

polar(AVA_adj.phase(2)*pi/180,AVA_adj.mag(2)/Max(2),'ok')
polar(VMEPphase(2)*pi/180,VMEPmag(2)/Max(2),'*k')

% Plot tab 8 adjustments
polar(AVA_adj.phase(3)*pi/180,AVA_adj.mag(3)/Max(3),'ob')
polar(VMEPphase(3)*pi/180,VMEPmag(3)/Max(3),'*b')
% Plot tab 6 adjustments
polar(AVA_adj.phase(4)*pi/180,AVA_adj.mag(4)/Max(4),'og')
polar(VMEPphase(4)*pi/180,VMEPmag(4)/Max(4),'*g')
% Plot tab 4 adjustments
polar(AVA_adj.phase(5)*pi/180,AVA_adj.mag(5)/Max(5),'om')
polar(VMEPphase(5)*pi/180,VMEPmag(5)/Max(5),'*m')

%%%%%%%%%%%%%%%%%%%%%%%%%%%%%%%%%%%%%%%%%%%%%%%%%%%%%%%%%%%%%%%%%%%%%%%%

```



```

function adj = LinearLongbow( vibsCmplx )
% This function calculates adjustments according to AVA coefficients.
% Input:
%   vibsCmplx = matrix of complex vibration data
% Output:
%   adj      = adjustment vector [hub weight(oz), pitch link(notch), 3 X
trim tab(oz)]
%

% Matrix of AVA coefficient magnitudes
mag = [0.0004936, 0.04448, 0,      0,      0;      % FPG100 (Lat)
       0.0004580, 0.15600, 0,      0,      0;      %   Hover (Lat)
       0.0004696, 0.03924, 0.1605, 0.3385, 0.6507; %   60 kts (Vert)
       0.0004546, 0.06359, 0.1714, 0.2886, 0.7391; %   80 kts (Vert)
       0.0004825, 0.11370, 0.1888, 0.3168, 0.6596; %  100 kts (Vert)
       0.0004547, 0.18190, 0.2161, 0.3747, 0.6992; %  120 kts (Vert)
       0.0004519, 0.24340, 0.3071, 0.4467, 0.9085]; %  140 kts (Vert)
% Matrix of AVA coefficient phases (deg)
phase = [163.0, 15.5, 0,      0,      0;      % FPG100 (Lat)
         171.2, 57.5, 0,      0,      0;      %   Hover (Lat)
         211.9, 286.6, 263.5, 270.6, 256.1;    %   60 kts (Vert)
         204.7, 273.2, 261.6, 261.3, 259.2;    %   80 kts (Vert)
         215.9, 262.0, 258.8, 268.4, 256.7;    %  100 kts (Vert)
         219.6, 256.1, 255.8, 258.6, 255.0;    %  120 kts (Vert)
         235.6, 247.2, 250.3, 260.5, 250.5];    %  140 kts (Vert)
% Convert the coefficients to complex numbers
A = mag.*(cos( phase*pi/180 ) + i*sin( phase*pi/180 ) );

% Calculate the adjustments
adjCmplx = A\vibsCmplx;
% Convert the adjustments to magnitude and phase
adj.mag = abs( adjCmplx );
adj.phase = angle( adjCmplx )*180/pi;

%%%%%%%%%%%%%%%%%%%%%%%%%%%%%%%%%%%%%%%%%%%%%%%%%%%%%%%%%%%%%%%%%%%%%%%%%%%%%%

%   Capt Miller
%   This function creates a single coefficient matrix from N coefficient
%   matrices by summing the squares of the N coefficient matrix
%   components
%   and then taking the square root.

function [LSC, standard]=Least_Squares_Coeff(Coeff)

numcoeff=length(Coeff);
numrows=length(Coeff{1}(:,1));
numcollumns=length(Coeff{1}(1,:));

C=zeros(numrows,numcollumns);

for j=1:numcoeff
    A.mag=abs(Coeff{j});
    A.phase=angle(Coeff{j});
    C=C+(A.mag.^2).*(cos( A.phase ) + i*sin( A.phase ) );
end

```

```

LSC.mag=sqrt(abs(C)/numcoeff);
LSC.phase=angle(C)*180/pi;
for j=1:numrows
    for k=1:numcollumns
        if LSC.phase(j,k) < 0
            LSC.phase(j,k) = LSC.phase(j,k)+360;
        end
    end
end

LSCcmplx = LSC.mag.*(cos(LSC.phase*pi/180)+i*sin(LSC.phase*pi/180));
for j=1:numcoeff

    diff{j}=abs(Coeff{j}-LSCcmplx);

end
for j=1:numrows
    for k=1:numcollumns
        for l=1:numcoeff
            temp(l)=diff{l}(j,k);
        end
        standard(j,k) = std(temp);
    end
end

%%%%%%%%%%%%%%%%%%%%%%%%%%%%%%%%%%%%%%%%%%%%%%%%%%%%%%%%%%%%%%%%%%%%%%%%%%

% Capt Miller

% This program will measure the difference between the VMEP adjustment
and
% the ad hoc adjustment for each flight. Plots are also generated of
ad
% hoc and VMEP adjustments.

clear;clc;close all;

load Coeff.mat
load Longbow_Vibes.mat
load Longbow_Coeff_Data.mat
load VMEPadj.mat
n=20;
[LSC, standard]=Least_Squares_Coeff(Coeff)
for j=1:length(Coeff)
    mag = Longbow_Vibes(j,[1 5 9 13 17 21 25])';
    phase = Longbow_Vibes(j,[2 6 10 14 18 22 26])';
    vibsCmplx = mag.*(cos( phase*pi/180 ) + i*sin( phase*pi/180 ) );
    pmag = Longbow_Vibes(j,[3 7 11 15 19 23 27])';
    pphase = Longbow_Vibes(j,[4 8 12 16 20 24 28])';
    pvibsCmplx = pmag.*(cos( pphase*pi/180 ) + i*sin( pphase*pi/180 )
);
    vibset(:,j) = -vibsCmplx+pvibsCmplx;
end

```

```

VMEPcplx = VMEPadj.mag.*(cos(VMEPadj.phase*pi/180) + ...
    i*sin(VMEPadj.phase*pi/180))
A = LSC.mag.*(cos( LSC.phase*pi/180 ) + i*sin( LSC.phase*pi/180 ) );

for j=1:10
    tmp{2*j-1,:}=Coeff{2*j};% tmp(odd) = A(even)
    tmp{2*j,:}=Coeff{2*j-1};% tmp(even) = A(odd)
end
clear Coeff;
Coeff=tmp;

for j=1:n

    %adj(j,:)=A\vibset(:,j); % This one for plotting RMS ad hoc
    adj(j,:)=Coeff{j}\vibset(:,j);%This one for plotting individual ad
hocs
end
for type=1:5
    subplot(2,3,type)
    polar(angle(adj(1:n,type)),abs(adj(1:n,type)),'ko')
    hold on
    polar(angle(VMEPcplx(1:n,type)),abs(VMEPcplx(1:n,type)),'k+')
end
for j=1:20
    diff(j,:)=abs(VMEPcplx(j,:) - adj(j,:));
end
diff
max(diff)
%figure(1)
subplot(2,3,1)
title('Weight')
%legend('Ad Hoc Adjustment','Actual Adjustment')
%figure(2)
subplot(2,3,2)
title('Pitch Link')
%legend('Ad Hoc Adjustment','Actual Adjustment')
%figure(3)
subplot(2,3,3)
title('Trim Tab 8-10')
%legend('Ad Hoc Adjustment','Actual Adjustment')
subplot(2,3,4)
title('Trim Tab 6-10')
subplot(2,3,5)
title('Trim Tab 4-10')

%%%%%%%%%%%%%%%%%%%%%%%%%%%%%%%%%%%%%%%%%%%%%%%%%%%%%%%%%%%%%%%%%%%%%%%%

% Capt Nathan A Mille
% This program generates the histograms showing difference between AH-
64D
% AVA adjustments from PC-GBS adjustments.

clear; clc;
load AVAadj.mat
load VMEPadj.mat

```

```

AVAcomplex = AVAadj.mag.*(cos( AVAadj.phase*pi/180 ) +...
    i*sin( AVAadj.phase*pi/180 ) );
VMEPcomplex = VMEPadj.mag.*(cos( VMEPadj.phase*pi/180 ) +...
    i*sin( VMEPadj.phase*pi/180 ) );
Magnitude_diff = abs(AVAcomplex - VMEPcomplex);

Rel_mag_diff = Magnitude_diff./AVAadj.mag;%max(VMEPadj.mag,
AVAadj.mag);

for i=1:20
    if abs(AVAcomplex(i,1)) < 113/2
        if abs(VMEPcomplex(i,1)) < 113/2
            Rel_mag_diff(i,1)=0;

            abs(AVAcomplex(i,1));
            abs(VMEPcomplex(i,1));
        end
    end

    if abs(AVAcomplex(i,2)) < 0.5/2
        if abs(VMEPcomplex(i,2)) < 0.5/2
            Rel_mag_diff(i,2)=0;

            abs(AVAcomplex(i,2));
            abs(VMEPcomplex(i,2));
        end
    end

    if abs(AVAcomplex(i,3)) < 0.5/2
        if abs(VMEPcomplex(i,3)) < 0.5/2
            Rel_mag_diff(i,3)=0;
        end
    end

    if abs(AVAcomplex(i,4)) < 0.5/2
        if abs(VMEPcomplex(i,4)) < 0.5/2
            Rel_mag_diff(i,4)=0;
        end
    end

    if abs(AVAcomplex(i,5)) < 0.5/2
        if abs(VMEPcomplex(i,5)) < 0.5/2
            Rel_mag_diff(i,5)=0;
        end
    end

end

X = ([0 1 2 3 4 5 6 7 8 9]+0.5)/10;
for i=1:5
    [n(i,:),xout(i,:)]=hist(Rel_mag_diff(:,i),X);
    subplot(1,5,i);
    bar(xout(i,:)*100,n(i,:)/0.2,'k');
    axis([0 100 0 100])
end
subplot(1,5,1)
title('Weight','FontSize',16)
ylabel('Percentage of Total Flights Sampled','FontSize',16)

```

```

subplot(1,5,2)
title('Pitch Link','FontSize',16)
subplot(1,5,3)
title('Tab 8-10','FontSize',16)
xlabel('Percent Difference of PC-GBS Adjustments from AVA Algorithm
Adjustments','FontSize',16)
subplot(1,5,4)
title('Tab 6-10','FontSize',16)
subplot(1,5,5)
title('Tab 4-10','FontSize',16)

%%%%%%%%%%%%%%%%%%%%%%%%%%%%%%%%%%%%%%%%%%%%%%%%%%%%%%%%%%%%%%%%%%%%%%%%

% Capt Miller Thesis
% This is a test program to determine if any mistakes were made
% during data entry. All AH-64D coefficients are plotted together.
Errors
% will show up as individual coefficients plotting grossly different
from
% the rest of the coefficients.
clear all; close all; clc;

load Coeff.mat
[LSC, standard]=Least_Squares_Coeff(Coeff);
[LSCgood, standardgood]=Least_Squares_Coeff(Coeff(1:5));
[LSCexd, standardexd]=Least_Squares_Coeff(Coeff(15:20));
b=1;
e=length(Coeff);
n=1;
for h=1:7
for j=b:e
value(h,j+1-b,:)=Coeff{j}(h,:);
end
end

end
vertvalue = value(3:7, :, :);
latvalue = value(1:2, :, :);
for h=1:7
max1(h)=max(abs(value(h, :, 1)));
max2(h)=max(abs(value(h, :, 2)));
max3(h)=max(abs(value(h, :, 3)));
max4(h)=max(abs(value(h, :, 4)));
max5(h)=max(abs(value(h, :, 5)));
end

for h=1:5
vertmax1(h)=max(abs(vertvalue(h, :, 1)));
vertmax2(h)=max(abs(vertvalue(h, :, 2)));
vertmax3(h)=max(abs(vertvalue(h, :, 3)));
vertmax4(h)=max(abs(vertvalue(h, :, 4)));
vertmax5(h)=max(abs(vertvalue(h, :, 5)));
end
for h=1:2
latmax1(h)=max(abs(latvalue(h, :, 1)));

```

```

        latmax2(h)=max(abs(latvalue(h,:,2)));
        latmax3(h)=max(abs(latvalue(h,:,3)));
        latmax4(h)=max(abs(latvalue(h,:,4)));
        latmax5(h)=max(abs(latvalue(h,:,5)));
end

for h=1:7
%figure(h)
subplot(3,3,h)
%polar(angle(value(h,:,1)),abs(value(h,:,1))/max1(h),'bx')
polar(angle(value(h,:,n)),abs(value(h,:,n)),'rx')
%hold on
%figure(2)
%subplot(3,3,h)
%polar(angle(value(h,:,2)),abs(value(h,:,2))/max2(h),'rx')
%figure(3)
%subplot(3,3,h)
%polar(angle(value(h,:,3)),abs(value(h,:,3))/max3(h),'gx')
%polar(angle(value(h,:,4)),abs(value(h,:,4))/max4(h),'mx')
%polar(angle(value(h,:,5)),abs(value(h,:,5))/max5(h),'cx')
end

subplot(3,3,1)
title('FPG100 Lat')
subplot(3,3,2)
title('Hover Lat')
subplot(3,3,3)
title('60 Kts Vert')
subplot(3,3,4)
title('80 Kts Vert')
subplot(3,3,5)
title('100 Kts Vert')
subplot(3,3,6)
title('120 Kts Vert')
subplot(3,3,7)
title('140 Kts Vert')

figure(2)
for i=1:5
    temp1 = max(vertmax1(i),vertmax2(i));
    temp2 = max(vertmax3(i),vertmax4(i));
    temp3 = max(temp1,temp2);
    maxval = max(temp3,vertmax5(i));

subplot(2,3,i)    % Each subplot is for a different lateral regime
polar(0,maxval,'w.')
hold on
polar(angle(vertvalue(i,:,1)),abs(vertvalue(i,:,1)),'kx')
polar(angle(vertvalue(i,:,2)),abs(vertvalue(i,:,2)),'kd')
polar(angle(vertvalue(i,:,3)),abs(vertvalue(i,:,3)),'k^')
polar(angle(vertvalue(i,:,4)),abs(vertvalue(i,:,4)),'kv')
polar(angle(vertvalue(i,:,5)),abs(vertvalue(i,:,5)),'kp')
end

figure(3)

```

```

for i=1:2
    temp1 = max(latmax1(i),latmax2(i));
    temp2 = max(latmax3(i),latmax4(i));
    temp3 = max(temp1,temp2);
    maxval = max(temp3,latmax5(i));

subplot(1,2,i)    % Each subplot is for a different lateral regime
polar(0,maxval,'w.')
hold on
polar(angle(latvalue(i,:,1)),abs(latvalue(i,:,1)*100),'kx')
polar(angle(latvalue(i,:,2)),abs(latvalue(i,:,2)),'kd')
polar(angle(latvalue(i,:,3)),abs(latvalue(i,:,3)),'k^')
polar(angle(latvalue(i,:,4)),abs(latvalue(i,:,4)),'kv')
polar(angle(latvalue(i,:,5)),abs(latvalue(i,:,5)),'kp')
end

figure(4)
polar(0,maxval,'w.')
hold on
polar(angle(latvalue(i,:,1)),abs(latvalue(i,:,1)*100),'ko')
polar(angle(latvalue(i,:,2)),abs(latvalue(i,:,2)),'kd')
polar(angle(latvalue(i,:,3)),abs(latvalue(i,:,3)),'k^')
polar(angle(latvalue(i,:,4)),abs(latvalue(i,:,4)),'kv')
polar(angle(latvalue(i,:,5)),abs(latvalue(i,:,5)),'kp')
title('Ad Hoc Coefficients for Hover(Lat) for AH-64A')

abs(LSCexd.mag-LSCgood.mag)./LSCgood.mag*100

```

Bibliography

1. Wroblewski, D., Branhof, R.W., and Cook, T., "Neural Networks for Smoothing of Helicopter Rotors," American Helicopter Society 57th Annual Forum Proceedings, Washington, DC, May 2001, pp. 1587-1594.
2. Wroblewski, D., Grabill, P., Berry, J.D., and Branhof, R.W., "Neural Network System for Helicopter Rotor Smoothing," IEEE 2000 Aerospace Conference Proceedings, Big Sky, Montana, March 2000, pp. 271-276.
3. Taitel, H., Danai, K., and Gauthier, D., "Helicopter Track and Balance With Artificial Neural Nets," *ASME Journal of Dynamic Systems, Measurement, and Control*, Vol. 117, No. 2, June 1995, pp. 226-231.
4. Meirovitch, Leonard. *Fundamentals of Vibrations*. New York: McGraw-Hill Book Co., 2001
5. Renzi, Michael J. *An Assessment of Modern Methods for Rotor Track and Balance*. MS thesis, AFIT/GAE/ENY/04-J11. Graduate School of Engineering and Management, Air Force Institute of Technology, Wright Patterson AFB OH, June 2004
6. Johnson, Lloyd. "HISTORY: Helicopter Rotor Smoothing." Article. n. pag. <http://www.dssmicro.com/theory/dsrothst.htm>. 25 August 2003.
7. Robinson, Mike. "Helicopter Track and Balance Theory." <http://www.amtonline.com/publication/article.jsp?pubId=1&id=844> February 1999.
8. Demuth, H., Beale, M., Hagan, M., "Neural Network Toolbox User's Guide," The Mathworks, Inc.
9. Branhoff, R.W., Keller, J.A., Grant, L., and Grabill, P., "Application of Automated Rotor Smoothing Using Continuous Vibration Measurements," Proceedings of the 61st Annual Forum of the American Helicopter Society, Grapevine, Texas, June 2005.

Vita

Captain Nathan A. Miller graduated from Tippecanoe High School in Tipp City, Ohio. He entered undergraduate studies at The Ohio State University in Columbus, Ohio where he graduated with a Bachelor of Science in Aeronautical and Astronautical Engineering in June 1996. He was commissioned through the PLC program as a Second Lieutenant in the United States Marine Corps.

His first assignment was at MCB Quantico as a student at The Basic School. In April 1997, he was ordered to NAS Pensacola to undergo flight training. In March 1999 he was designated a Naval Aviator and, following initial flight training in the CH-53E, was assigned to Marine Heavy Helicopter 461 at MCAS New River, North Carolina. He deployed with the 24th Marine Expeditionary Unit from April to October 2001 and again with the 22nd MEU from February to July 2004. While with the 22nd MEU, he participated in combat operations in Afghanistan. In August 2004, he entered the Graduate School of Engineering and Management, Air Force Institute of Technology. Upon graduation, he will be assigned to Naval Air Depot Cherry Point, North Carolina.

REPORT DOCUMENTATION PAGE				Form Approved OMB No. 074-0188	
<p>The public reporting burden for this collection of information is estimated to average 1 hour per response, including the time for reviewing instructions, searching existing data sources, gathering and maintaining the data needed, and completing and reviewing the collection of information. Send comments regarding this burden estimate or any other aspect of the collection of information, including suggestions for reducing this burden to Department of Defense, Washington Headquarters Services, Directorate for Information Operations and Reports (0704-0188), 1215 Jefferson Davis Highway, Suite 1204, Arlington, VA 22202-4302. Respondents should be aware that notwithstanding any other provision of law, no person shall be subject to a penalty for failing to comply with a collection of information if it does not display a currently valid OMB control number.</p> <p>PLEASE DO NOT RETURN YOUR FORM TO THE ABOVE ADDRESS.</p>					
1. REPORT DATE (DD-MM-YYYY) 23-03-2006		2. REPORT TYPE Master's Thesis		3. DATES COVERED (From – To) June 2005 – March 2006	
4. TITLE AND SUBTITLE A Comparison of Main Rotor Smoothing Adjustments Using Linear and Neural Network Algorithms				5a. CONTRACT NUMBER	
				5b. GRANT NUMBER	
				5c. PROGRAM ELEMENT NUMBER	
6. AUTHOR(S) Miller, Nathan, A., Captain, USMC				5d. PROJECT NUMBER N/A	
				5e. TASK NUMBER	
				5f. WORK UNIT NUMBER	
7. PERFORMING ORGANIZATION NAMES(S) AND ADDRESS(S) Air Force Institute of Technology Graduate School of Engineering and Management (AFIT/EN) 2950 Hobson Way WPAFB OH 45433-7765				8. PERFORMING ORGANIZATION REPORT NUMBER AFIT/GAE/ENY/06-M24	
9. SPONSORING/MONITORING AGENCY NAME(S) AND ADDRESS(ES) N/A				10. SPONSOR/MONITOR'S ACRONYM(S)	
				11. SPONSOR/MONITOR'S REPORT NUMBER(S)	
12. DISTRIBUTION/AVAILABILITY STATEMENT APPROVED FOR PUBLIC RELEASE; DISTRIBUTION UNLIMITED.					
13. SUPPLEMENTARY NOTES					
<p>14. ABSTRACT Helicopter main rotor smoothing is a maintenance procedure that is routinely performed to minimize airframe vibrations induced by non-uniform mass and/or aerodynamic distributions in the main rotor system. This important task is both time consuming and expensive, so improvements to the process have long been sought. Traditionally, vibrations have been minimized by calculating adjustments based on an assumed linear relationship between adjustments and vibration response. In recent years, artificial neural networks have been trained to recognize non-linear mappings between adjustments and vibration response. This research was conducted in order observe the character of the adjustment mapping of the Vibration Management Enhancement Program's PC-Ground Base System (PC-GBS). Flight data from the UH-60, AH-64A, and AH-64D were utilized during the course of this study. What has been determined is that the neural networks of PC-GBS produce adjustments that can be reproduced by a linear algorithm, thus implying that the shape of the mapping is in fact linear.</p>					
15. SUBJECT TERMS Helicopter Rotors, Vibration, Neural Nets, Optimization, Helicopter Main Rotor Smoothing					
16. SECURITY CLASSIFICATION OF:			17. LIMITATION OF ABSTRACT	18. NUMBER OF PAGES	19a. NAME OF RESPONSIBLE PERSON Donald L. Kunz (ENY)
a. REPORT	b. ABSTRACT	c. THIS PAGE			19b. TELEPHONE NUMBER (Include area code) (937) 255-3636, ext 4548 (Donald.kunz@afit.edu)
U	U	U	UU	146	